

UNIVERSITÀ  
DEGLI STUDI  
DI PADOVA

Sede Amministrativa: Università degli Studi di Padova

Dipartimento di Geoscienze

SCUOLA DI DOTTORATO DI RICERCA IN: Scienze della Terra  
CICLO XXVI

**DEMISE OF CARNIAN PLATFORMS: LARGE SCALE GEOMETRIES AND MECHANISMS  
OF PRECIPITATION**

**Direttore della Scuola** : Ch.mo Prof. Massimiliano Zattin

**Supervisore** : Dr. Nereo Preto

**Co-supervisore** : Dr. Anna Breda

**Dottorando**: Giovanni Gattolin



# Demise of Carnian platforms: large scale geometries and mechanisms of precipitation

*Giovanni Gattolin*

2014



# *Contents*

---

<b>Abstract (English)</b> .....	<b>7</b>
<b>Riassunto (italiano)</b> .....	<b>9</b>
<b>Preface</b> .....	<b>11</b>
<b>Chapter 1: Introduction</b> .....	<b>13</b>
• 1.1 Introduction and setting	
• 1.2 Methods and aim	
<b>Chapter 2: From large scale high-relief platforms to small mounds</b> .....	<b>19</b>
• 2.1 Lithozones	
<b>Chapter 3: Demise of Late Triassic carbonate platforms triggered the onset of a tide-dominated depositional system in the Dolomites, Northern Italy</b> .....	<b>27</b>
• Abstract	
• 3.1 Introduction	
• 3.2 Geological setting	
• 3.3 Methods	
• 3.4 Facies analysis	
◦ 3.4.1 Stratigraphic intervals description and interpretation	
• 3.5 Discussion	
◦ 3.5.1 Paleoenvironment and paleogeography	
◦ 3.5.2 Relative sea level changes	
◦ 3.5.3 Similarities with Plio-Pleistocene deposits of the central Mediterranean Sea	
◦ 3.5.4 First occurrence of a strait developed between two demised carbonate platforms?	
• 3.6. Conclusions	
<b>Chapter 4: Sequence Stratigraphy after the demise of a high-relief carbonate platform (Carnian of the Dolomites): sea-level and climate disentangled</b> .....	<b>53</b>
• Abstract	
• 4.1 Introduction	

- 4.2 Geological setting
- 4.3 Methods
- 4.4 Lithozones
- 4.5 Sequence stratigraphy
- 4.6 Discussion
  - 4.6.1 Role of 3D modeling in identification of depositional geometries
  - 4.6.2 What triggered the platform demise?

**Chapter 5: General conclusion .....77**

**Chapter 6: Possible implications .....79**

**References .....83**

## *Abstract (English)*

---

During the Late Triassic, a climate change known as the Carnian Pluvial Event (CPE) resulted in a major crisis for carbonate producers. In the western Tethys, the change in carbonate production led to a dramatic modification of depositional geometries. The steep clinoforms of the high relief pre-crisis carbonate platforms were replaced by low angle ramp geometries. A quantitative three dimensional modeling of the geometry of sedimentary bodies in the Cortina d'Ampezzo area (North-eastern Italy) formed before, during and after the Carnian crisis, coupled with facies analysis, was performed in order to investigate in detail how the changes in shallow water carbonate precipitation influenced the depositional geometries of carbonate platforms.

Facies and depositional geometries suggest that after the demise of high-relief, microbial dominated carbonate platforms, a phase of intermediate sedimentation took place, in which microbial carbonate mounds and loose carbonate and terrigenous sediments coexisted. The subsequent evolution to a ramp is characterized by the onset of a tide-dominated environment. In the study area, the sedimentary succession developed in a marine strait connecting two small basins. Both ebb and flood paleocurrents are documented and their directions are in agreement with the strait orientation, as inferred from the paleogeographic position of relict high-relief carbonate platforms. Facies and sedimentary structures related to variations in the hydraulic regime have been observed, including planar cross stratification, herringbone cross stratification, flaser to wavy to lenticular bedding and cyclical alternations of mainly oolitic-siliciclastic vs. mainly bioclastic-muddy laminae. The peculiarity of this tidal system is that, differently from all other known cases, it did not develop in a tectonically confined submarine graben or canyon, but in a marine passage between relict high-relief carbonate platforms.

Sedimentary facies analysis, coupled with geological three dimensional modeling, led also to constrain the sequence stratigraphy of this complex stratigraphic interval, in which the eustatic and climatic signals can be disentangled. The climate change predates the sea-level drop and caused the demise of the microbial-dominated high-relief carbonate platforms. A surface similar to a drowning unconformity was thus generated, even though a transgression was not taking place. Only small isolated microbial carbonate mounds survived the crisis of high-relief platforms. The complete disappearance of microbial carbonates (i.e. mounds) and the definitive switch of the shallow water carbonates to loose-sediment dominated ramps coincides with a subsequent sea-level drop. Thus the demise of the Upper Triassic microbial dominated high-relief platforms of the Dolomites can be interpreted as a two step process: at first a climatic event killed the km-scale high-relief platforms; later a drop in sea level led to the definitive disappearance of the microbial carbonates.



## Riassunto (italiano)

---

Nel tardo Triassico un cambiamento climatico noto come *Carnian Pluvial Event* (CPE) determinò una profonda crisi degli organismi produttori di carbonato di calcio. Ciò si tradusse in una importante modifica delle geometrie deposizionali delle piattaforme carbonatiche della Tetide occidentale. Piattaforme carbonatiche caratterizzate da alto rilievo morfologico e scarpate molto acclivi vennero sostituite da rampe a basso angolo.

Allo scopo di comprendere come le variazioni occorse allo stile di precipitazione del carbonato di calcio influenzarono le geometrie deposizionali delle piattaforme carbonatiche è stata eseguita l'analisi di *facies* e la modellazione geologica tridimensionale di alcuni corpi sedimentari depositatisi nell'area di Cortina d'Ampezzo (Italia Nord-orientale) prima, durante e dopo la crisi carnica.

*Facies* e geometrie deposizionali suggeriscono che la morte delle piattaforme microbiali ad alto rilievo fu seguita da un periodo in cui piccoli duomi di carbonato microbiale (*mound*) crescevano contemporaneamente alla deposizione di carbonati e sedimenti di origine detritica. La seguente evoluzione verso un sistema di rampa fu caratterizzato dall'instaurarsi di un ambiente sedimentario dominato dalle maree. Nell'area di studio la successione sedimentaria si sviluppò in uno stretto marino che connetteva due piccoli bacini. Sono state rilevate strutture sedimentarie generate da correnti di marea con verso opposto e in accordo con l'orientazione del paleo-stretto che può essere dedotta dalla paleogeografia delle piattaforme ad alto rilievo pre-crisi. Si osservano *facies* e strutture sedimentarie come stratificazioni incrociate planari, stratificazioni incrociate di tipo *herringbone*, laminazioni *flaser*, *wavy* e lenticolari, alternanze cicliche di lamine prevalentemente oolitico-silicoclastiche e lamine prevalentemente bioclastiche-fangose dovute a variazioni del regime idraulico. La particolarità di questo sistema tidale è che, diversamente dagli altri casi noti in letteratura, non si sviluppò in un *graben* o in un *canyon* di origine tettonica, bensì in un corridoio marino delimitato dai relitti di due piattaforme ad alto rilievo.

L'analisi di *facies*, unitamente all'utilizzo di tecniche di modellazione geologica tridimensionale, ha permesso inoltre di interpretare dal punto di vista sequenziale questo complesso intervallo stratigrafico, permettendo di riconoscere e separare segnale eustatico e segnale climatico. Il cambiamento climatico è precedente alla caduta eustatica ed è la causa della morte delle piattaforme microbiali ad alto rilievo. La morte di queste piattaforme determina la creazione di una superficie stratigrafica simile ad una *drowning unconformity*, nonostante non sia in atto una trasgressione. I *mound* microbiali rappresentano il tentativo della *carbonate factory* microbiale, che caratterizzava le piattaforme carbonatiche ad alto rilievo, di tenere testa al cambiamento climatico. La completa scomparsa del carbonato microbiale (i *mound*) e il definitivo passaggio dei carbonati di mare basso a sistemi di rampe dominate da sedimento sciolto, é coeva a un abbassamento del livello marino. Riassumendo, la morte delle piattaforme microbiali ad alto rilievo tardo triassiche delle Dolomiti può essere interpretata come un processo in due fasi: inizialmente un evento climatico uccide le grandi piattaforme ad alto rilievo; successivamente la caduta del livello marino porta alla definitiva scomparsa dei carbonati microbiali.

The structure of this thesis is the following:

Chapter 1 is a brief introduction to the work, presenting aims, settings and methods.

Data are presented in chapters 2; 3 and 4.

Chapter 2 describes in detail the sedimentary facies of the lower portion of the studied stratigraphic interval.

Chapter 3 (*published on Sedimentary Geology and cited in chapter 4 as Gattolin et al., 2013*) describes sedimentary facies and depositional environments of the upper part of the studied stratigraphic interval.

Chapter 4 (*submitted to Palaeogeography, Palaeoclimatology, Palaeoecology*) concerns the sequence stratigraphic interpretation of the whole stratigraphic interval of interest.

Chapter 5 presents the general conclusions of the thesis.

Chapter 6 considers possible implications of the work.

As Chapter 3 and Chapter 4 derive from papers already published on, or submitted to, international peer reviewed journals, these chapters are structured as the papers. Thus, each of these chapters include their own introduction, firstly in order to give the reader an high quality text, as resulted from the peer-review process, secondly in order to give the opportunity to those who read a single chapter to have a complete view of the topic. On the other hand, Chapter 2 is the unpublished description of the lower portion of the studied stratigraphic interval and is written to provide a complete overview of the entire depositional sequence. Its interpretation is provided in Chapter 4.

Calcium carbonate precipitation in marine environments is generally the result of a complex interaction between different processes, which may be abiotic, biologically controlled, biologically induced and biologically influenced (Lowenstam, 1981; Lowenstam and Weiner, 1989; Schlager, 2003; Dupraz et al., 2009). The term microbialite (sensu Burne and Moore 1987) is used in this thesis to indicate in situ carbonate precipitation inferred to result from organomineralization s.l. processes, on the basis of microfabrics comparable to modern microbialites.

## **1.1 Introduction and setting**

Carbonate platforms are sedimentary bodies composed of autochthonous and/or parautochthonous carbonate, with morphological relief. Present examples are the atolls of Indian and Pacific oceans (e.g. the Maldives, the French Polynesia islands, the Cook islands, among others), the Bahamas and the Great Barrier Reef of Australia. Shallow water benthic biological communities whose organisms control or promote the precipitation of calcium carbonate, called "carbonate factories", create carbonate platforms. Carbonate factories can be classified according to their prevalent mode of calcium carbonate precipitation (Schlager, 2003): in mud-mound or M-factories, carbonate precipitation is biotically induced, mostly by microbes; in tropical or T-factories, precipitation is controlled by autotrophs as green algae or corals; in cool water type or C-factories, precipitation is controlled by heterotrophs as molluscs or echinoderms. Each type of factory generates carbonate platforms with specific geometries and skeletal associations (Fig. 1.1; Schlager, 2003; 2005), leading thus to the formation of sedimentary bodies with specific shapes and facies.

Due to the scarcity of calcareous plankton, the carbonate precipitation in pre-Jurassic seas occurred essentially in shallow water environments (Stanley and Hardie, 1998), and is testified in the rock record by extensive carbonate platforms, as those that characterize the Triassic of Tethys (e.g. the Chinese Great bank of Guizhou, Lehrmann et al., 1998). The Southern Alps, i.e., the S-vergent portion of the Alpine belt outcropping in Lombardy, Trentino Alto Adige, Veneto and Friuli (northern Italy, Fig. 1.2), is a type area for the study of the Triassic carbonate platforms of the Tethys, as the reduced tectonic deformation allowed the preservation of sedimentary facies, depositional geometries and platform-basin relationships. The geometry of Triassic carbonate platforms is particularly well preserved in the Dolomites, a ca. 35 km large pop-up structure in which tectonic deformation is minimal and mostly confined at the bounding faults (see Castellarin and Vai, 1982 and Castellarin and Doglioni, 1985 for tectonics; von Mojsisovics, 1879; Bosellini, 1984; De Zanche et al.,

1993; Harris, 1993; Gianolla et al., 1998; Keim and Schlager, 1999; 2001; Bosellini et al., 2003; Blendinger et al., 2004; Preto et al., 2011 among others for facies and depositional geometries).

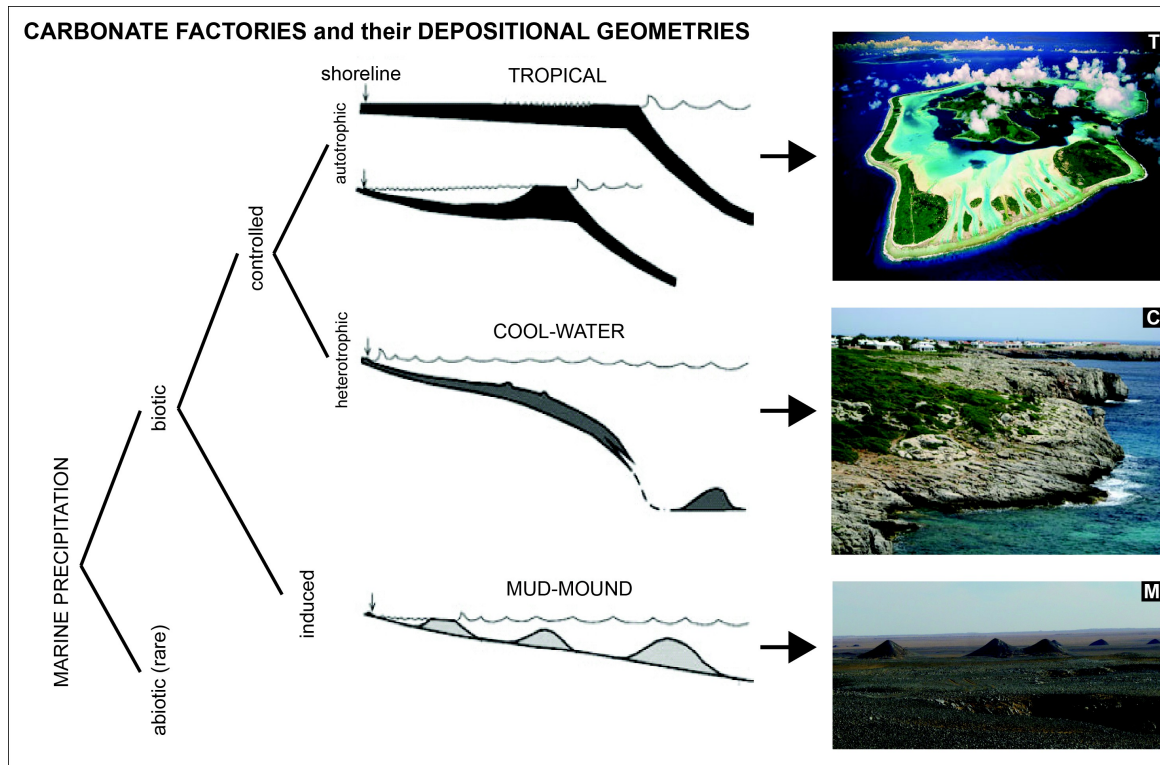


Figure 1.1. Carbonate precipitation modes and resulting depositional geometries of the three most important carbonate factories (modified after Schlager et al., 2003). Examples of resulting carbonate platform geometries are provided on the right. (T) Bora Bora, French Polynesia, Recent. (C) Menorca, Spain, Tortonian. (M) Azzel Matti, Algeria, Devonian.

The end Permian mass extinction severely hit the marine realms and caused the wiping of the 62% of the marine invertebrate families (McKinney, 1985) and up to the 96% of the species (Raup, 1979). The Dolomites are not an exception. Here, the nucleation of the first sporadic carbonate platforms after the Permo-Triassic extinction dates back to the Olenekian-Anisian boundary (Fig. 1.3; Lower Serla Dolomite and later M.te Rite Fm., Senowbari-Daryan et al., 1993; Neri et al., 2007) but only in the late Anisian a complete and widespread recovery of carbonate platforms is observed (Fig. 1.3; Contrin Fm., Masetti and Neri, 1980 and later Sciliar Lower Edifice, Gaetani et al., 1981; De Zanche et al., 1993; Gianolla et al., 1998). From Anisian to Carnian, the carbonate platforms of the Dolomites

grew in the framework of a complex palaeogeography, featuring small isolated carbonate platforms (up to 12 km in diameter) with progradational to backstepping geometries (Bosellini, 1984), locally emerged lands or exposed volcanic buildups, and deep basins with either carbonate or mixed to siliciclastic sedimentation. These carbonate platforms were dominated by the M-factory, with a secondarily contribution by the T-factory (Blendinger, 1994; Russo et al., 1997; Keim and Schlager, 2001; Marangon et al., 2011). They developed depositional geometries, with steep (up to 40°) carbonate slopes often lacking clear clinoform beds. This was the result of the combination of two main factors: the high subsidence rates which were characterizing the area in this period (Maurer, 2000; Emmerich et al., 2005), and the fact that the slope was in part made up of boundstone (Blendinger, 1994; Keim and Schlager, 1999; 2001; Bosellini et al., 2003; Marangon et al., 2011).

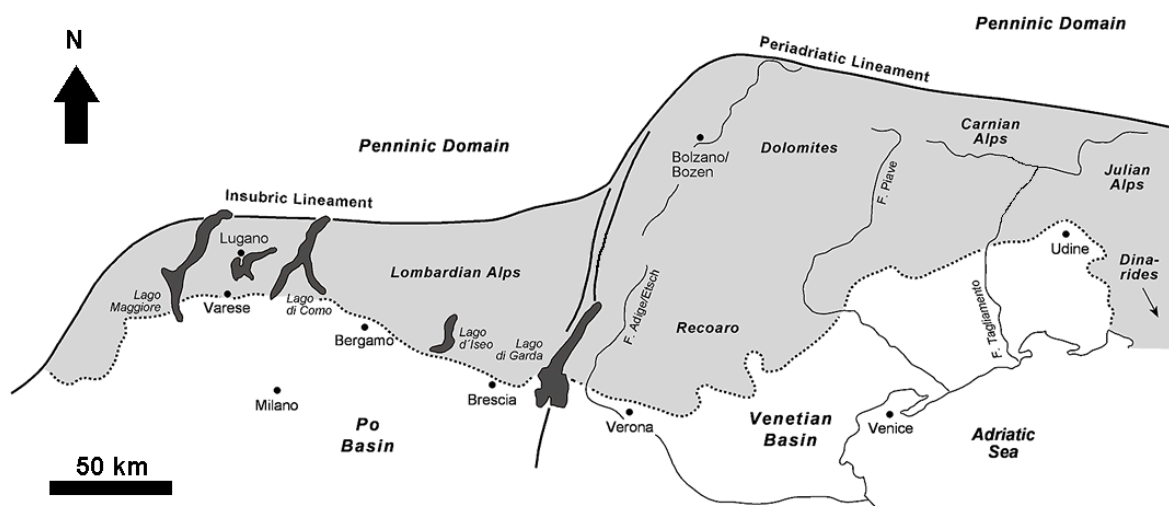


Figure 1.2. The Southern Alps are the S-vergent portion of the Alpine mountain belt and are here indicated in light gray (modified after Feist-Burkhardt et al., 2008). They outcrop in northern Italy, to the South of the Periadriatic/Insubric lineament. Names of the main areas are indicated. This thesis is focused on Upper Triassic carbonate platforms of the Dolomites.

At the end of the Early Carnian, a sudden change in the carbonate factory is observed. Shallow water carbonate systems of the Dolomites switched from mainly microbial carbonates (M-factory) to carbonates with skeletal associations typical of a C-factory (Preto and Hinnov, 2003, see also the transition from Cassian 2 high-relief platforms to Heiligkreutz Fm. In Neri et al., 2007). Consequently, in terms of depositional geometries, the high-relief steep-slope carbonate platforms were substituted by low angle ramps (Fig. 1.1). Along with the turnover of the carbonate factories and platforms, a huge volume of siliciclastics was supplied to marginal seas, so that all the topographical complexity inherited from the Early Carnian was leveled out.

This change in carbonate factories and platform geometries is related to a “crisis” in carbonate production, but what exactly happened to carbonate platforms during the Carnian crisis is still only partially understood. Some authors suggest that the demise of high-relief platforms is related to a shift to more humid conditions (the Carnian Pluvial Event; Simms and Ruffell, 1989; Preto et al., 2010; Dal Corso et al., 2012), while others indicate sea level drop as a possible cause (De Zanche et al., 1993; Gianolla et al., 1998; Bosellini et al., 2003) that led to subaerial exposure and consequent karstification of the platforms and to the erosion of adjacent high-lands.

## **1.2 Methods and aim**

This work has been focused on the relationship between the changes in main carbonate-producing biota and the changes in depositional geometries that resulted from it. The sedimentary bodies deposited during the Carnian carbonate-factory turnover have been investigated through standard facies analysis methods (e.g. Tucker and Wright, 1990; Flügel, 2004). The interpretation of the depositional geometry of geological bodies has been carried out with the aid of three dimensional modeling methods (i.e., photogrammetry and terrestrial laser scanner) in order to avoid misinterpretation driven by perspective distortions, and in order to resolve long-standing controversies on the significance of Carnian outcrops of the Dolomites on the light of a quantitative geological field data. A



sequence stratigraphic interpretation of the studied interval has been carried out following the standard terminology of Catuneanu et al. (2009; 2011).

All the presented data have been collected in the Cortina d'Ampezzo area (North-eastern Italy; Fig 3.1).

The aim of this work are:

- To detail the Carnian carbonate factory turnover;
- To reconstruct the sedimentary environment of the area during the Carnian crisis;
- To refine the sequence stratigraphy of the studied interval;
- To disentangle the role played by climate and eustacy in the carbonate factory turnover.

Figure 1.3 (next page). Schematic sequence stratigraphic reconstruction of the Triassic sequences of the Dolomites (after De Zanche et al., 1993; Gianolla et al., 1998; Neri et al., 2007). The stratigraphic interval object of this thesis is highlighted in red.



## ***2. From large scale high-relief platforms to small mounds***

---

The lower portion of the stratigraphic interval object of this study span from the last generation of high-relief Carnian carbonate platforms (Cassian 2 platforms *sensu* De Zanche et al., 1993; Gianolla et al., 1998; Neri et al., 2007; Fig. 1.3) to the basal portion of the Heiligkreutz Fm. (Figs. 1.3; 3.2; lower portion of the Borca Mb. *sensu* Neri et al., 2007; Durrenstein Fm. Lithofacies A, B and C *sensu* Preto and Hinnov, 2003). It was surveyed in the Cortina area, on the southern wall of the Tofana di Rozes and at Dibona Hut (Figs. 3.1; 4.3a; 4.4a).

### **2.1 Lithozones**

#### *Lithozone 1 (L-1)*

The first and oldest lithozone (L-1) of this interval (i.e. the high-relief Cassian 2 carbonate platform *sensu* De Zanche et al., 1993; Fig. 1.3) was observed only in its slope facies at Tofana di Rozes where it constitutes a sort of wedge pinching out toward the East. Its maximum thickness, measured on the western side of the outcrop, is ~ 200 m (see L-1 in Fig. 4.3 c). It is constituted by thick clinostratified beds of completely dolomitized limestone, dipping ~ 20-30° to the East. Megabreccia boulders, with sizes ranging from m to tens of m, were identified. Dolomitization hampers the observation of original sedimentary facies. The correspondent margin and platform top facies are not observable in the Tofane area, but have been described in neighboring outcrops at Falzarego Pass (see Fig. 3.1 for location) where a thinning upward succession of subtidal facies, constituted by fine grained fossiliferous dolomites (bioclasts are gastropods, bivalves and corals), alternate with m-scale tepee structures, pisolitic beds and stromatolites of supratidal origin, thus constituting m- scale peritidal sedimentary cycles (Hardie et al., 1986; Breda et al., 2009). Detailed description on the original facies of this generation of carbonate platforms can only be given on the base of reef boulders fallen in the adjacent basins and preserved from diagenesis that affected the

platforms. In situ carbonate facies are in fact completely dolomitized, with only a few exceptions (e.g., Keim and Schlager, 1999). The facies of the Cassian olistoliths embedded in basinal marls and claystones were described by, e.g., Russo et al. (1997). In these works, the prevailing microbial nature of the lower Carnian Cassian platform was highlighted: for example, the well preserved olistoliths (the so-called Cipit boulders) of Punta Grohmann are dominated by microbialites (Fig. 2.1; Russo et al., 1997).

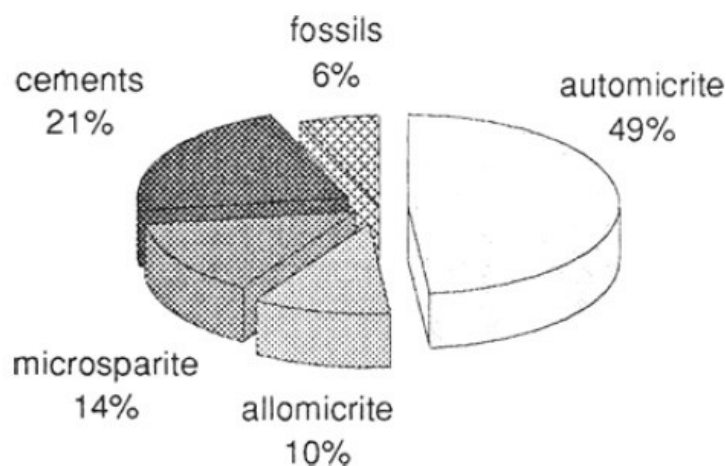


Fig. 2.1. Main components of the Cassian platform (*sensu* De Zanche et al., 1993) derived Cipit boulders determined with point counting (from Russo et al., 1997). The term automicrite is an equivalent of the term microbialite as used in this work.

According to these authors, the amount of skeletal elements (bioclasts) is minor and comprised between 0 % and 10 %. Similar observations were made by Keim and Schlager (1999; 2001) for the coeval Sella Platform. Here the horizontally dm- m- scale bedded platform top bears less than 10 % of skeletal grains, while the amount of microbialites is ~ 40 % (Fig. 2.2). On the m- scale bedded 25-35° inclined slopes the microbialites amount decreases to ~ 30 % (Fig. 2.2) and megabreccias are accumulated in the lower slope. Keim and Schlager (1999) observed that, despite the extensive occurrence of microbialites, no mounds developed on the steep slopes of the Sella platform.

In sum, except for lower slope portion, which is often characterized by megabreccias, the Cassian high-relief platforms were dominated by microbialites and, similarly to all the Middle Triassic carbonate platforms of the Dolomites, developed steep slopes.

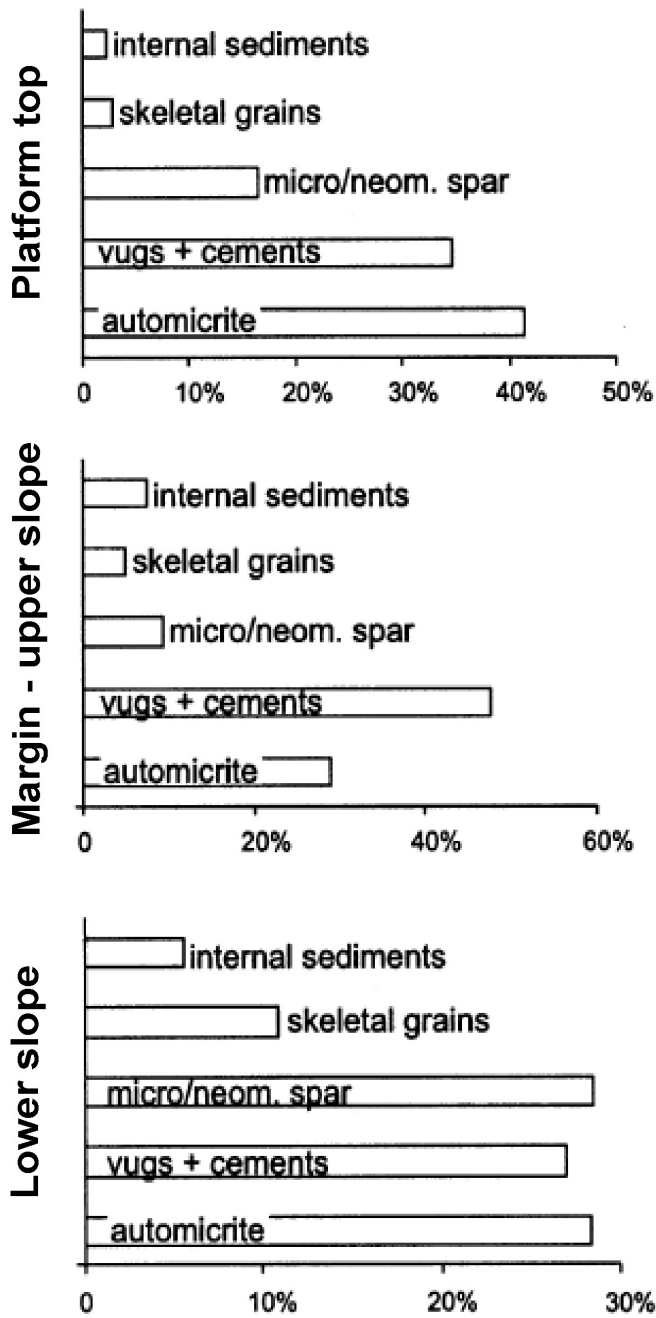


Fig. 2.2. Modal composition of the platform top, margin - upper slope, and lower slope of the Cassian (*sensu* De Zanche et al., 1993) Sella carbonate platform (modified after Keim and Schlager, 2001). Automicrite is used here as a synonym of microbialite.

### *Lithozone 2 (L-2)*

The boundary between the first and the second lithozone (L-2) was observed at Tofana di Rozes and is constituted by a sharp, ~ 20° East dipping by-pass surface which coincides with the top of the last slope clinoform of the Cassian high-relief platform

(boundary between L-1 and L-2 in Fig. 4.3c). A series of lenticular-shaped carbonate bodies (mounds) nucleated on the bypass surface, which are mainly made up of boundstone (Fig. 4.5), and are interlayered and overlapped by dm thick beds of arenaceous grainstones with bivalves, gastropods, peloids, plant remains, and by less common cm- dm- thick beds of shale and calcisiltite (Figs. 4.6; 4.7). In order to compare the mode of precipitation of carbonate of these mounds to that of the lower Carnian high-relief Cassian Platform, a quantitative petrographic digital image analysis of mounds was carried out on 80x50 mm thin sections of eleven particularly well preserved samples coming from the Dibona Hut area (Fig. 2.3). Rock components were classified and divided into eight classes:

- algae (mainly dasycladaceans)
- calcareous sponge (mainly Sphinctozoa e Inozoa)
- corals (mainly scleractinian)
- other metazoans (Hydrozoans and *incertae sedis*)
- skeletal grains (bivalves, gastropods, brachiopods and foraminifers)
- microbialites (stromatolites, leiolites, clotted peloidal micrite, calcimicrobes and agglutinated tubes)
- cement (acicular and radial fibrous cement, sideritic cement)
- cavities (inter o intraparticle, open or filled by debris and/or glauconite and/or cement)

The average contribution of frame builders, like corals (less than 5%) and calcareous sponges (less than 14%), is negligible while microbialites account for ~ 44% of the whole rock volume (Fig. 2.4a). This value rises to ~ 70% if the volume of cements and cavities is subtracted (Fig. 2.4b).

The modal composition of the carbonate mound facies on top of the bypass surface is similar to that observed by Russo et al. (1997) and Keim and Schlager (2001) in the Cassian platforms in terms of proportion of microbialites and skeletal grains. Mounds are the dominant facies at Tofana di Rozes, where they present maximum size (10-100 m), while arenaceous grainstone beds prevail in the Dibona Hut area (Figs. 4.5; 4.6). Here, the average size of mounds decrease to 1-5 m.

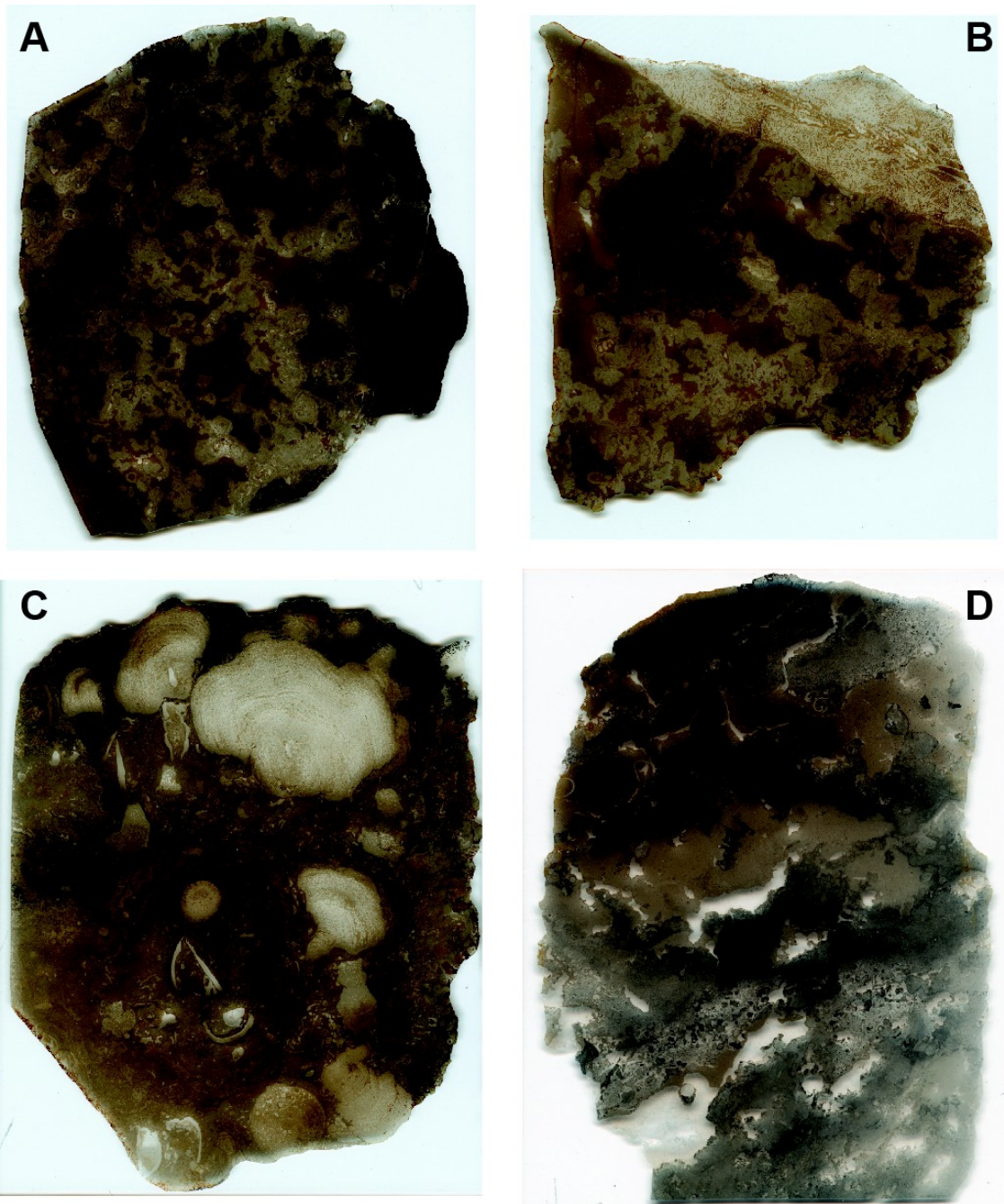


Fig. 2.3. Four 80x50 mm thin sections mounds located near the Dibona Hut. The majority of the rock volume is composed by microbialites. (B) Note in the upper portion of the thin section an Hydrozoan. (C) Note the presence of calcareous sponges and mollusks.

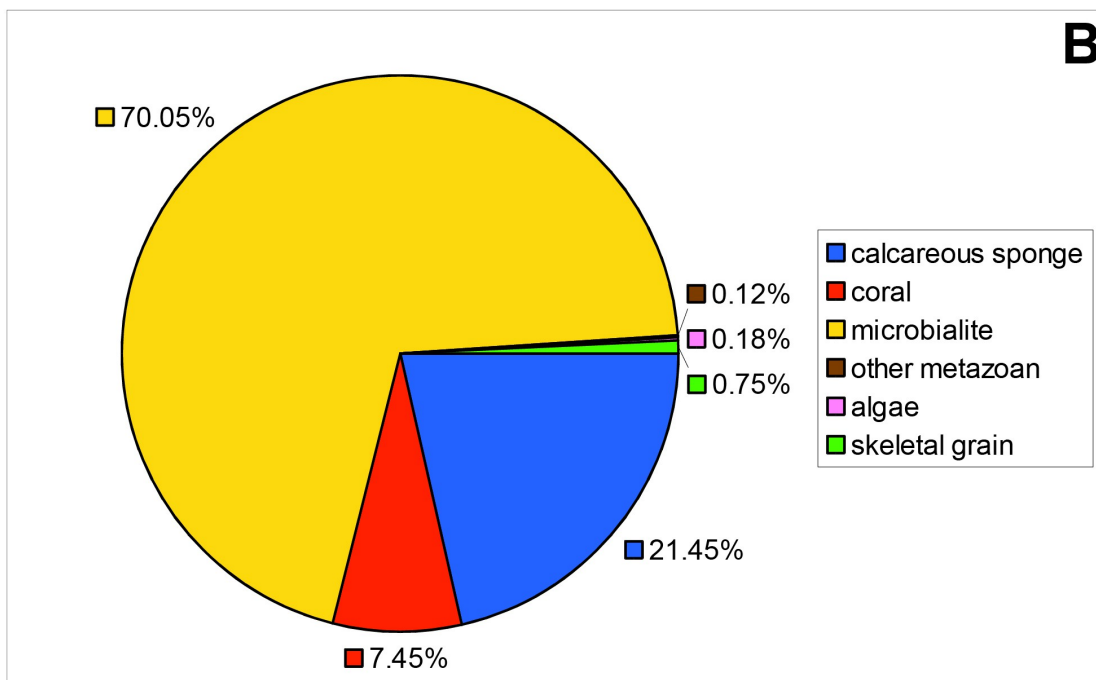
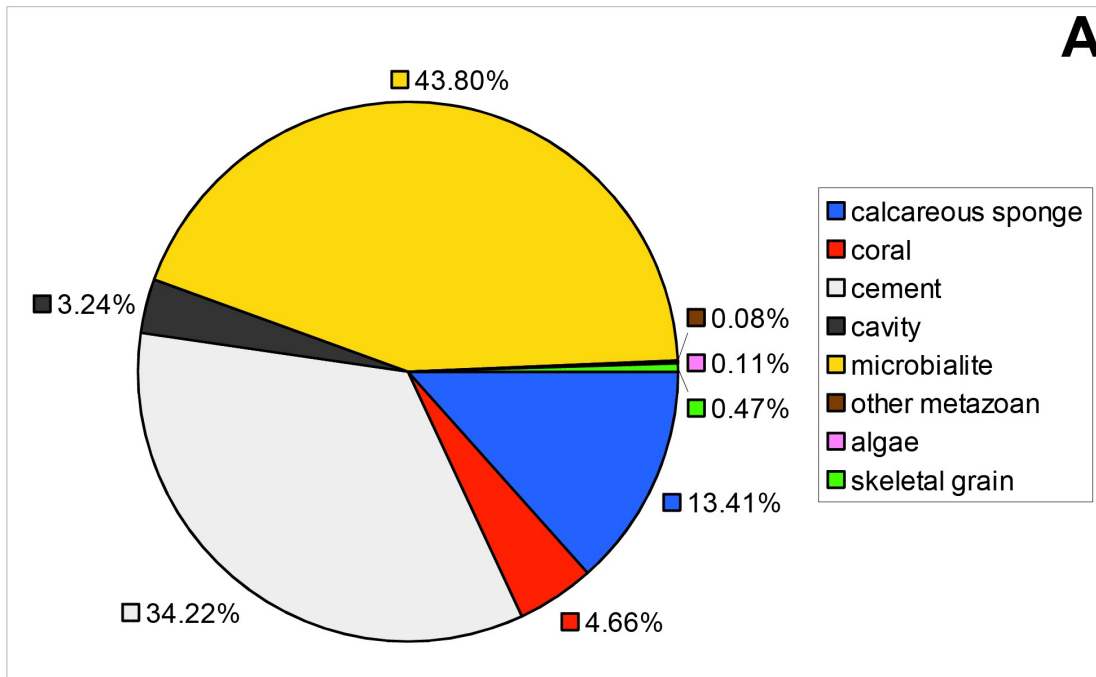


Fig. 2.4. (A) Main components of mounds of the Dibona Hut area as resulting from the digital image analysis. In (B) the contribution of cements and cavities has been subtracted. The majority of the rock volume is constituted by microbialites, while frame builders (corals, sponges and some other metazoans) constitute less than 20%.



Above the mounds, at Dibona Hut this lithozone (L-2) is represented by a ~ 5 m thick sequence of m-scale beds, characterized by highly erosive bases (Fig. 2.5; Preto and Hinnov, 2003; Breda et al., 2009). These beds are mainly made up of mixed carbonate-siliciclastic conglomeratic arenites. The siliciclastic fraction increases upward and is constituted by quartz and volcanic rock fragments, while carbonate grains are mainly bivalves, gastropods and echinoderms. Plant remains and amber droplets are present too. These coarse grained beds are overlain by a ~ 30 m thick clinostratified body (Fig. 2.5; L-2-CLINO in Fig. 4.4c) which dm-scale beds are made up of intensively dolomitized well sorted arenaceous grainstone. Main components are bivalves, gastropods, peloids, plant remains, echinoderms, quartz and volcanic rock fragments, bed joints are plane parallel. Beds are grouped in bedsets which present foresets dipping ~ 25° toward the East (after correction of tectonic tilt) and topsets are stair stepping lowered moving from West toward the East (Fig. 4.4c). The stair stepping surface that cap the clinostratified body is overlapped by a series of tabular horizontal dm to m thick beds of highly dolomitized arenaceous grainstone made up of abundant plant remains, bivalves, gastropods, few echinoderms, peloids, quartz and volcanic rock fragments (L-2-ONLAP in Fig. 4.4c).

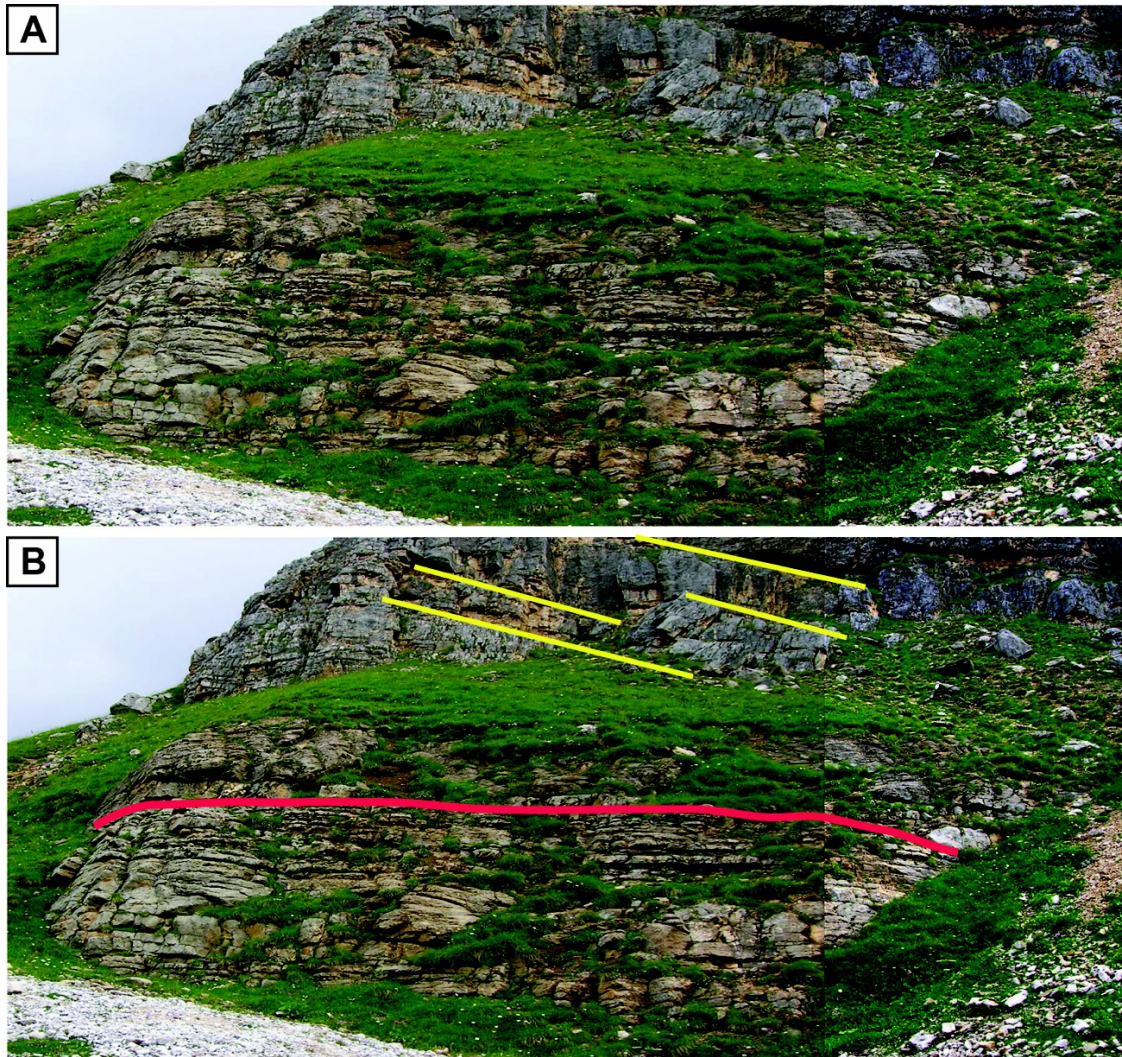


Fig. 2.5. (A) western corner of the Dibona Hut outcrop and (B) its interpretation. Over the red line, thick beds of mixed carbonate-siliciclastic conglomeratic arenites crop out, characterized by erosive base and upward increase in siliciclastics. These beds are overlain by the clinostatified body visible in Fig. 4.4 and which bedding is highlighted in this figure by yellow lines.

# **3. Demise of Late Triassic carbonate platforms triggered the onset of a tide-dominated depositional system in the Dolomites, Northern Italy**

*(published on Sedimentary Geology and cited in Chapter 4 as Gattolin et al., 2013)*

---

## **Abstract**

Facies analysis of the mixed carbonate–siliciclastic Upper Triassic Heiligkreuz Formation in the Cortina–Tofane area (Dolomites, Northern Italy) shows a tide-dominated sedimentary succession developed in a marine strait environment connecting two small sub-basins on the western margin of the Tethys Ocean. Both ebb and flood paleocurrents are preserved and their directions are in agreement with the strait orientation, as inferred from the geographic position of high-relief carbonate platforms in the substrate. Facies and sedimentary structures including planar cross stratification, herringbone cross stratification, flaser to wavy to lenticular bedding and cyclical alternations of mainly oolitic–siliciclastic vs. mainly bioclastic–muddy laminae related to variations of the hydraulic regime have been described and compared with other tide-dominated systems developed in confined marine conditions, and in particular with the Plio-Pleistocene deposits of the central Mediterranean Sea. However, in contrast with all other known cases, this tidal system did not develop in tectonically confined submarine grabens or canyons, but rather in a narrow marine passage between two relict high-relief carbonate platforms.

## **3.1 Introduction**

Tidal systems and tidal deposits are widely studied in the geologic record and especially in the Cenozoic (e.g., Martel et al., 1994; Anastas et al., 1997; Longhitano and Nemeč, 2005; Betzler et al., 2006; Martín et al., 2009; Longhitano et al., 2010; Longhitano, 2011), and in contemporary systems (Beets and van der Spek, 2000; Kraus, 2000;

Anthony, 2002; Reeder and Rankey, 2009; Rankey and Reeder, 2011; Berkeley and Rankey, 2012). The interest in this kind of sedimentary system goes beyond the mere scientific appeal and the beauty of the sedimentary structures which are often preserved. The study of tidal deposits and sequences is the key to understanding the factors and dynamics controlling the evolution of specific coastal environments. In the rock record, tidal deposits often have good reservoir properties. We here present a Late Triassic tidal system the onset of which is unusual in the geological record.

The case study presented here comes from the Dolomites (NE Italy, Fig. 3.1). During the Middle Triassic, this area was characterized by a paleogeography featuring high-relief isolated carbonate platforms and deep (up to thousands of meters depth) inter-platform basins (Bosellini, 1984; Bosellini et al., 2003; Preto et al., 2005). At the end of the early Carnian (Late Triassic, ca. Julian–Tuvanian substages boundary), an important change in depositional geometries is observed and corresponds to the crisis of high-relief carbonate platforms and to a progressive filling of basins (De Zanche et al., 1993; Gianolla et al., 1998; Bosellini et al., 2003; Keim et al., 2006). Some authors suggest that the demise of carbonate platforms was triggered by a climatic event (Simms and Ruffell, 1989; Rigo et al., 2007; Dal Corso et al., 2012), whereas others attribute it to a sea level drop (De Zanche et al., 1993; Gianolla et al., 1998; Bosellini et al., 2003). This work focuses on the sedimentary environment that developed in the aftermath of the carbonate platforms crisis in the Cortina–Tofane area (Fig. 3.1).

The quantity and quality of diagnostic sedimentary structures and the areal distribution of paleocurrents were used to identify the onset of a marine strait dominated by tidal currents. This system developed, exploiting the inherited paleogeography of the basins and the high-relief carbonate platforms. It displays many similarities with some Plio-Pleistocene deposits of the central Mediterranean Sea (Longhitano, 2011). This study shows how the demise of carbonate platforms can create adequate conditions for the onset of a tidal controlled sedimentary environment.

### **3.2 Geological setting**

The Dolomites are located in NE Italy and constitute a ca. 35 km large pop-up structure in the S-vergent portion of the Alpine belt (Castellarin and Doglioni, 1985). Thanks to little tectonic deformation, mostly confined near the bounding faults, and the absence of

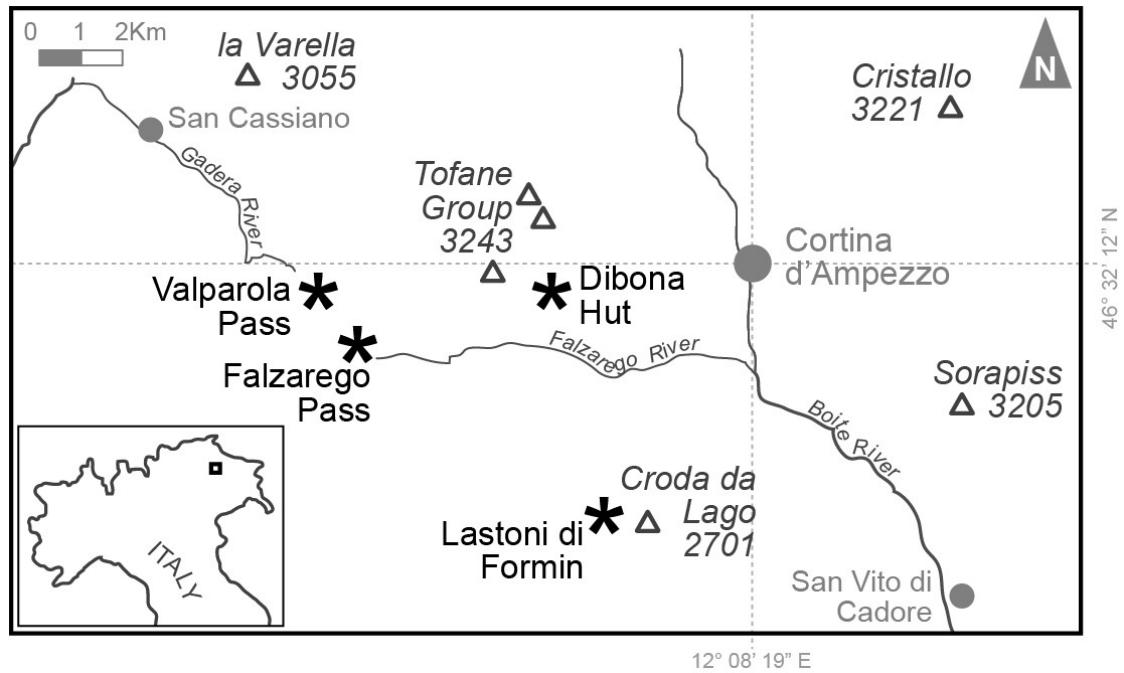


Fig. 3.1. Location and map of the study area. Stars indicate the studied outcrops, triangles the major peaks (elevations in meters) and dots the main towns.

Alpine metamorphism, the Dolomites constitute a type area for the study of Late Permian to Early Jurassic sedimentary and volcanic successions (De Zanche et al., 1993; Gianolla et al., 1998).

In the early Carnian (Late Triassic) the Dolomites were placed in the SW portion of the Tethys Ocean (Ziegler, 1988; Dercourt et al., 1993) at northern tropical latitudes (Muttoni et al., 1996; Broglio Loriga et al., 1999; Flügel, 2002). This area was characterized by a complex paleogeography, featuring high-relief, small (6 km in diameter), mostly isolated carbonate platforms with mainly climbing progradational geometries (Cassian Dolomite; Von Mojsisovics, 1879; Assereto et al., 1977; Bosellini, 1984; Keim and Schlager, 1999, 2001), and deep basins with either carbonate or mixed carbonate–siliciclastic sedimentation (San Cassiano Formation; De Zanche et al., 1993; Keim et al., 2006; Neri et al., 2007). At the end of the early Carnian, a significant change from this complex paleotopography to a flat coastal area is observed. This change is due to three main factors:

1) An important carbonate factory turnover. Highly productive microbial to tropical factories (sensu Schlager, 2003) responsible for carbonate production on high-relief

platforms were substituted by less productive cool-water to tropical (*sensu* Schlager, 2003) factories which produced ramp geometries (Bosellini et al., 2003; Preto and Hinnov, 2003).

2) A conspicuous siliciclastic input was supplied to marginal basins, so that by the end of this period all the topographical complexity inherited from the early Carnian was leveled out by the infilling of the basins.

3) A progressive slowdown of the high subsidence rates that characterize the area during the Middle Triassic and early Carnian.

What provoked the carbonate factory turnover and the increase in siliciclastic input is still under debate. Some authors suggest it is related to a shift to more humid conditions (i.e., the Carnian Pluvial Event; Simms and Ruffell, 1989; Preto et al., 2010; Dal Corso et al., 2012; see also Reingrabener Wende of Schlager and Schöllnberger, 1974) in turn triggered by the eruption of the Wrangellia large igneous province (Furin et al., 2006; Greene et al., 2010). Other authors suggest a sea level drop (De Zanche et al., 1993; Gianolla et al., 1998; Bosellini et al., 2003) that caused subaerial exposure and consequent karstification of the Cassian platforms and the erosion of adjacent highlands. It is likely that both climatic change and sea level fall have to be taken into account.

Our study focuses on the sedimentary system whose deposition immediately follows the shut-off of high-relief carbonate platforms, which is known as the Heiligkreuz Formation (HKS) (Neri et al., 2007; Breda et al., 2009; ex Durrenstein Fm. Auctorum; Fig. 3.2a, b). The age of this formation is well constrained by ammonoid biostratigraphy: it belongs to a short time interval encompassing part of the austriacum and dilleri ammonoid subzones of Mietto and Manfrin (1995), across the early to late Carnian boundary. From a sequence stratigraphic point of view, the HKS represents a complete third-order depositional sequence (Fig. 3.2b; Russo et al., 1991; De Zanche et al., 1993; Gianolla et al., 1998; Neri and Stefani, 1998) deposited during the regressive phase of a long term transgressive–regressive eustatic cycle (Gianolla and Jacquin, 1998). The presence of tidal-current generated sedimentary structures in the HKS is suggested by Bosellini et al. (1978) in particular for the outcrops of the Falzarego Pass (see Fig. 3.1 for location).

The HKS is overlain by the Travenanzes Formation (Fig. 3.2a, b; Neri et al., 2007; Breda and Preto, 2011; ex Raibl Fm. Auctorum) and by the Dolomia Principale (Neri et

al., 2007) which testify to the return to more arid conditions and the start-up of a large (thousands of km wide) epicontinental carbonate platform (De Zanche et al., 2000; Gianolla et al., 2003; Breda and Preto, 2011).

### **3.3 Methods**

Field observations took place in the Cortina–Tofane area at the four localities shown in Fig. 3.1.

At Dibona Hut, a key locality for the study of the Southern Alpine Carnian succession, the stratigraphic section of De Zanche et al. (1993) and Preto and Hinnov (2003) was remeasured for the interval of interest (from 58 to 115 m of Preto and Hinnov, 2003) and detailed sedimentological descriptions were made (Fig. 3.3). Bed by bed facies analysis was used to better define the facies associations and sedimentary environments. Paleocurrent measurements were also taken, and plotted on rose diagrams using Openstereo, an open source software developed by the Instituto de Geociencias—Universidade de Sao Paulo (<http://www.igc.usp.br/index.php?id=openstereo>).

### **3.4 Facies analysis**

The HKS is characterized by pure siliciclastic to pure carbonatic sedimentary facies with grain sizes ranging from clay to pebbles. A total of 18 sedimentary facies was observed. Their sedimentological description and interpretation is provided in Table 3.1. In the study area, and in particular in the Dibona section (Fig. 3.3) four intervals or lithozones can be distinguished. Each is characterized by a specific facies association.

#### **3.4.1. Stratigraphic intervals description and interpretation**

##### *Interval 1*

Description. This interval, ca. 22 m thick, roughly corresponds to the “Lithofacies Association D” of Preto and Hinnov, 2003, and was observed at Dibona Hut where it constitutes the base of the stratigraphic section presented in Fig. 3.3 and, although much more condensed, at Lastoni di Formin. It mainly consists of an alternation of dm to m

thick dolostone beds, rich in peloids, often capped by cm thick stromatolitic lamination, planar fenestrae and sheet cracks (facies F5, Table 3.1, see Fig. 4f of Preto and Hinnov, 2003), and dm calcarenite beds where feeble cross bedding is sporadically visible (facies M1, Table 3.1). Both facies F5 and M1 often display burrows and usually present a rooted cm to dm thick portion at the top of the beds (Fig. 3.4b). In places, over the karstified top of dolostone (F5) or calcarenite beds (M1), clays and shales generally cm, rarely dm thick are present (facies F1, Table 3.1, Fig. 3.4a). These levels are generally dark in color and display the presence of roots, plant fragments, amber, pyrite and coal. Sporadic dm beds of massive arenites (facies M7, Table 3.1) were observed in this interval.

Interpretation. The lower portion of the dolostone beds (F5) reflects a shallow-water subtidal environment and the stromatolitic laminated cap, often displaying planar fenestrae and sheet-cracks, is evidence of supratidal conditions. This observation is confirmed by the widespread presence of roots and hard grounds on the upper portion of dolostone beds. This means that, on the whole, facies F5 represents peritidal cycles. Similar observations can be made at the calcarenite beds (M1) which show the same sedimentary environment of peritidal dolostones (F5), but they represent a more high-energy counterpart. Organic rich clay and shale beds (facies F1) with roots and plant remains indicate episodic soil development (Fig. 3.4a). Observed soils belong to the Histic and Spodic-soil category and developed in a wet climate (Breda et al., 2009). The presence of karst affecting the beds which usually underlie this facies confirms this observation. The widespread presence of coal and pyrite allow these soils to be attributed to a swamp environment. Massive arenites (facies M7) are rare, grains are essentially allochthonous and indicate an extra-basinal origin. The stacking of these four facies suggests a peritidal/paralic environment where facies F5 and M1 represent the normal peritidal cycles. Facies F1 represents the transition to more paralic (quasi-continental) conditions and development of littoral swamps. Beds of massive arenites (M7) suggest rare episodes of increased continental sediment discharge into the basin, probably related to flood events.



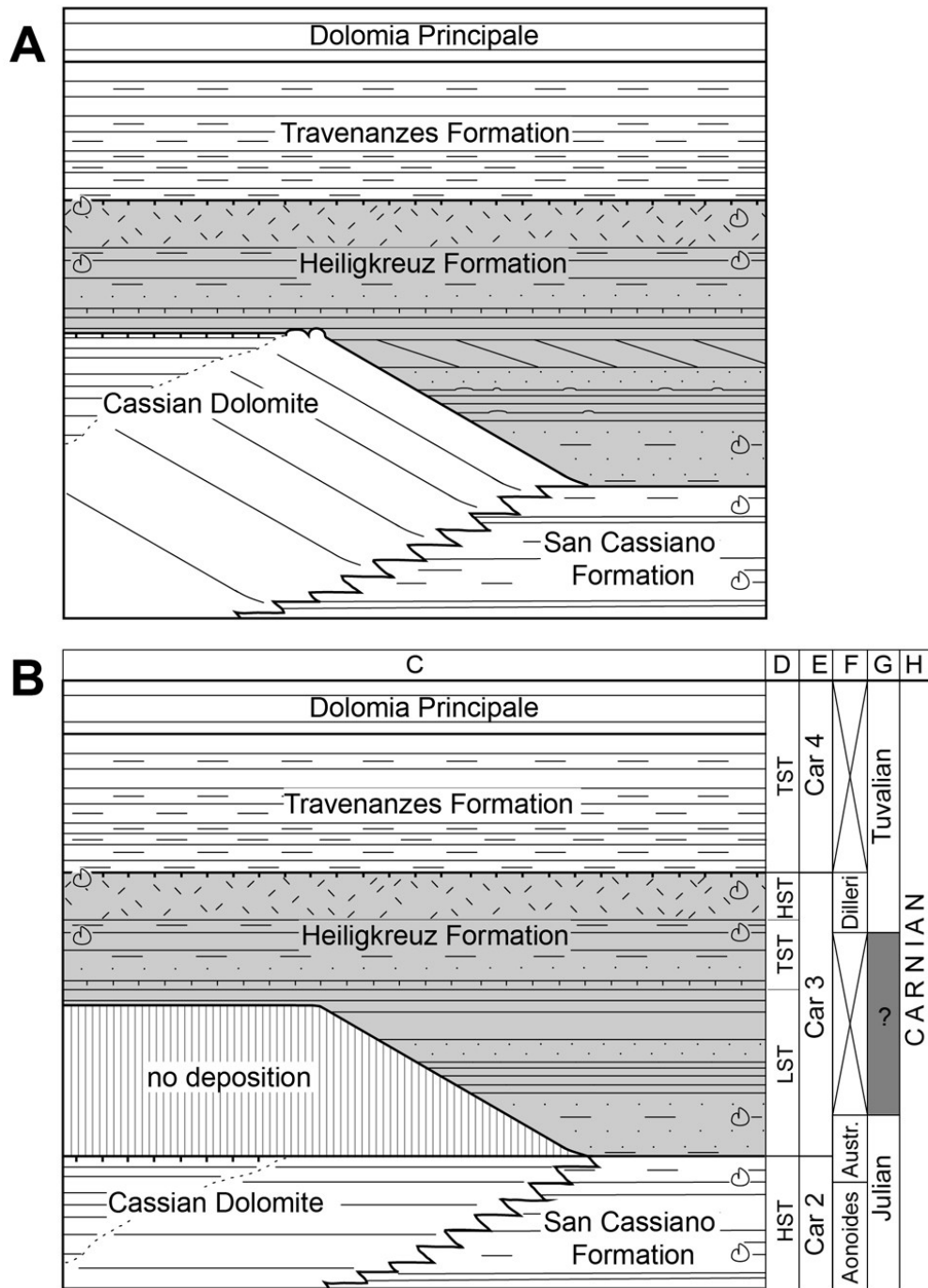


Fig. 3.2. (A) Lithostratigraphic scheme (modified from Preto and Hinnov, 2003) and (B) Wheeler type diagram of the studied interval in the Cortina-Tofane area. The Heiligkreuz Formation, which is the object of this study, is highlighted in gray. The platform settings (to the left) corresponds to Falzarego Pass and Valparola Pass areas, the basinal settings (to the right) corresponds to Dibona Hut area while Lastoni di Formin area should be considered intermediate to these two conditions (see Fig. 3.8 for a three dimensional view of the paleogeography). Ammonoid symbols indicate ammonoid occurrences in the area. (C) Names of lithostratigraphic units (from Neri et al., 2007). (D) System tracts (from De Zanche et al., 1993). (E) Third order depositional sequences (from De Zanche et al., 1993). (F) Ammonoid biostratigraphy (from Mietto and Manfrin, 1995). (G-H) Chronostratigraphy stages and substages.

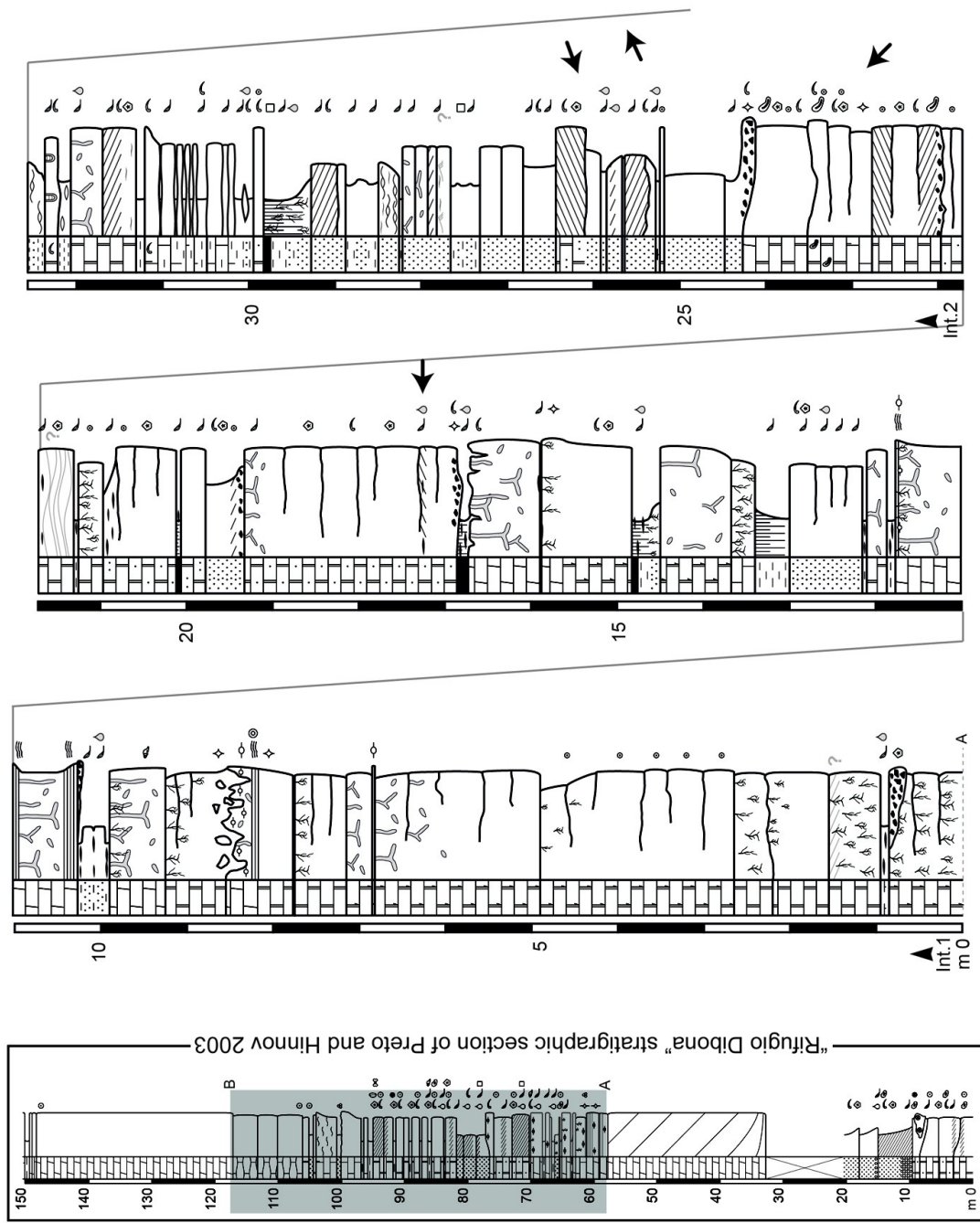


Fig. 3.3. Stratigraphic section measured at Dibona Hut. It corresponds to the interval between 58 and 118 m of the "Rifugio Dibona" section of Preto and Hinnov, 2003 (gray rectangle). Measured paleocurrents are expressed by arrows with azimuthal orientation. Every stratigraphic interval base is marked with its own acronym. Scale in m. Due to outcrop conditions, this stratigraphic section is the result of the merging of two minor stratigraphic sections (the first from 0 to 41 m, the second from 41 to 66 m) 30 meters far from each other.

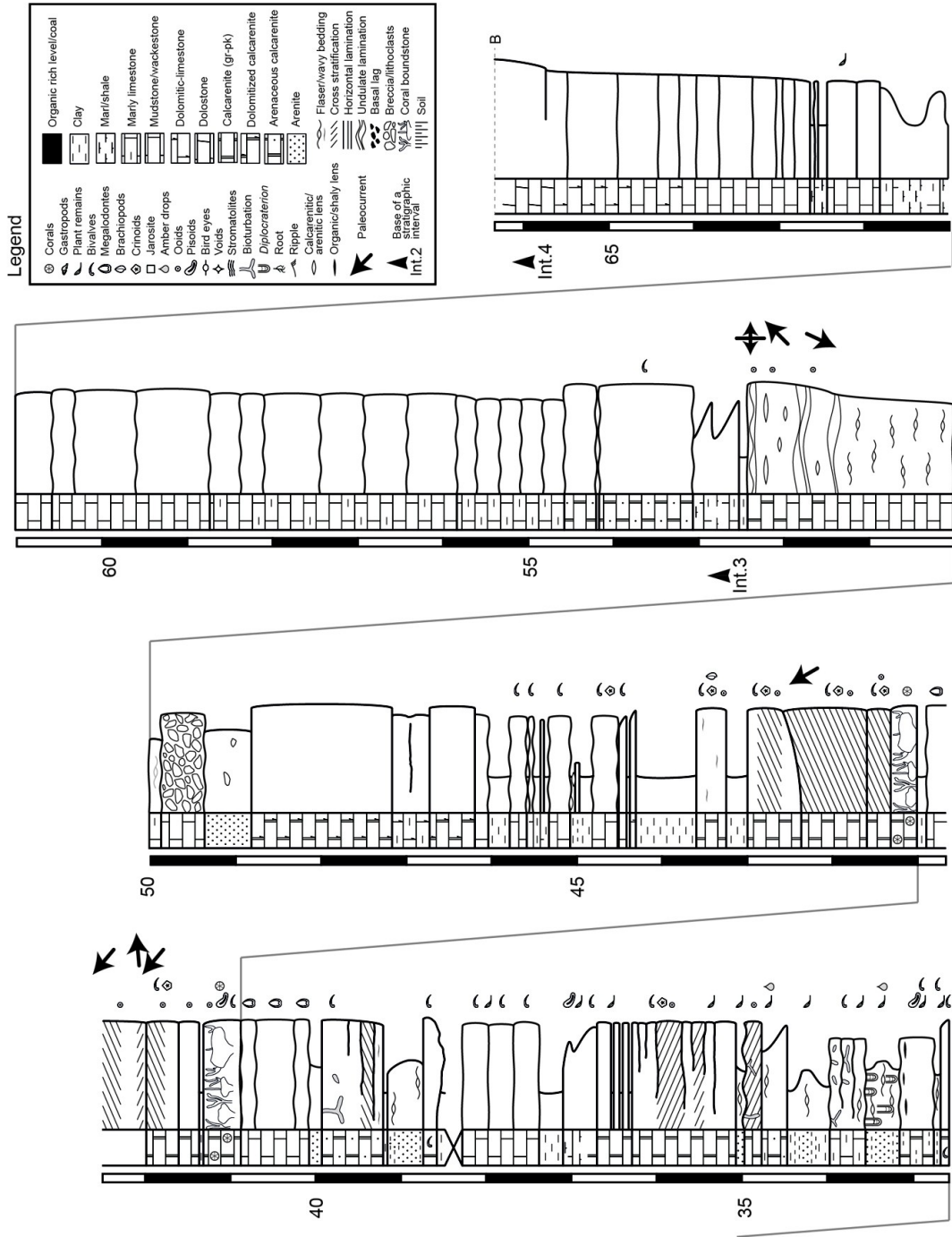


Fig 3.3 (continued).

## *Interval 2*

Description. The second interval observed at Dibona Hut spans 22.0–52.5 m of the stratigraphic section presented in Fig. 3.3. It outcrops also at Lastoni di Formin although more condensed. It roughly corresponds to the sum of “Lithofacies Association E and F” of Preto and Hinnov (2003), and a relatively high number of sedimentary facies are here represented. In the outcrop, the most evident beds, dm thick, are made up of oolitic–bioclastic calcarenites. Siliciclastic grains are less commonly observed (facies M2, Table 3.1). When burrows are not pervasive, this facies displays a well developed planar cross stratification, with an angular to sigmoidal lower contact (Fig. 3.5b, c), generally organized in 10 to 50 cm thick sets, bounded by horizontal bed joints. Sets alternately migrating in two opposing directions can be found. Moreover in some of them an alternation of mm bioclastic (rarely muddy) laminae and cm oolitic (less commonly siliciclastic) laminae is seen (Fig. 3.5d, e). Often bioclastic–muddy laminae are well preserved at the basal contact and tend to disappear upwards (Fig. 3.5f). Dm beds of arenites, made up of quartz, chert, feldspar, lithics and other minor components (facies M3, Table 3.1) are another well represented lithology in this stratigraphic interval. Grain size ranges from fine to medium sands, rarely up to granules and sporadically cementation is poor. Also in this facies, when the presence of burrows is moderate, it is possible to notice a cm- to dm-scale cross stratification, at times migrating in two opposing directions. Intermediate facies between M2 and M3 were locally observed. Cm thick levels of grainstones–packstones essentially made up of imbricated bivalve shells (Coquina, facies M6, Table 3.1) can be found. Generally they occur at the base of a bed and pass upwards towards facies M2 and M3. Dm beds of calcsiltites to calcarenites with mm mud interbeds, characterized by a widespread presence of cm ripples (facies FM1, Table 3.1) are common. The main constituent of this facies is peloids but other siliciclastic and carbonatic components can be observed. The general structure of this facies range from a flaser-bedding to a wavy-bedding as a function of variable mud content (Fig. 3.4d). Burrows and in particular *Diplocraterion* traces are common (Fig. 3.4e). In outcrop, when this facies is particularly poor in mud content and rich in peloids, it can exhibit an aspect similar to a nodular mudstone (Fig. 3.4d). Dark shales and siltites rich in plant remains constitute some cm, rarely dm, beds (facies F6, Table 3.1). Lenticular bedding is locally induced by the presence of lenses or

isolated ripples made up of more competent calcarenites (Fig. 3.4c). Facies from white carbonatic wackestone to gray marly limestone, not showing evident sedimentary structures, generally constitute dm beds (facies F4, Table 3.1). Here burrows are common and associated with nodular bed joints. Dm beds of massive mixed carbonate–siliciclastic to pure siliciclastic arenites (facies M7, Table 3.1) were observed. One of these in particular exhibits a coarse sand grain size and contains cm rip-up clasts of limestone (at 49 m on Fig. 3.3). Megalodon bafflestone facies (B1, Table 3.1), coral boundstone facies (B2, Table 3.1), oncoidal floatstone facies (L1, Table 3.1), flat pebble breccia facies (L2, Table 3.1) and rooted dark clays/siltites (facies F1, Table 3.1) occur.

*Interpretation.* The most interesting aspect of this stratigraphic interval is the widespread presence of diagnostic tidal sedimentary structures. The planar cross stratification (Fig. 3.5b, c), alternately migrating in two opposing directions (facies M2) is clear evidence of a tide dominated subtidal setting. Alternation of mainly oolitic–siliciclastic laminae and mainly bioclastic laminae is probably linked to the variation in the hydraulic section and hence the velocity of tidal currents (Fig. 3.5d, e; Longhitano et al., 2010; Longhitano, 2011). The fact that bioclastic–muddy laminae are often eroded in their upper part seems to testify to the alternation between different energy currents and thus the development of erosion during higher velocity current periods (Fig. 3.5f). In facies M3, the more homogeneous composition of grains led to the development of less clear planar cross stratification and the absence of stacked laminae. A tidal dominated environment is highlighted also by facies FM1 and F6 (Fig. 3.4c, d). They both present ripples generally made up of calcarenites interbedded with muddy/shaly levels. Ripples reflect tidal currents while less competent interbeds represent suspension fallout during slack water intervals and/or deposition under lower energy tidal currents. Wackestones to marly limestones (facies F4, Table 3.1) indicate episodes of deposition of parautochthonous carbonate. This can be possible only in a low energy setting such as areas not reached by waves or tidal currents. The bed made up of coral boundstone (facies B2, Table 3.1) indicates the growth of a biostrome in photic, clean water, normal salinity conditions, in a niche protected from tidal currents. Monospecific mollusc association (facies B1, Table 3.1) with a high population density is typical of marine environments stressed by salinity variations or by current action or, more probably, by turbidity pulses (Dalrymple and Choi, 2007). Both oncoidal floatstone (facies L1, Table

3.1) and flat pebble breccia (facies L2, Fig. 3.5a) indicate a high energy subtidal environment, and in particular are attributed to the presence of tidal channels. Levels of coquina (facies M6, Table 3.1) indicate bivalve concentrations due to sporadic high energy events. As in interval 1, beds of massive arenites (facies M7, Table 3.1) show an increased continental sediment supply related to flood events. One episode of prolonged subaerial exposure is testified by the presence of a well developed soil (facies F1, Table 3.1) at 29.5 m (Fig. 3.3).

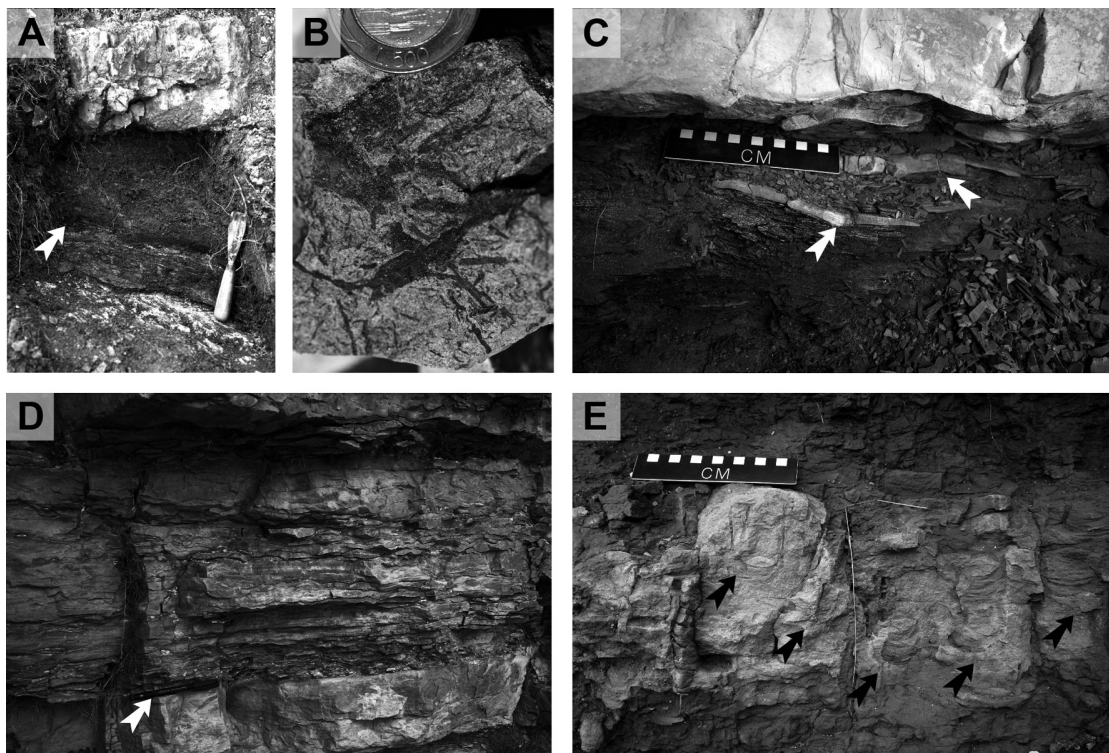


Fig. 3.4. Facies of the Heiligkreuz Fm. observed at Dibona Hut. (A) Paleosol (facies F1; interval 1). The white arrow indicates a coal-rich horizon. (B) Roots at the top of a calcarenite bed (facies M1, interval 1). (C) Lenticular bedded dark shale level (facies F6; interval 2). White arrows indicate isolated calcarenite ripples. (D) Flaser bedding in fine grained calcarenite (facies FM1, interval 2). Pencil (white arrow) as scale. (E) Highly bioturbated calcsiltites to calcarenite facies (facies FM1, interval 2). Black arrows indicate *Diplocraterion* traces.

### *Interval 3*

Description. This stratigraphic interval is comprised between 52.5 and 65.5 m of the Dibona Hut section (Fig. 3.3). It corresponds to the “Lithofacies Association G” of Preto and Hinnov (2003). It mainly consists of a stacking of dm to m thick beds of limestones and marly limestones, often affected by dolomitization (facies F2, Table 3.1). Bed joints are generally nodular. From these levels some ammonoids were collected in the Col dei Bos area (between Dibona Hut and Valparola Pass in Fig. 3.1). Rare cm to dm beds of dark gray marls, rich in Chondrites (see Fig. 4m of Preto and Hinnov, 2003) and locally with pyrite nodules (facies F3, Table 3.1) were observed.

Interpretation. The nodular bed joints, absence of tractional sedimentary structures and evidence for subaerial exposure, together with fossil content (ammonoids), suggest a completely subtidal origin for this interval, deeper than the one that produced interval 2. Marl facies (F3, Table 3.1) testifies to episodes of increased clay input and, as highlighted by the presence of pyrite nodules and Chondrites traces, for low sea bottom oxygenation.

### *Interval 4*

Description. This interval is found above 65.5 m in the Dibona Hut stratigraphic section (Fig. 3.3, see the “Rifugio Dibona” stratigraphic section of Preto and Hinnov, 2003 to observe the entire thickness of this unit), but the most interesting observations of this interval are found at Lastoni di Formin, Falzarego Pass and Valparola Pass. At Dibona Hut it consists of ca. 30 m of massive dolostone where ooids are rarely recognizable (facies M4, Table 3.1) and sedimentary structures are completely obliterated by dolomitization. At Falzarego Pass and Valparola Pass, this interval is constituted by dm to m beds of mixed oolitic–siliciclastic sandstones displaying dm- to m-scale cross stratification, often planar (facies M5, Table 3.1; Figs. 3.6, 3.7d, e, f), and dm-scale herringbone cross stratification with nearly opposite foresets. At Lastoni di Formin the lower portion of this interval shows facies similar to Falzarego Pass and Valparola Pass (i.e., facies M5, Table 3.1), that rapidly grade into dm to m beds of cross stratified dolostone (facies M4, Table 3.1). Here, dolomitization did not erase sedimentary

structures that are similar to those of facies M5 (Table 3.1; Fig. 3.7b). Moreover, siliciclastic grains aligned along bedding planes are often visible (Fig. 3.7a).



Fig. 3.5. Facies of the Heiligkreuz Fm. observed at Dibona Hut. (A) Flat pebble breccia made up of unconsolidated rip-up clasts (facies L2; interval 2). Both lithoclasts and matrix are constituted of lime-mudstone (B) Calcarenite bed displaying well developed planar cross stratification with an angular basal contact (facies M2; interval 2). White dashed line highlights the stratification. (C) Calcarenite bed displaying well developed planar cross stratification with a tangential basal contact (facies M2; interval 2). Note the yellowish bioclastic-muddy interbeds. (D) Calcarenite bed displaying alternation between mainly oolitic laminae and mainly bioclastic laminae (facies M2; interval 2). Black arrows indicate whitish bioclastic levels. (E) Calcarenite bed displaying alternation between mainly oolitic-siliciclastic laminae and mainly bioclastic-muddy laminae (facies M2; interval 2). Black arrows indicate yellowish bioclastic-muddy levels. (F) Calcarenite bed displaying alternation between mainly oolitic-siliciclastic laminae and mainly muddy laminae (facies M2; interval 2). The black arrow indicates a yellowish muddy lamina which decreases in thickness towards the upper contact.



Interpretation. Cross stratified dolostones (facies M4, Table 3.1) and cross stratified sandstones (facies M5, Table 3.1) reflect similar mechanisms of sediment transport and deposition, water depth, and sedimentary environment. The main differences between the two facies are due to the nature of the sediment: mainly carbonate grains (probably ooids) in M4, mixed carbonate (ooids) and siliciclastic grains in M5. At Lastoni di Formin, facies M5 rapidly grades into facies M4. Moreover a small siliciclastic input during facies M4 deposition is still testified by the presence of siliciclastic grains aligned along bedding planes, highlighting cross-lamination (Fig. 3.7a). Both facies M4 and M5 are medium grained, well sorted and free of muddy matrix or fine clastic intercalations. Both exhibit the absence of subaerial exposure surfaces and the presence of the same sedimentary structures such as planar cross stratification and hummocky cross stratification (Fig. 3.7b–f).

Similarly to interval 2, interval 4 is characterized by subtidal environments, dominated by tidal currents. In interval 4 evidences of subaerial exposure are totally absent.

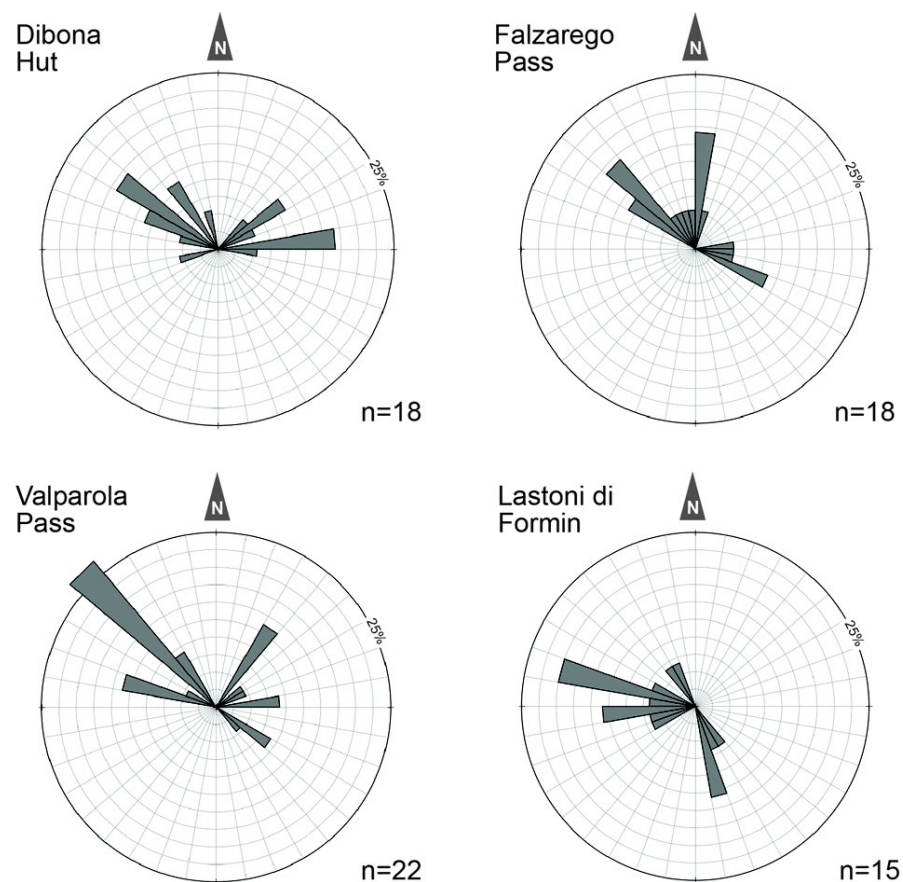


Fig. 3.6. Rose diagram displaying paleocurrents dispersion at studied sites.

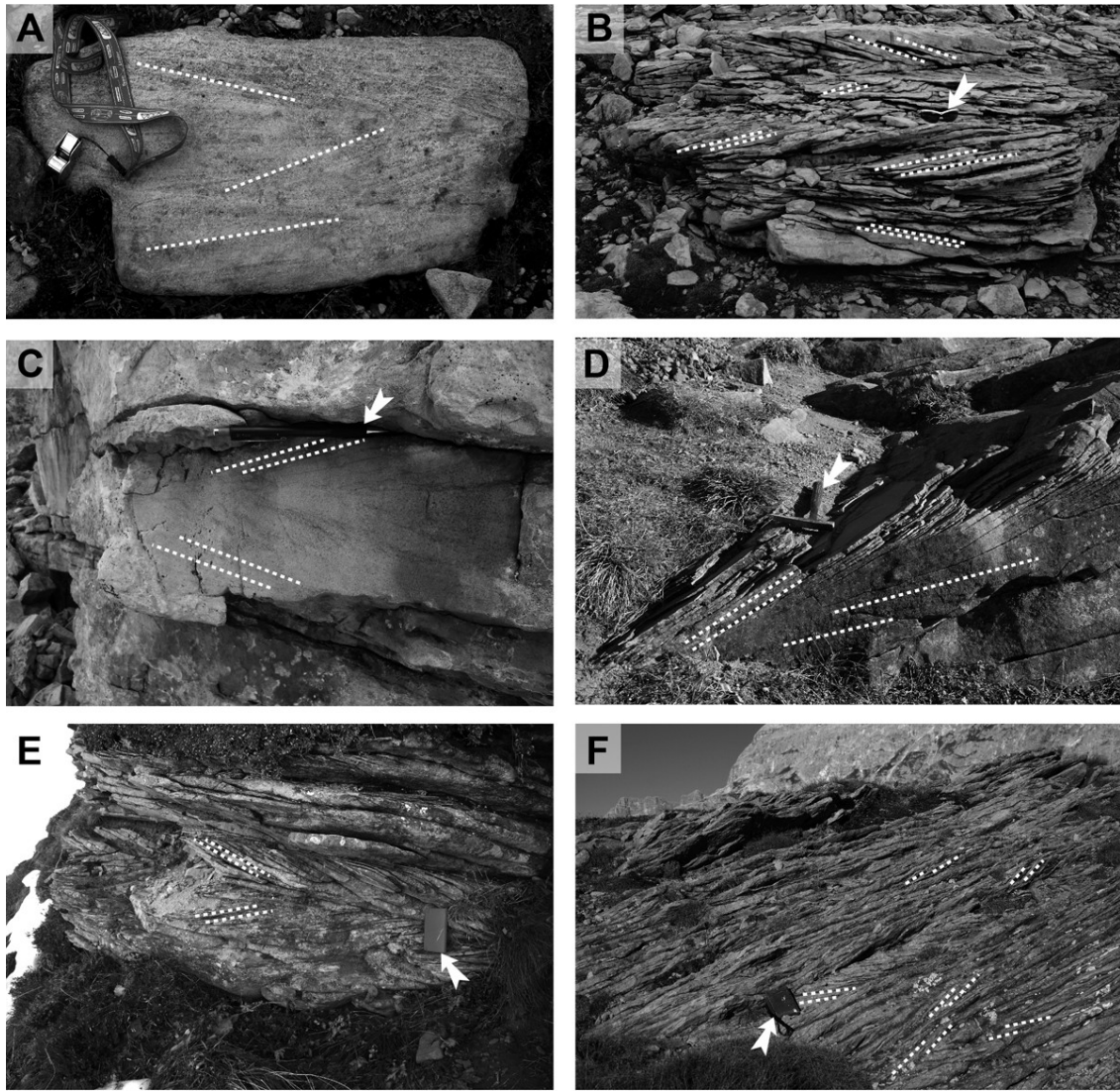


Fig. 3.7. Facies of the Heiligkreuz Fm. observed in the study area. White dashed lines highlight the most evident stratifications. (A) Cross stratified arenaceous dolostone from Lastoni di Formin with siliciclastic grains aligned along bedding planes (facies M4; interval 4). (B) Dolostones from Lastoni di Formin characterized by planar stratification dipping in opposing directions (facies M4; interval 4). Sunglasses indicated by the white arrow as scale. (C) Dolostone bed from Lastoni di Formin displaying herringbone cross stratification (facies M4; interval 4). Some siliciclastic grains are aligned along bedding planes. Pencil indicated by the white arrow as scale. (D) Sandstones from Falzarego Pass displaying planar cross stratification dipping on opposing directions (facies M5; interval 4). Hammer indicated by the white arrow as scale. (E) Sandstones from Valparola Pass displaying herringbone cross stratification (facies M5; interval 4). Notebook indicated by the white arrow as scale. (F) Sandstones from Valparola Pass characterized by cross (often planar) stratification dipping in opposing directions (facies M5; interval 4). Compass indicated by the white arrow as scale.

Table 3.1 (next pages). Summary of facies classifications and interpretations for the studied outcrop of the Cortina area. The prefix of the facies code means: F = dominance of fine grain sizes (<0.063 mm), M = dominance of medium grain sizes (0.063–2 mm), L = dominance of large grain sizes (>2 mm), B = dominance of boundstone facies.

Facies code	Sedimentary facies and structures	Interpretation
<b>Low to mid energy facies</b>		
F1	Clays, shales and arenaceous shales. Black to red. Karst can affect underlying beds. Roots, plant remains, amber, pyrite are often present such as coal on the top of the beds. Rare Jarosite. Cm, rarely dm beds.	Histic and spodic paleosols (Fig. 3.4a) related to subaerial exposure in a wet climate or to a swamp environment.
F2	Dolomitic limestones. Generally dolomitized marly limestones. Gray to dark gray, often with nodular joints. Rare bioclasts and plants fragments. Ammonoids were found at Col dei Bos (between Dibona Hut and Valparola Pass in Fig. 1.1). Dm to m beds.	Low-energy subtidal environment.
F3	Marls with <i>Chondrites</i> (see Fig. 4m of Preto and Hinnov 2003). Dark gray. Pellets have been observed and pyrite nodules. Cm to dm beds.	Same as F2 but developed with a considerable input of clay.
F4	Wackestones to marly limestones. White to gray. Bivalves, including ostreids, and plant remains. Echinoderms and agglutinate foraminifers are rare. Burrows often associated to nodular bed joints. An hard ground at the top of a bed was observed. Dm beds.	Low energy setting. Marly limestones facies indicate an appreciable continental input while wackestones indicate more clean water conditions.
F5	Peritidal dolostones. Peloids and lumps, vadose pisoids are less common. Plant fragments and gastropods. Stromatolitic lamination, planar fenestrae, sheet cracks on the top. Widespread presence of borrows, possible presence of roots and hard grounds on the upper portion of the beds (see Fig. 4f of Preto and Hinnov 2003). Dm beds.	Peritidal cycles. The peloidal portion is expression of subtidal environment. Stromatolites, roots, sheet cracks, and fenestrae are expression of supratidal conditions.
F6	Heterolithic shales and siltites. Dark gray. Plant fragments. Locally lenticular bedding due to the presence of cm lenses/isolated ripples of more competent calcarenite (Fig. 3.4c). Cm, rarely dm beds.	Lenses/isolated ripples are expression of sediment migration under peak tidal currents velocity while mud represent suspension fallout during slack water.
FM1	Calcsiltites to calcarenites with mm mud interbeds. Peloids. Other carbonatic and siliciclastic components can be observed. Pervasive presence of ripples with rectilinear crests (~1 cm high, ~ 5 cm wavelength). From flaser (Fig. 3.4d) to wavy bedding in relation to mud content. Burrows including <i>Diplo craterion</i> traces (Fig. 3.4e). Dm beds.	Similar to F6 but high energy tidal currents. <i>Diplo craterion</i> traces confirm the presence of high energy currents (Seilacher 2007).
B1	<i>Megalodon</i> bafflestones. <i>Megalodon</i> (cm-bivalves) in life position, matrix is mudstone. Nodular bed joints. On the top of the bed bivalves dissolution can be observed. One dm bed.	Monospecific molluscs association grown in an environment stressed by salinity variations or by currents action or, more probably, turbidity pulses.
B2	Coral boundstone. Corals in life position. Matrix is a grainstone-rudstone made up of bivalves, pisoids and oolites. One dm bed.	Biostrome. Indicates photic, clean water, normal salinity conditions.
<b>Mid to high energy facies</b>		
L1	Oncoidal floatstones. Matrix is constituted by oolites and bioclasts. Dm beds.	High energy subtidal sedimentation, probably in a tidal channel.
L2	Flat pebble breccias, made up of unconsolidated rip	High-energy subtidal sedimentation,

	up clasts with dimensions ranging between 2 mm and 5 cm. Clasts are spherical-elliptical in shape with the longest axis lying horizontally. Lithoclasts and matrix are constituted of lime-mudstone (Fig. 3.5a). Dm beds.	probably in a tidal channel.
M1	Peritidal calcarenites, from peloidal–bioclastic packstones to oolitic-bioclastic grainstones. Bioclasts are bivalves, gastropods, echinoderms and plant fragments plus rare amber. Roots can be observed at the beds top (Fig. 3.4b). Sporadic cm-dm scale cross stratification. Dm beds.	Peritidal cycles. The lower portion of the beds is expression of a subtidal environment, roots on the upper portion indicates supratidal conditions.
M2	Oolitic–bioclastic grainstones with intraclasts and extraclasts. Echinoderms, bivalves, gastropods, peloids, plant fragments, marine and terrestrial vertebrate bones and teeth occur. Planar cross stratification with basal contact from angular to tangential (Figs. 3.5b, 3.5c), organized in 10–50 cm thick sets, bounded by horizontal bed joints, and locally alternatively migrating in two opposing directions. An alternation of mm bioclastic (rarely muddy) laminae and cm oolitic (less commonly siliciclastic) laminae can be observed (Figs. 3.5d, 3.5e). Bioclastic-muddy laminae are seen near the basal contact and tend to vanish upwards (Fig. 3.5f). Burrows occurs. Dm beds.	Deposition of tidal dunes in a subtidal high-energy setting. Each bed testifies one preferential current verse (ebb or flood). Alternation between mainly bioclastic laminae and mainly oolitic laminae is due to variation in the velocity of tidal currents (Longhitano et al., 2010; Longhitano 2011).
M3	Cross bedded arenites. Fine to medium grained, locally up to granules size. Quartz, chert, feldspars, and lithics, rare allochemis. Plant fragments, amber. Locally cm- to dm-scale cross stratification migrating in two opposing directions. Burrows occurs. Dm beds.	Similar to M2 but the more homogeneous composition of laminae lead to the development of less clear planar cross bedding.
M4	Cross stratified dolostones. Ooids are rarely recognizable. Siliciclastic grains may be present aligned along bedding planes (Fig. 3.7a). Cross (often planar) stratification and herringbone cross stratification (h =10–50 cm) with opposite foresets (Figs. 3.7b, 3.7c). Dm to m beds.	Subtidal migration of ooids under high-energy, ebb and flood tidal currents. They represent a stacking of tidal dunes.
M5	Cross stratified sandstones. Medium grained, made up of siliciclastic grains and ooids. Dm- to m-scale cross (often planar) stratification, herringbone cross stratification (h =10–50 cm) with opposite foresets (Figs. 3.7d, 3.7e, 3.7f). Dm to m beds.	As M4 but different sediment source.
<b>Highest energy facies</b>		
M6	Coquinas. Grainstone-packstone, rarely wackestone-floatstone, made up of imbricated bivalve shells. Occur in cm lags at the base of beds, and pass with a gap in intermediate grain sizes, towards arenites-calcarenites facies described above (M2 and M3).	Bivalves concentration due to sporadic high energy events.
M7	Massive arenites. Dark gray to green. From fine to coarse grained, made up of quartz, chert, lithics and feldspars; plants remain, amber and crinoids can occur. In one level rip up clasts made of limestone were found. Generally cm to dm beds.	Episodes of continental sediment supply. Probably produced by sediment gravity flows related to flood events.

## 3.5. Discussion

### 3.5.1. Paleoenvironment and paleogeography

Discussion is mainly concentrated on stratigraphic intervals 2 and 4 where sedimentary structures point clearly to tidal depositional processes and consequently to a tide-dominated sedimentary environment. The observed planar cross stratified deposits that sometimes display an alternation between bioclastic and siliciclastic laminae (Figs. 3.5b–e, 3.7b, d, f), and, as already observed by Bosellini et al. (1978), the presence of herringbone cross stratification (Fig. 3.7c, e), are clear evidence of a tide-dominated environment. In interval 2 this is strengthened by the contemporaneous presence of flaser to wavy to lenticular bedding (Fig. 4c, d) and tidal channel deposits. Paleocurrent measurements are in agreement with those measured by Bosellini et al. (1978) (their Fig. 8), and highlight the coexistence of two principal directions of sediment transport that represent ebb and flood currents (Fig. 3.6). These paleocurrent directions are not perfectly collinear (Fig. 3.6); the angle between the ebb and flood paleocurrent directions is ca. 150°. This is not surprising and has been noted in several tidal dominated environments (Blondeaux et al., 1982; D'alpaos and Martini, 2005; Rankey and Reeder, 2011). This may reflect mutually evasive channels (Dalrymple and Choi, 2007) or differential lateral confinement (Rankey and Reeder, 2011).

In the geological and present-day sedimentary record, structures as those described above are observed in two tide-dominated environments: straits/canyons (Longhitano and Nemeč, 2005; Reeder and Rankey, 2009; Shanmugam et al., 2009; Longhitano et al., 2010, 2012a; Longhitano, 2011) and embayed gulfs (Tape et al., 2003; Davis, 2006; Dalrymple and Choi, 2007). The presence of a marine strait can act as a funnel for tide induced water mass movements, and thus to development of appreciable tidal currents in microtidal settings (Longhitano and Nemeč, 2005; Longhitano, 2011; Longhitano et al., 2012b). Bays and gulfs with adequate shape, dimension and depth can produce such tide amplification (Pugh, 1987; Sztanò and De Boer, 1995; Dalrymple and Choi, 2007). Field observations across the Cortina–Tofane area suggest that our case study is an E–W elongated marine paleostrait, bordered on the northern and on the southern sides by two relict high-relief carbonate platforms, the Lagazuoi/Tofane Cassian platform to the north, and Lastoni di Formin/Averau–Nuvolau Cassian platform to the south (Figs. 3.1,

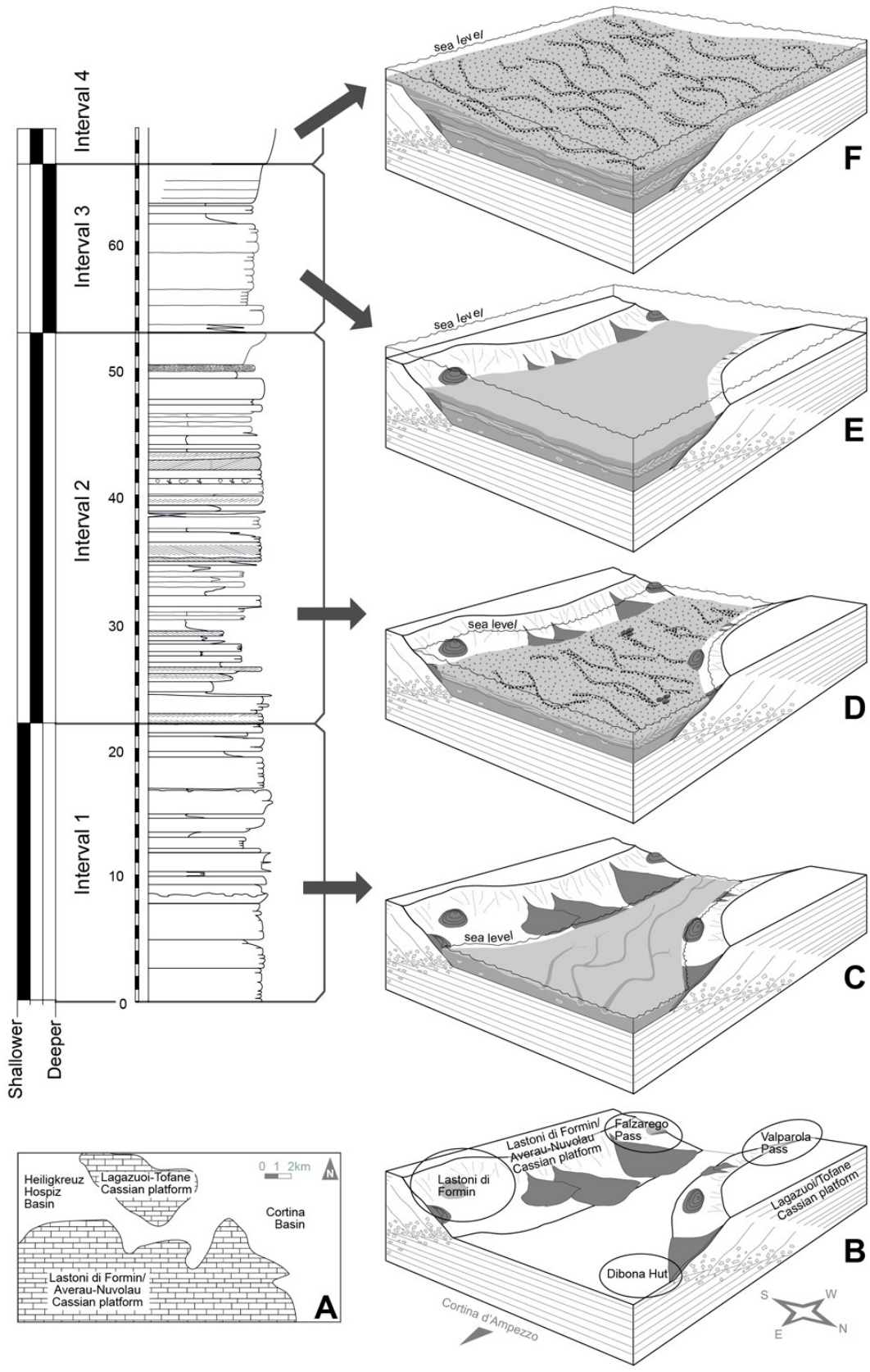
3.8; Neri et al., 2007). Across the Dolomites region in the Carnian there existed a basinal area to the east, and a complex coastline, roughly trending N–S, to the west (Breda et al., 2009; Gianolla et al., 2011). Within this coastline, the paleostrait described in this paper was connecting a basin characterized by open marine, fairly deep-water successions to the east (the Cortina Basin of Neri et al., 2007), with another basin which was subjected to restriction, and thus to deposition of poorly oxygenated facies with an oligotypic, eurihaline fossil association, to the west (the Heiligkreuz Hospiz Basin of Keim et al., 2006; Fig. 3.8a). We thus suggest that the flood current was flowing westward, and produced the bedforms dipping 300–330° (Fig. 3.6). The ebb current produced the bedforms dipping to the east. The siliciclastic sedimentary input was preferentially from the south (Hofmann, 1972; Siorpaes and Gianolla, 1991; Breda et al., 2009) while the carbonate input (i.e. mainly oolitic) was probably parautochthonous, from the adjacent shallow marine areas.

### 3.5.2. Relative sea level changes

In agreement with De Zanche et al. (1993) and Preto and Hinnov (2003), the facies associations' superposition in the Cortina–Tofane area can be interpreted as the sedimentary response to a transgressive–regressive cycle. Stratigraphic interval 1 shows a peritidal–paralic environment and thus the shallowest observed conditions (Fig. 3.8c). This lithozone was found at Dibona Hut which occupies the most basinal position with respect to the other outcrops presented here (Fig. 3.8b) and, although much more condensed, at Lastoni di Formin. During deposition of interval 1, Falzarego Pass and Valparola Pass were probably emerged or at least subjected to sediment bypass (Fig. 3.8c). Interval 2 displays a slightly deeper (mainly subtidal) sedimentary environment. Taking into account the paleogeography of the area it reveals a rise of relative sea-level (Fig. 3.8d). Due to bad outcrop conditions and the presence of thrust faults, it was not possible to verify this interval at Falzarego Pass and Valparola Pass. An appreciable rise of relative sea level is visible in the third stratigraphic interval (Fig. 3.8e). The fine grained facies lacking sedimentary structures (Dibona Hut) but with a fossil content (ammonoids from Col dei Bos) suggests that this interval is the expression of the maximum marine ingressions (Fig. 3.8e). Being in a more proximal position with respect to Dibona Hut, this facies association is almost absent at Lastoni di Formin where

interval 2 is directly overlain by interval 4. Interval 4 was observed across the whole study area. The only difference between different outcrops is the relative abundance of facies M4 vs. M5, i.e., a difference only in terms of the type of supplied sediment and not in sedimentary processes. Observed sedimentary structures point to a tide-dominated environment while the homogeneity of sediments and sedimentary structures suggests a similar water depth for each studied site (Fig. 3.8f). Although completely subtidal, this suggests a return to shallower marine conditions with respect to interval 3 (a marine regressive phase). The absence of the fine grained siliciclastic fraction (mud) indicates that emerged high lands had nearly disappeared at the time of deposition of interval 4.

Fig. 3.8 (next page). Paleogeography of the Cortina–Tofane area and response of the sedimentary environment to the relative sea level changes during deposition of the Heiligkreuz Fm. The stratigraphic column to the left is a simplification of that shown in Fig. 3.3. (A) Paleogeographic map of the study area (Breda et al., 2009, modified). (B–F) Evolution of depositional environments. Arrows indicate approximate time periods at deposition relative to stratigraphic column.





### 3.5.3. Similarities with Plio-Pleistocene deposits of the central Mediterranean Sea

In addition as evidence of tidal currents, facies M2 is similar to the “rhythmic siliciclastic stratification” described by Longhitano in the Plio-Pleistocene deposits of central Mediterranean Sea, southern Italy (Longhitano and Nemeč, 2005; Longhitano et al., 2010; Longhitano, 2011). Both southern Italy facies and facies M2 observed in the Cortina–Tofane area present dm thick beds, a well developed planar cross stratification and sometimes bioturbation. In the outcrops studied by Longhitano, paleocurrents only follow one main direction (e.g., see Fig. 4 in Longhitano et al., 2010) while in the Dolomites outcrops presented here, two opposing current directions are preserved (Fig. 3.6). This suggests that in the Cortina–Tofane area both ebb and flood currents were equally dominant. Moreover the dominance of structures which testify only one of the two tidal currents is a common feature in mainly siliciclastic systems, while in mainly carbonatic systems the preservation of structures generated by both ebb and flood tidal currents is common (Hayes, 1975; Fitzgerald, 1984; Reeder and Rankey, 2009). In southern Italy an alternation between cm siliciclastic and bioclastic laminae was described, while in the Dolomites the alternation is between cm oolitic to mixed oolitic–siliciclastic, and mm bioclastic, rarely muddy, laminae (Fig. 3.5d, e). In tide-dominated systems the alternation between laminae made of grains differing in terms of shape and density, and so in hydraulic portability, is generally related to variations in hydraulic section and thus in tidal current velocity (Longhitano and Nemeč, 2005; Longhitano et al., 2010; Longhitano, 2011). In particular, in the Plio-Pleistocene of the central Mediterranean, the alternation between siliciclastic and bioclastic laminae is interpreted as an effect of short (diurnal) variations in current energy (Longhitano et al., 2010; Longhitano, 2011). This model could probably also explain the laminae alternation observed in facies M2 with differences in the sediment sources: mainly oolites instead of siliciclastics and a limited presence of mud which is completely absent in the southern Italy facies. Laminae intercalations in the Dolomites outcrops can represent the alternation between tidal current driven sedimentation (oolites laminae) versus slack water phase sedimentation (bioclastic and muddy laminae). Bioclastic–muddy laminae are generally well preserved near the basal contact and tend to vanish upwards (Fig. 3.5f). This may indicate an alternation between different velocity currents in which the

faster current is able to erode the sediment deposited by the slower. The main difference between facies M2 and southern Italy tidalites deals with the regularity of laminae thicknesses. In most of the outcrops studied by Longhitano (2011), a cyclical variation in laminae thickness has been recognized and interpreted as the effect of the variations in average current velocity that occurred every neap–spring tidal cycle, i.e. every 28 days (Williams, 1989; Tape et al., 2003; Mazumder and Arima, 2005; Kvale, 2006). A cyclicity in laminae thickness variation was observed in only one bed of facies M2 (Fig. 3.9) at Dibona Hut. In the other cross bedded beds the variations in laminae thickness seem random. This may be due to an inconstant sediment supply or to the complexity of transport processes which might include, complex currents in the basin, indented coastlines, and paleogeography which resulted in lower tidal current acceleration. Facies M5 has a medium grain size and sedimentary structures similar to M2 but here an alternation between oolitic–siliciclastic and bioclastic–muddy laminae was not observed. This is probably related to a more homogeneous sediment supply in which bioclasts and a mud fraction were almost absent.

#### 3.5.4. First occurrence of a strait developed between two demised carbonate platforms?

Throughout the geologic record, sedimentary environments dominated by tidal currents similar to that observed in the Cortina–Tofane area were generally hosted by narrow marine passages (straits). A considerable number of these straits are related to the development of submarine grabens (e.g., Barrier, 1987; Mercier et al., 1987; Galloway, 2002; Betzler et al., 2006; Folkestad and Satur, 2008; Martín et al., 2009; Longhitano, 2011; Longhitano et al., 2012a, 2012b). In contrast to this sedimentary environment, the system described in this paper does not occupy a tectonic graben or sub-marine canyon, but rather lies between two relict carbonate platforms whose proximity has allowed the development of a marine strait (Fig. 3.8a, b). Similarities with the case study presented in this paper can be observed in the recent geological record of the Maldives (Betzler et al., 2013a, 2013b; Lüdmann et al., 2013). Here the formation of marine passages between atolls dominated by bidirectional currents, even if they are reversing monsoonal currents, follows the partial drowning of the carbonate platform that occurred in the upper Miocene. This partial drowning is probably related to the onset of monsoon-triggered marine upwelling, and thus to an injection of nutrients, in turn linked

to the Himalayan uplift (Betzler et al., 2013b). Although episodes of drowning of carbonate platforms related to the onset of marine upwelling were hypothesized in the Dolomites during the Middle Triassic (the Cernerera drowning of Preto et al., 2005), this phenomenon cannot be invoked as the cause for the demise of the Upper Triassic Cassian platforms. During the Carnian crisis a complete and simultaneous demise of all the highrelief carbonate platforms is documented in the whole Dolomites area (De Zanche et al., 1993; Gianolla et al., 1998). The cause of the shut-off of carbonate production of high-relief platforms is not a drowning but a sea level drop (De Zanche et al., 1993; Gianolla et al., 1998; Bosellini et al., 2003) and/or a climate change (Schlager and Schöllnberger, 1974; Simms and Ruffell, 1989; Preto et al., 2010; Dal Corso et al., 2012).



Fig. 3.9. Cyclical variation in laminae thickness observed in M2 at Dibona Hut related to cyclical variations of the current velocities during the neap–spring tidal cycle. Dark laminae are of siliciclastic–oolitic grainstone and white layers of bioclastic–oolitic grainstones.

### **3.6. Conclusions**

Detailed facies analysis carried out in the Carnian (Late Triassic) Heiligkreuz Fm. of the Cortina–Tofane area (Dolomites, Northern Italy) identifies a sedimentary environment dominated by tidal currents. The development of this system had been possible thanks to the particular paleogeography of the area featuring an E–W elongated marine strait that, in contrast to those cases known in the literature, is bounded on the northern and on the southern sides by two demised high-relief carbonate platforms. Four stratigraphic intervals formed in different paleodepth conditions, were defined and two opposing paleocurrent directions trending to the northwest (ebb) and east (flood), were measured. A tidal depositional environment is given by the presence of planar cross stratification with opposing dipping laminae, herringbone cross stratification and flaser to wavy to lenticular bedding. Alternating mainly oolitic and mainly bioclastic laminae within planar cross stratified beds is similar to those observed in some Plio-Pleistocene tidal deposits of the central Mediterranean Sea and is the effect of variations in the hydraulic section, and thus of changing current velocity, during the tidal cycle.

# ***4. Sequence Stratigraphy after the demise of a high-relief carbonate platform (Carnian of the Dolomites): sea-level and climate disentangled***

*(submitted to Palaeogeography, Palaeoclimatology, Palaeoecology)*

---

## **Abstract**

Sedimentary facies analysis, coupled with geological 3D modeling, led to constrain the sequence stratigraphy of a complex stratigraphic interval in the Late Triassic of the Dolomites, in which both sea level and climate changes were penecontemporaneously interacting. This multidisciplinary approach is the key to disentangle the timing of the two events (climatic change vs. sea level fluctuation) and their effects on the shallow water carbonates realm. The climate change predate the sea-level drop and is the cause of the demise of the microbial-dominated high-relief carbonate platforms. After the high-relief platforms demise a period of coexistence between small microbial carbonate mounds and loose arenaceous carbonates is documented. The subsequent sea-level fall determine the complete disappearance of microbial carbonates (i.e. mounds) and the definitive switch of the shallow water carbonates to loose sediment dominated ramps. Thus the demise of the Upper Triassic microbial dominated high-relief platforms of the Dolomites can be interpreted as a two step process: first a climate event killed the km-scale platforms; second a fall of the sea level led to the definitive disappearance of the microbial carbonates. Moreover it is shown as a climate-induced crises of shallow water carbonate systems can generate geological surfaces similar to drowning unconformities when a transgression is not taking place.

## **4.1 Introduction**

Sequence stratigraphy is a powerful tool to understand the history and the evolution of depositional systems and sedimentary basins (e.g., Vail et al., 1991; Catuneanu, 2006;

Catuneanu et al., 2011). It has been successfully applied in a variety of geodynamic settings to both siliciclastic (Galloway and Williams, 1991; Helland-Hansen, 1992; Mellere and Steel, 1995; Miall and Arush, 2001; Catuneanu et al., 2002; Cantalamessa et al., 2005; Breda et al., 2007; Galloway, 2008; Miall et al., 2008; among others) and carbonate systems (De Zanche et al., 1993; Pasquier and Strasser, 1997; Gianolla et al., 1998; Gianolla and Jacquin, 1998; Pomar and Tropeano, 2001; Mateu-Vicens et al., 2008; among others). However, the sequence stratigraphic interpretation of carbonate systems still has significant limitations, related to the capability of some carbonate platforms to produce sediment in situ, at a rate that is influenced by oceanographic and climatic parameters more than by sea level change (Schlager, 1991; 1993; Schlager et al., 1994; Pomar, 2001). One singularity of carbonate platforms is that they can drown, that is, the platform top can be submerged below the photic zone; in that case, the platform cannot catch up to sea level and the carbonate production is irreversibly shut down (Schlager, 1981; 1999a, b; Hallock and Schlager, 1986). The geometry and facies of drowned carbonate platforms mime a rise of the sea level even during periods of sea level stability. In the specific case of carbonate platforms drowning, the special behavior of carbonate systems has been often related to a change in the ecology or biology of carbonate producers, in turn commonly related to climate and/or environmental changes (Schlager, 1981; Hallock and Schlager, 1986; Jenkyns, 1991; Mutti et al., 1997, 2005; Weissert et al., 1998; Wilson et al., 1998; Mutti and Hallock, 2003; Schlager, 2003; Pomar et al., 2004; Föllmi and Godet, 2013; Godet et al., 2013; among others). In the Triassic of the Dolomites (North-eastern Italy, Fig. 4.1a), sedimentary sequences are dominated by carbonates. During the last decades, several sequence stratigraphic interpretations of these successions were proposed (Brandner, 1984; De Zanche et al., 1992; De Zanche et al., 1993; Ruffer and Zühlke, 1995; Neri and Stefani, 1998; Gianolla et al., 1998; Neri et al., 2007) that had to face the paradox of drowning platforms, at times of prolonged and intense subsidence as the Middle Triassic (De Zanche et al., 1995; Blendinger et al., 2004; Preto et al., 2005; Brack et al., 2007).

At the end of the early Carnian, a major event of carbonate platform demise is recorded in the Dolomites: carbonate production in high relief platforms suddenly shuts off and is substituted by the deposition of a mixed carbonate-siliciclastic succession deposited on a low-relief ramp depositional profile (Heiligkreuz Formation in Neri et al., 2007, ex

Dürrenstein Formation of De Zanche et al., 1993; Preto and Hinnov, 2003; Fig. 4.2). This crisis of high-relief carbonate platforms has been related to an episode of climate change (Schlager and Schöllenger, 1974; Simms and Ruffell, 1990) known as the "Carnian Pluvial Event" (CPE; Simms and Ruffell, 1989; Preto et al., 2010; Stefani et al., 2010), and corresponds to a major perturbation of the global carbon cycle (Dal Corso et al., 2012). In the Dolomites, the interpretation of the stratigraphic interval around the CPE, in terms of sequence stratigraphy, is challenging.

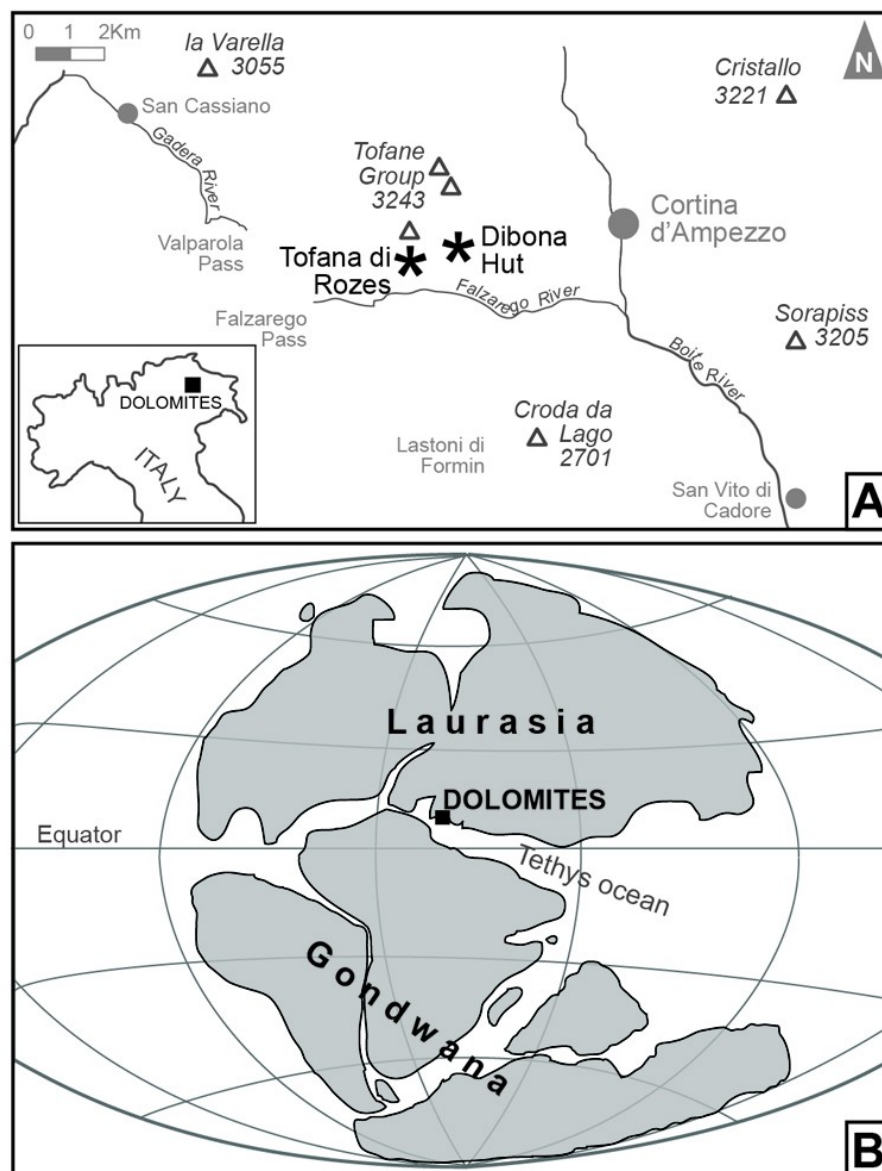


Fig. 4.1. (A) Location and map of the study area. Stars indicate the studied outcrops (see Fig. 4.3a, 4.4a), triangles the major peaks (elevations in meters) and dots the main towns. To help the reader other localities are indicated in grey. (B) Position of the Dolomites during Middle-Late Triassic.

According to De Zanche et al. (1993) and Gianolla et al. (1998), the ramp deposits formed after the demise of high relief early Carnian platforms make up for a complete 3<sup>rd</sup> order depositional sequence, and a sea level fall at the base of this interval caused the demise of the underlying high relief carbonate platforms (De Zanche et al., 1993; Gianolla et al., 1998; Bosellini et al., 2003). However, this interpretation does not explain the change in the type of carbonate sediments and is incongruous with most of the documented episodes of carbonate platform drowning and demise (Schlager, 1981; 1999a, b; 2005; Weissert et al., 1998). In this work, a reappraisal of the sequence stratigraphy of the Heiligkreuz Formation is presented. The focus is put on the lower sequence boundary interval, with the aim of disentangling the roles of sea level change and environmental factors on the demise of high-relief carbonate platforms. We applied 3D acquisition and modeling techniques coupled with facies analysis to assess the relative timing of the platform demise with respect to the sedimentary record of sea level fall and subaerial exposure. Our data suggest that the demise of high relief carbonate platforms occurred before sea level fall and the consequent subaerial exposure; depositional geometries mimicking a sequence boundary were thus generated and are unrelated to an actual decrease in accommodation, in analogy to typical drowning unconformities (type 3 SB of Schlager, 1999b). Differently from episodes of drowning of the Middle Triassic, however, the CPE and the related demise of high-relief carbonate platforms occurred at a time of tectonic quiescence, at the end of a long-term depositional cycle (Gianolla and Jacquin, 1998), when accommodation in the area was created at a slow rate. The case study of the Carnian of the Dolomites thus shows that climate-induced crises of carbonate systems can generate surfaces similar to drowning unconformities outside of times of prolonged transgression.

## **4.2 Geological setting**

During the Middle-Late Triassic, the Dolomites (North-eastern Italy, Fig. 4.1a) were located in the western portion of the Tethys Ocean (Ziegler, 1988; Dercourt et al., 1993) at northern tropical latitudes (Fig. 4.1b; Muttoni et al., 1996; Broglio Loriga et al., 1999; Flügel, 2002). The area was characterized by a “chess-board-like” paleotopography featuring domains with different subsidence rates (horsts and grabens) and bounded by roughly North-South and East-West faults (Masetti and Neri, 1980; Blendinger, 1986;



De Zanche et al., 1993; Gianolla et al., 1998; Preto et al., 2011). Often, horsts hosted the onset of isolated high relief carbonate platforms dominated by Microbial to Tropical carbonate factories (*sensu* Schlager, 2003), while in grabens a carbonate to siliciclastic basinal sedimentation took place (Masetti and Neri, 1980; Gaetani et al., 1981; Bosellini, 1984; Bosellini et al., 2003; Neri et al., 2007; Preto et al., 2011; among others).

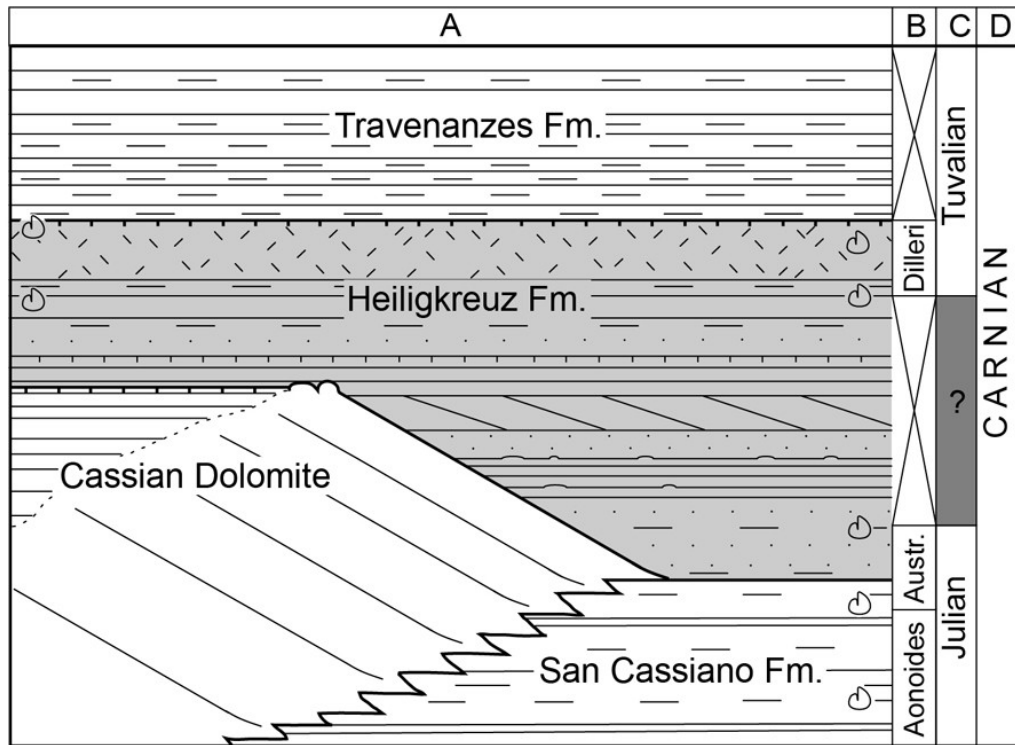


Fig. 4.2. Lithostratigraphic scheme (modified from Preto and Hinnov, 2003) of the studied interval in the Cortina-Tofane area. The Heiligkreuz Formation, is highlighted in grey. The platform settings (to the left) corresponds to Tofana di Rozes area, the basinal settings (to the right) corresponds to Dibona Hut area. Ammonoid symbols indicate ammonoid occurrences in the area. (A) Names of lithostratigraphic units (from Neri et al., 2007). (B) Ammonoid biostratigraphy (from Mietto and Manfrin, 1995). (C-D) Chronostratigraphy stages and substages. According to Preto and Hinnov (2003), the clinostratified body of Dibona Hut, is represented in this figure as tabular prograding body. In this study it has been highlighted as, this clinostratified body, is thus characterized by an offlapping geometry, and shows an overall progradation of the shoreline along a descending, low angle trajectory (see chapters 4.4 and 4.5 and Fig. 4.4)

Toward the end of the early Carnian, a progressive slowdown of the high subsidence rates along with a strong siliciclastic input to marginal basins resulted in the flattening of this complex paleotopography. Contemporaneously, an important turnover in

carbonate factories and carbonate platform geometries occurred and Microbial to Tropical factories were replaced by Cool-water to Tropical factories (*sensu* Schlager, 2003) which originated ramp geometries (Bosellini et al., 2003; Preto and Hinnov, 2003; Stefani et al., 2010). The demise of the last generation of high relief Carnian carbonate platforms (Fig. 4.2; Cassian 2 platforms in De Zanche et al., 1993) is attributed to two main factors: (1) the subaerial exposure they suffered following an important sea level drop and (2) the considerable siliciclastic input (in turn triggered by the sea level drop) which can be detrimental to the carbonate production (Russo et al., 1991; Keim et al., 2001; Bosellini et al., 2003). This sea level drop constitutes the lower sequence boundary of a third order depositional sequence (Fig. 4.2; Car 3 in De Zanche et al., 1993; Gianolla et al., 1998), object of this study.

### 4.3 Methods

A three-dimensional model of the southern walls of Tofana di Rozes (see Fig. 4.1a for location; Fig 4.3a) was created with the photogrammetric software Agisoft™ Photoscan. Forty-six highly overlapping photographs were taken from a working distance of ~ 4 km using a Sony α200 DSLR camera (resolution = 10.2 megapixel) coupled with a Minolta AF 100-200 f4.5 zoom lens (selected focal length = 100mm, f = 9). To scale and georeference the model, the GPS position of 20 points, well recognizable both on the field and on the photographs, was taken with the aid of a Royaltek RBT-2200 bluetooth GPS (average uncertainty in the specific conditions ~ 1 – 5 m) coupled with a HP iPAQ 214 handheld pc running Esri® ArcPAD™ 7.0. A three-dimensional model of the Dibona Hut outcrop (Fig. 4.1a for location; Fig. 4.4a) was acquired through an Optech Ilris 3D terrestrial laser scanner (wavelength 1500 nm, acquisition speed 2500 points per second). The working distance was ~ 60 m and the resolution of the point clouds is ~ 1 point every 4 cm. To georeference the model, the GPS position of 6 targets was taken using a high precision Base-Rover Topcon HiPer® Pro system (uncertainty ~ 3 cm).

Sedimentary facies were defined in the field and through petrographic analysis, using standard sedimentology methods (e.g., Tucker and Wright, 1990; Flügel, 2004).

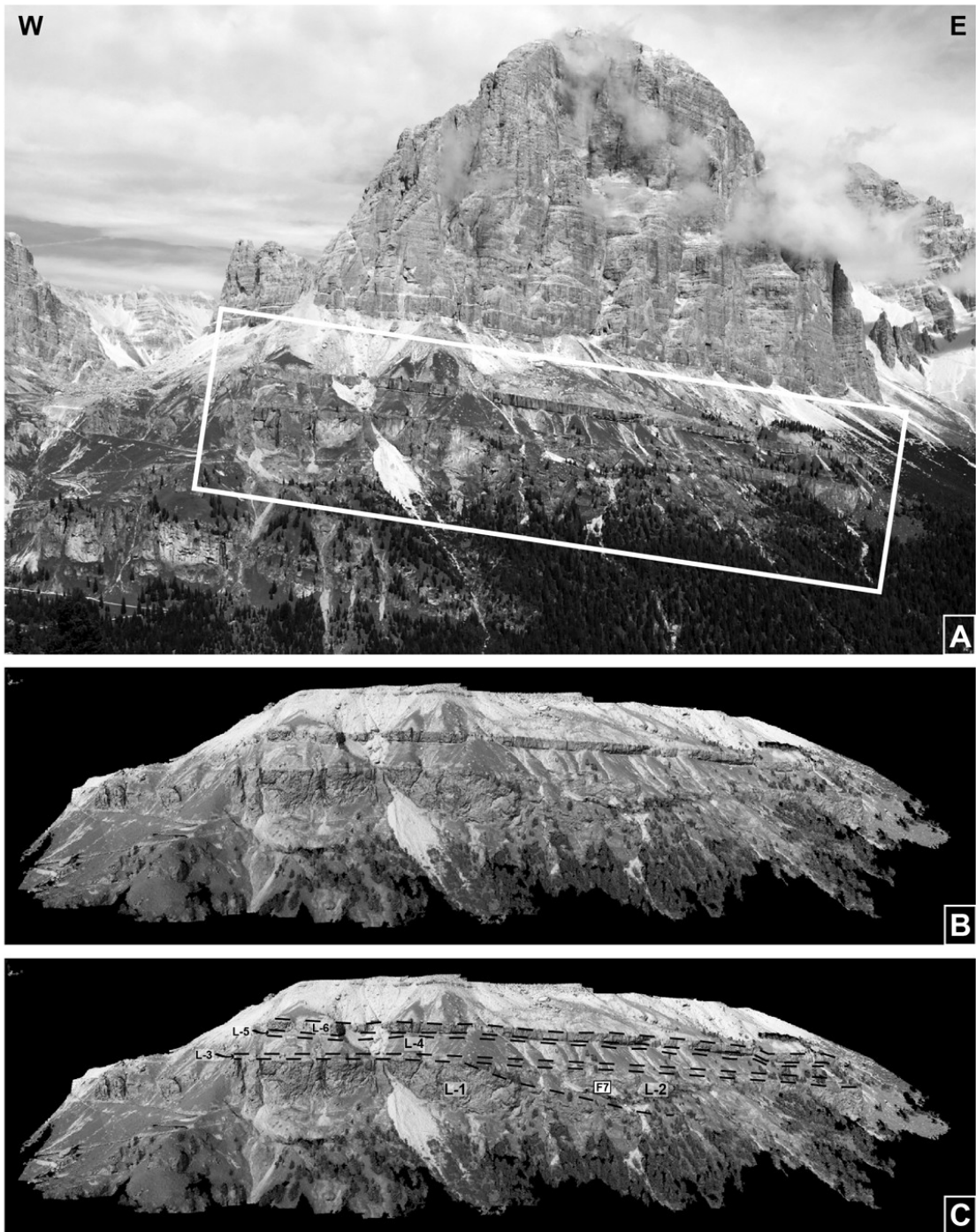


Fig. 4.3. (A) The outcrop on the southern wall of the Tofana di Rozes. The white rectangle indicates the area of interest i.e. the stratigraphic interval object of this study. (B) Photogrammetric three dimensional model of the outcrop (only the area of interest was modeled). (C) Line drawing of the outcrop. Black dashed lines indicate the lithozones limits (see the Lithozones chapter for a description of facies and stratal relationships). F7 indicates the location of Fig. 4.7.

## 4.4 Lithozones

The sedimentary succession was divided into six lithozones. Each of these lithozones is characterized by a different facies association, stratal patterns and depositional geometries. A brief description of lithozones is provided below; for a more detailed description the reader is referred to Preto and Hinnov (2003) and Gattolin et al. (2013).

### *Lithozone 1 (L-1)*

This lithozone was observed only at Tofana di Rozes, where it constitutes a wedge pinching out toward the East. Its maximum thickness is ~ 200 m on the western side of the outcrop (Figs. 4.3b, c). It is mainly constituted by m thick clinoforms of pervasively dolomitized limestone. Locally megabreccias, with m to tens of m large boulders, were identified. Dolomitization hampers the observation of original facies. L-1 pertains to the platform slope of one of the Carnian high-relief carbonate platforms (Cassian 2 of De Zanche et al., 1993; Gianolla et al., 1998). The correspondent margin and platform top facies are not observable in the Dibona and Tofane area, but have been described in neighboring outcrops at Falzarego Pass (Fig. 4.1a; Breda et al., 2009). The microbial character of these platforms is known, however, from allocthonous boulders and carbonate grains in the adjacent basins (Russo et al., 1997; Keim and Schlager, 1999; 2001; Preto, 2012). Except for the toe of slope portion, which is often characterized by megabreccias, they are dominated by microbial boundstones.

### *Lithozone 2 (L-2)*

The boundary between the first and the second lithozone was observed at Tofana di Rozes. It is constituted by a sharp, ~ E dipping by-pass surface on top of the last slope clinoform of L-1. L-2 is constituted by lenticular-shaped carbonate bodies (mounds) mainly made up of microbial boundstone (Figs. 4.3b, c; 4.5), interlayered and laterally onlapped by dm thick beds of arenaceous grainstones with bivalves, gastropods, peloids, plant remains (Fig. 4.6). Mounds are the dominant facies at Tofana di Rozes, where they present maximum size (10-100 m), while arenaceous grainstones prevail at Dibona Hut (Figs. 4.5; 4.6). Cm- dm thick beds of calcsiltite and shale are rare at both localities

(Fig. 4.7).

At Dibona Hut, the last part of this lithozone is constituted by a ~ 5 m thick sequence of m-scale beds with a highly erosive base, made up of arenaceous-conglomeratic grainstones (main components are volcanic rock fragments, quartz, molluscs, echinoderms, plant debris and rare amber droplets; Breda et al., 2009) which testifies the onset of mass flows. These coarse grained beds are overlaid by a 30 m thick clinostratified body (L-2-CLINO in Fig. 4.4c) which dm-scale beds are essentially made up of arenaceous grainstone (main components are bivalves, gastropods, peloids, plant remains and echinoderms), with plane parallel bed joints. Beds are grouped in bedsets which present foresets dipping ~ 25° toward the E (after correction of tectonic tilt) and topsets progressively lowered toward the E (Fig. 4.4c). These clinostratified bedsets represent the two-dimensional along-dip cut of a sedimentary body which along-strike geometry is not visible due to exposure bias. As the three dimensional geometry of clinofolds is not observable, it is not possible to actually interpret the sedimentary body. The high dip-angle of the beds and the amplitude of the bedsets constrain the shortlist to two possibilities: a delta (implying an along-strike lobate shape of clinofolds) or a coastal prograding wedge (implying an along-strike rectilinear shape of clinofolds), but a further distinction between them is not possible. The clinostratified body is overlapped by tabular dm to m beds of often dolomitized arenaceous grainstone (L-2-ONLAP in Fig. 4.4c).

### *Lithozone 3 (L-3)*

This lithozone consists of an alternation of dm to m thick dolostone beds, with peloids, often capped by stromatolitic lamination, sheet cracks and planar fenestrae, and dm-scale calcarenite beds. Both facies are characterized by burrows and by a rooted or karstic horizon at the top of the beds. Over the karstified top of some beds, thin layers of dark clays and shales are present and display roots, plant fragments, amber, pyrite and coal. Rare dm beds of massive arenites were observed and among them the most evident are located in the lower portion of this lithozone. This stacking of facies suggests a peritidal/paralic environment (see interval D of Preto and Hinnov, 2003 and interval 1 of Gattolin et al., 2013).

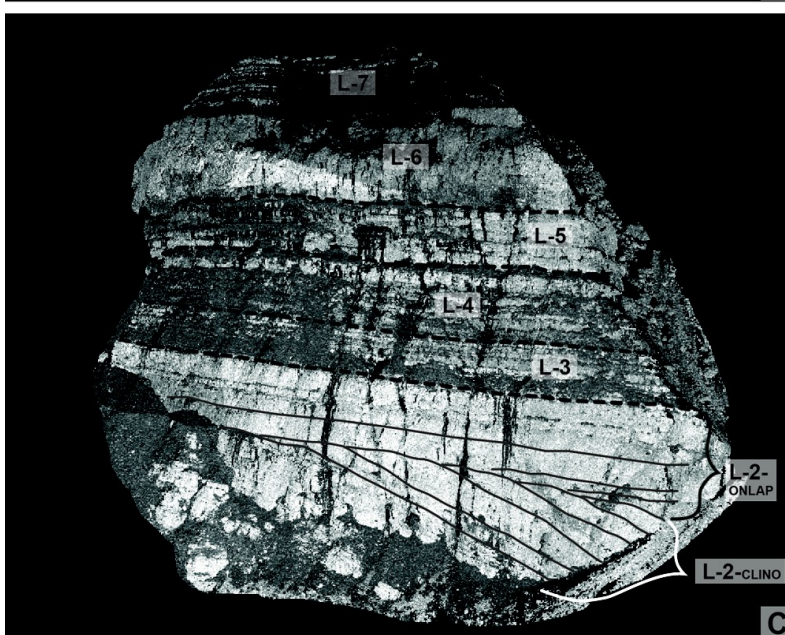
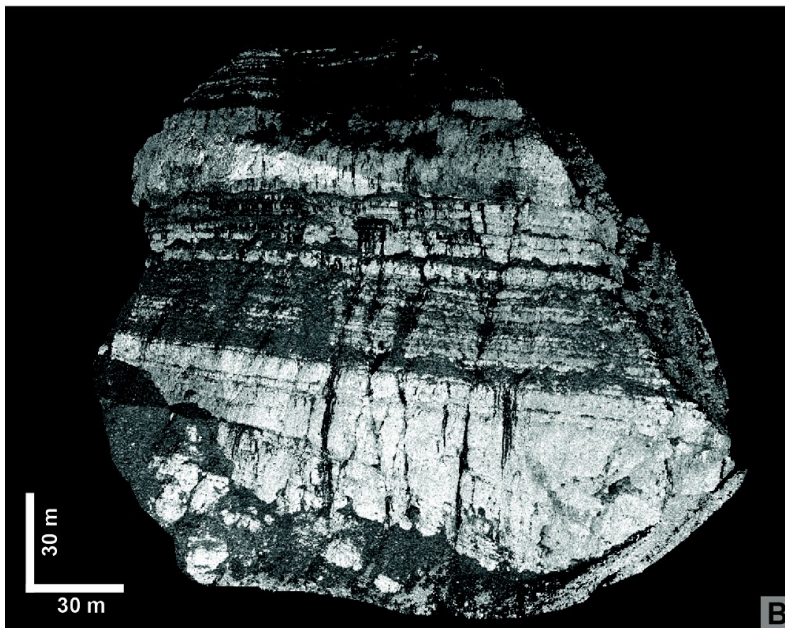


Fig. 4.4. (A) The Dibona Hut outcrop. (B) Three dimensional model of the outcrop. This model is a three dimensional point cloud obtained by a terrestrial laser scanner. (C) Line drawing of the outcrop. Black dashed lines indicate the lithozones limits, grey continuous lines the bedding in the second lithozone (see the Lithozones chapter for a description of facies and stratal relationships).



Fig. 4.5. Outcrops at the boundary between L-1 and L-2 at Tofana di Rozes and their interpretation. The boundary between L-1 and L-2 is constituted by a E dipping by-pass surface which developed on the top of the youngest L-1 clinoform. This surface is onset by lenticular-shaped carbonate bodies (mounds) mainly made up of microbial boundstone.

Dolostones and grainstones represent the normal peritidal cycles, clays and shales the development of littoral swamps (paralic). Massive arenites are rare episodes of high continental sediment discharge into the basin while some of them represent lags. At Tofana di Rozes, the boundary between L-2 and L-3 is marked by a well developed karstic surface that toward the West interests also L-1 (Fig. 4.8). At Dibona Hut, L-3 directly overlies L-2-ONLAP and no evidences of karstification have been observed between them.

#### *Lithozone 4 (L-4)*

The limit between the third and the fourth lithozone is gradational. Due to the absence of a sharp boundary between them it has been arbitrary placed at the first occurrence of

well developed planar cross stratification within the succession. Those sedimentary structures are common in L-4 and were observed in dm thick beds, mainly made up of oolitic-bioclastic calcarenites. Sets of laminae alternately migrating in two opposing directions can be found. Dm-scale beds of fine to medium grained arenite, mainly made up of quartz, chert, feldspar and lithic grains are also observed, with local presence of cm to dm-scale cross stratification, at times migrating in two opposing directions. Levels of imbricated bivalve shells (Coquina) can be found at the base of calcarenites and arenites. Dm thick beds of calcsiltites to calcarenites with mud interbeds, characterized by the presence of ripples, are common. The most represented grains in this facies are peloids. The general structure of this facies is flaser-bedding to wavy-bedding as a function of variable mud content. Cm- dm thick beds of dark shales and siltites rich in plant remains are locally characterized by the presence of isolated ripples made up of calcarenites, producing lenticular bedding. White wackestone to grey marly wackestone, not showing sedimentary structures, and massive dm beds of mixed carbonate-siliciclastic to pure siliciclastic arenites, were rarely observed. The whole L-4 is often interested by burrows. The facies stacking pattern suggests that L-4 deposited in a subtidal environment. Calcarenites and arenites with planar cross bedding and foresets alternatively migrating in opposing directions, as well as flaser to wavy to lenticular bedding, indicate that the dominant mechanism of sediment transport was reversing tidal currents. Episodes of subaerial exposure are almost absent (see interval 2 of Gattolin et al., 2013 for details).

#### *Lithozone 5 (L-5)*

The boundary between L-4 and L-5 is gradational, it has been placed at the complete disappearance of tractional sedimentary structures. L-5 consists of dm to m thick nodular beds of often dolomitized limestones and marly limestones. Ammonoids and conodonts were found at Dibona. Some ammonoids were collected also in the Col dei Bos area, ~ 500 m West of Tofana di Rozes (Preto and Hinnov, 2003; Breda et al., 2009). Cm to dm beds of gray marls with *Chondrites* and locally with pyrite nodules were locally observed. The absence of tractional sedimentary structures and of evidences of subaerial exposure, together with the nodular bed joints and the fossils content (ammonoids), suggest a completely subtidal origin for this lithozone, deeper



than L-4, and a temporary partial starvation of the system (see interval 3 of Gattolin et al., 2013 for details).

### *Lithozone 6 (L-6)*

The sixth lithozone (L-6, Figs. 4.3c and 4.4c) consists of ~ 30 m of massive dolostone. Sedimentary structures are obliterated by dolomitization, only ooids are locally recognizable. Observations on the same interval carried out by Gattolin et al. (2013, see their interval 4) on outcrops neighboring the Dibona and Tofane area, reveal the presence of dm to m thick beds of dolostones (Lastoni di Formin; Fig. 4.1a) and mixed oolitic-siliciclastic arenites (Falzarego Pass, Valparola Pass, Lastoni di Formin; Fig. 4.1a) with planar cross bedding and herringbone cross bedding. The absence of subaerial exposure surfaces and the presence of planar and herringbone cross bedding suggest that L-6 deposited in a subtidal environment, dominated by tidal currents. The top of L-6 is marked in the whole area by a well developed karstic surface (Fig. 4.9).

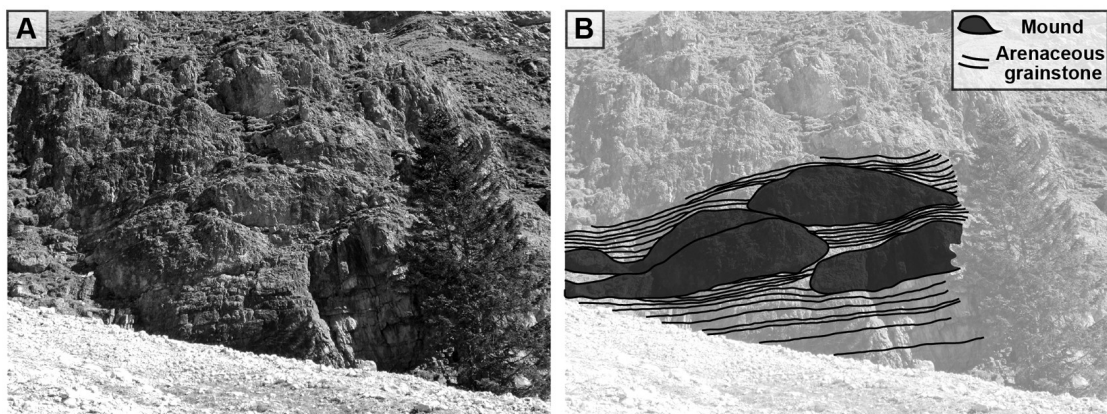


Fig. 4.6. (A) Outcrop of L-2 at Dibona Hut and (B) its interpretation. Lenticular-shaped carbonate bodies (mounds) mainly made up of microbial boundstone are interlayered and laterally onlapped by dm thick beds of arenaceous grainstones.

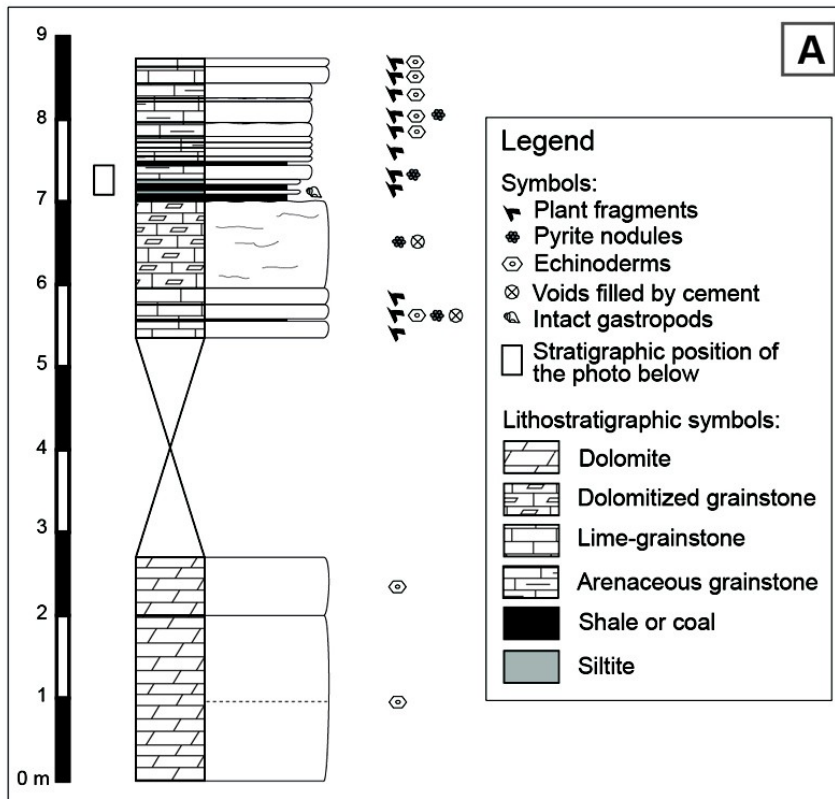


Fig. 4.7. (A) Stratigraphic log of a loose sediment intercalation in the L-2 at Tofana di Rozes and (B) a detail of it. This intercalation lies between two carbonate mounds and is mainly made up of cm- dm thick beds of grainstone (and its dolomitized counterpart), arenaceous grainstones, calcisiltite and shales. The location of this stratigraphic log is highlighted in Fig. 4.3c.



### *Lithozone 7 (L-7)*

This lithozone (L-7; Figs. 4.3c and 4.4c) consists of dm thick beds of aphanitic, mottled dolostones alternated to dark clays and represents a marginal marine/paralic environment. L-7 constitutes the basal part of the Travenanzes Formation, a mixed siliciclastic/carbonate succession of alluvial plain to floodbasin to tidal flat environments that deposited during Upper Carnian on a wide, low-relief coastal area (Breda and Preto, 2011).

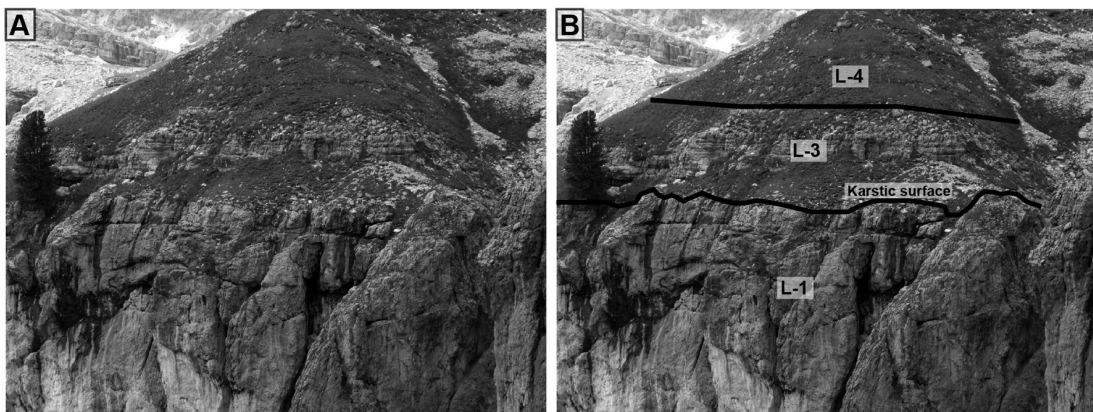


Fig. 4.8. (A) Western portion of Tofana di Rozes outcrop and (B) its interpretation. Here the L-1 is directly overlaid by the L-3. The boundary between L-1 and L-3 is constituted by a karstic surface.



Fig. 4.9. Karst at the top of the L-6 at Lastoni di Formin (see Fig. 4.1a for location).

## 4.5 Sequence stratigraphy

The described succession, together with observations made on stratal patterns, depositional geometries and erosional surfaces led to disentangle the sequence stratigraphy of the studied interval. The sequence stratigraphic interpretation of the succession is provided below using the standard terminology of Catuneanu et al. (2009; 2011). As in the previous sequence stratigraphic interpretations of this interval (De Zanche et al., 1993; Gianolla et al., 1998) the depositional sequences subdivision has been carried out following the approach suggested by Vail et al. (1991).

### 1<sup>st</sup> depositional sequence

#### *Highstand system tract*

The pervasively dolomitized clinostratified sedimentary body outcropping at the base of the Tofana di Rozes outcrop (L-1; Fig. 4.3) represents the slope of the last generation of high relief carbonate platforms developed during Carnian in the Dolomites area (Cassian 2 of De Zanche et al., 1993; Gianolla et al., 1998). In terms of geometry, the toe of slope rapidly advances basinward. The shoreline trajectory, which is marked by the trajectory of the platform margin, is not observable in this outcrop, but it is known that this generation of carbonate platforms always presents a downward-concave prograding shoreline trajectory, suggesting a gradual decrease of the accommodation rate (e.g. Sella platform of Bosellini, 1984). This observation enables to interpret the L-1 as an HST (Fig. 4.10; Car 2 HST of De Zanche et al., 1993; Gianolla et al., 1998).

The upper bed joint of the youngest cliniform of L-1 paleoslope is characterized by the presence of a by-pass surface without evident erosion features (e.g., karst). At Tofana di Rozes, L-2 is dominated by carbonate mounds directly overlaying this surface (Fig. 4.5) which occur along the whole slope length. Here, the maximum altitude reached by the mounds of facies L-2 is exactly the same of the shelf break of the underlying high-relief platform, from which the cliniforms of facies L-1 originate (Fig. 4.3). This testifies that, during the deposition of L-2, the sea level was still as high as during the deposition of L-1, so that L-2 is still part of the highstand system tract of the first depositional sequence (Fig. 4.10). The difference in the abundance of carbonate mounds vs. arenaceous grainstones observed in L-2 between Tofana di Rozes and Dibona Hut

outcrops (Figs. 4.5; 4.6) is due to their different paleotopographic location. Tofana lies on the high paleo-slope of the Cassian platform, while Dibona was closer to the basin depocenter (Gattolin et al., 2013).

## **2<sup>nd</sup> depositional sequence**

### *Falling stage system tract*

The ~ 5 m thick coarse grained interval found at the top of L-2 and representing the onset of mass flow deposits, is interpreted as the beginning of the sea level fall and consequent increase of sediment discharge in the basin. A sharp increase in sediment grain size is testified also at the coeval outcrop of Borca di Cadore and in the whole Cadore area (Neri et al., 2007; Breda et al., 2009). The basal surface of forced regression (Hunt and Tucker, 1992) can be placed at the base of this coarse grained interval (Fig. 4.10). At Tofana di Rozes, this surface coincides with a well developed subaerial exposure surface, showing karst development (Fig. 4.8). The clinostatified bedsets, made up of arenaceous grainstones, which constitute the lower portion of the cliff observed at Dibona Hut (L-2-CLINO; Fig. 4.4), irrespective of their interpretation as a delta body or a coastal prograding wedge, record a fall of the sea level (e.g., Massari et al., 1999; Hernández-Molina et al., 2000; Tropeano and Sabato, 2000; Pomar and Tropeano, 2001; Massari and D'Alessandro, 2010). The offlapping geometry evidences an overall progradation of the shoreline along a descending, low angle trajectory. Consequently, together with the last coarse grained portion of the L-2, the L-2-CLINO represents the falling stage system tract of the second depositional sequence (Fig. 4.10; Car 3 of De Zanche et al., 1993; Gianolla et al., 1998). The stair-stepping surface at the top of the clinostatified sedimentary body (L-2-CLINO; Fig. 4.4) represents the correlative conformity (*sensu* Hunt and Tucker, 1992, Fig. 4.10). Being in a paleotopographical higher position with respect to Dibona (Gattolin et al., 2013), the falling stage system tract is not recorded at Tofana di Rozes. Instead, a well developed karstic surface is produced by subaerial exposure on top of L-2 (subaerial unconformity of Sloss et al., 1949; Figs. 4.8, 4.10). More to the West, e.g., at Falzarego Pass (Fig. 4.1a), this karstified surface lies on top of the platform interior facies of the older Cassian platform, a time equivalent of facies L-1 (Fig. 4.10).

### *Lowstand system tract*

At Dibona Hut, above the correlative conformity (*sensu* Hunt and Tucker, 1992), the dolomitized arenaceous grainstones beds (L-2-ONLAP; Fig. 4.4) onlapping the clinofolds represent the base of the lowstand system tract (Fig. 4.10). This interval, coherently with the paleotopography of the area, deposited only at Dibona Hut which was in a more basinal setting than Tofana di Rozes.

### *Transgressive system tract*

At Dibona Hut, the basal portion of L-3 often displays massive arenites with basal lags, which lie on the karstified top of the underlying peritidal cycles and evolve into the subtidal portion of the following cycle. These are thus interpreted as transgressive lags formed on a formerly emerged coastal area and are evidence of a transgressive ravinement surface (Cattaneo and Steel, 2003). The L-3 marks a sharp change in lithology with respect to the pervasively dolomitized L-2 ONLAP (see Fig. 4.4c) and is characterized by shallow water peritidal-paralic deposits of tidal-flat/lagoon, cyclically subjected to subaerial exposure and soil development (interval D of Preto and Hinnov, 2003; interval 1 of Gattolin et al., 2013). At Tofana di Rozes, L-3 directly overlies in disconformity the karstic surface on top of L-2 and L-1 (i.e. the sequence boundary; Figs. 4.3; 4.10). The transition from L-3 to L-4 is gradual. The facies association observed in L-4 is typical of a mainly subtidal environment dominated by tidal currents and therefore identifies a marked deepening of the depositional environment with respect to L-3 (interval E-F of Preto and Hinnov, 2003; interval 2 of Gattolin et al., 2013). Deepening takes on in L-5, which finer grain-size and nodular bed joints testify the deepest environment of the entire depositional sequence (interval 3 of Gattolin et al., 2013). Lithozones L-3, L-4 and L-5 represent the transgressive system tract of the second depositional sequence (Fig. 4.10; Car 3 of De Zanche et al., 1993; Gianolla et al., 1998). The maximum flooding surface (Frazier, 1974; Posamentier et al., 1988) is likely placed within L-5 as confirmed by the occurrence of open marine fossils (ammonoids and conodonts; Preto and Hinnov, 2003) and the absence of indicators of high hydraulic energy, implying sedimentation below the wave base.

### *Highstand system tract*

Above, L-6 is coarser grained and characterized by well developed planar to herringbone cross bedding, thus recording a return to shallower conditions with respect to L-5. The observed facies association suggests a subtidal, tide dominated sedimentary environment similar to that of facies association L-4. L-6 is observed in the whole Dolomites area (interval H of Preto and Hinnov, 2003; Neri et al., 2007) and testifies for an important shift of the coast line toward the basins (interval 4 of Gattolin et al., 2013). This lithozone constitutes the highstand system tract of the second depositional sequence (Fig. 4.10; Car 3 of De Zanche et al., 1993; Gianolla et al., 1998).

The well developed karstic surface on top of L-6 in the study area is observed at a regional scale in the Dolomites and beyond, and is the subaerial unconformity that mark the boundary with the subsequent depositional sequence (Fig. 4.9; Car 4 of De Zanche et al., 1993; Gianolla et al., 1998). Above it, an abrupt landward shift in facies is observed, with the deposition of the coastal sediments of the Travenanzes Formation, here represented by dm thick beds of aphanitic and mottled dolostones alternated with dark clays (L-7) and suggesting marginal/paralic environments (Breda and Preto, 2011).

## **4.6 Discussion**

### 4.6.1 Role of 3D modeling in identification of depositional geometries

During the last three decades, several interpretations were proposed for the stratigraphic succession outcropping at Dibona Hut, and in particular for the clinostratified body of L-2-CLINO (Fig. 4.4). Bosellini et al. (1982) and later Doglioni and Carminati (2008) interpreted this body as a tectonically tilted block, bounded by an angular unconformity at its top. Preto and Hinnov (2003) instead interpreted this sedimentary body as a prograding shoal barrier with a tabular geometry. The inaccessibility of this outcrop is the main cause for the lack of an unambiguous interpretation which had been carried out on the basis of local observations of sedimentary facies coupled to panoramic views (in the field or on photographs), which are essentially bi-dimensional, and thus affected by perspective distortion.

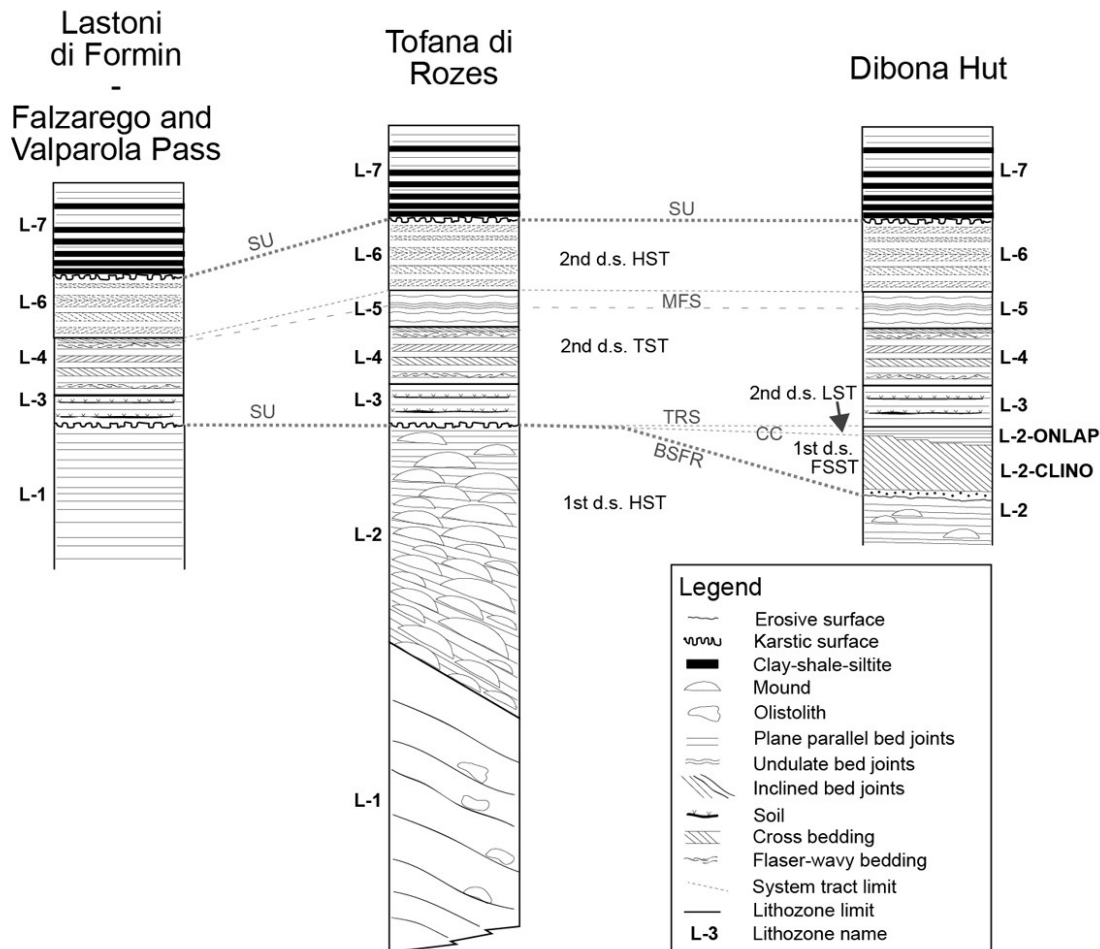


Fig. 4.10 Sequence stratigraphic correlation of three schematic stratigraphic logs representing the sequences outcropping at Tofana di Rozes, Dibona Hut and Lastoni di Formin/Falzarego Pass/Valparola Pass (see Fig. 4.1a for locations). The Lastoni di Formin/Falzarego Pass/Valparola Pass log has been summarized according to Bosellini et al. (1978), Preto and Hinnov (2003); Gattolin et al. (2013). The figure not in scale, the thickness of lithozones is only indicative. HST = high stand system tract, FSST = falling stage system tract, LST= low stand system tract, TST = trassgressive system tract. SU = subaerial unconformity (Sloss et al., 1949), BSFR = basal surface of forced regression (Hunt and Tucker, 1992), CC = correlative conformity (*sensu* Hunt and Tucker, 1992), TRS = trassgressive ravinement surface (Cattaneo and Steel, 2003); MFS = maximum flooding surface (Frazier, 1974; Posamentier et al., 1988).

Only the use of three dimensional acquisition and modeling techniques allowed to retrieve quantitative information and observe the true geometry of the outcrop (see in particular L-2-CLINO and L-2-ONLAP in the Lithozones paragraph; Fig. 4.4). The stair stepping surface at the top of L-2-CLINO, which was a key feature to identify and define the falling stage system tract of the second depositional sequence, could only be



recognized and traced on the remote-sensed 3D geological model of the outcrop (Fig. 4.4). Differently from the previous sequence stratigraphic interpretation (De Zanche et al., 1993; Gianolla et al., 1998), the lower portion of the Heiligkreuz Formation is now interpreted to be the last part of the highstand system tract (L-2) of the first depositional sequence (Fig. 4.10; Car 2 in De Zanche et al., 1993; Gianolla et al., 1998) and not as the low stand system tract of the second depositional sequence (Car 3 in De Zanche et al., 1993; Gianolla et al., 1998). This is confirmed by the observations carried out from the 3D model of the Tofana di Rozes outcrop. Here, the maximum altitude reached by the mounds of facies L-2 is the same of the shelf break of the underlying high-relief platform. This implies that during the growth of mounds the sea level was still high as during the development of high-relief platform and so the L-2 s.s. is part of the first depositional sequence high stand.

Photogrammetry and terrestrial laser scanning are methods which allow the rapid acquisition of field data on a variety of scales, from a metre-scale outcrop to the km scale of a mountain slope. These data can be used as the base for accurate three-dimensional models of sedimentary bodies. Here we have shown that not only 3D acquisition techniques can speed-up the field work and increase accuracy, but also provide the means for interpretations that would be otherwise impossible on inaccessible or exceedingly wide outcrops. In this case, the identification of a amended and more accurate sequence stratigraphy across the Carnian Pluvial Event in the Dolomites was only possible using the 3D reconstruction of outcrops.

#### 4.6.2 What triggered the platform demise?

The demise of the Carnian high relief carbonate platforms (L-1; the Cassian 2 of De Zanche et al., 1993; Gianolla et al., 1998) was attributed by the previous authors (De Zanche et al., 1993; Gianolla et al., 1998) to a subaerial exposure and a sequence boundary (*sensu* Vail et al., 1991) was placed just above the demised platform (base of Car 3 sequence in De Zanche et al., 1993; Gianolla et al., 1998). In this work, the sedimentological evidence of sea level fall was identified, but occurs at a later stage with respect to the high-relief platform demise. After the Cassian platform demise, small, mainly microbial mounds nucleated all along the abandoned slopes (cf. also Keim et al., 2006). The nucleation of mounds was probably possible because of the shut

down of the underlying high-relief platform (Fig. 4.5). Boulders and other platform-derived sediments, typical of the Cassian platforms (e.g., Reijmer, 1998; Preto, 2012), are in fact not found associated with mounds of lithozone L-2. Rather, mounds are interfingered with arenaceous grainstones made up of prevailing skeletal grains (Figs. 4.6; 4.7), which are only a minor component in the high-relief Cassian platforms (Kenter, 1990, Russo et al., 1997, Reijmer, 1998; Keim and Schlager, 1999; 2001). These observations are confirmed at Lavarella by Keim et al. (2001, 2006; see Fig. 4.1a for location). Microbial carbonate mounds (Fig. 4.5) can be interpreted as relics of the Cassian Microbial factory (*sensu* Schlager, 2003) that try to hold up the crisis. They are tightly interfingered with arenaceous grainstones that highlight the onset of a important siliciclastic input and of a different carbonate factory producing mostly loose skeletal grains (Figs. 4.6, 4.7). At Tofana di Rozes, this unit onsets the Cassian platform slope up to the shelf break (Fig. 4.3) and is capped by the same karstic surface found at the top of the Cassian platform (Fig. 4.8), thus, the main episode of sea level fall is subsequent to the high relief carbonate platform demise and to the establishment of mounds on the abandoned slope. Sea level fall thus could not have triggered the crisis of the high relief microbial platform.

In Late Triassic high-relief carbonate platforms of the Dolomites (Cassian *sensu* De Zanche et al., 1993), the carbonate production was dominated by microbialites (Russo et al., 1997; Keim and Schlager, 1999, 2001). Being independent from light availability, microbialites are less influenced by sea level variations with respect to metazoan reefs. Microbial platforms are usually characterized by a carbonate production zone spread from shallow to deep waters (down to 200-300 m depth; Kenter, 1990; Della Porta et al., 2003; 2004; Kenter et al., 2005; Marangon et al., 2011). Data from the geological record demonstrate that carbonate production rates of healthy Tropical and Microbial carbonate factories are high enough to keep the pace with eustatic variations (Schlager, 1981; 1999a,b; 2003), and in fact the demise of a carbonate platform is generally caused by pulses of tectonic subsidence or by climatic events (Schlager, 1981). In the Dolomites, a slow down of subsidence is observed during the development of the last generations of Carnian high relief platforms (Bosellini, 1984; Gianolla and Jacquin, 1998; Bosellini et al., 2003; Stefani et al., 2010). The following depositional sequence (second depositional sequence of this work) testifies the complete filling of sedimentary

basins and a flattening of the paleotopography (Fig. 4.2), so that important subsidence pulses can be excluded. The most probable trigger for the demise of Cassian platforms is thus an episode of climatic or oceanographic change, and specifically the onset of the Carnian Pluvial Event (CPE of Simms and Ruffell, 1989; Preto et al., 2010; Dal Corso et al., 2012). Being a humid period, the CPE determined an increase of hinterland weathering and rivers runoff, reflected in a important input of siliciclastics. This may have been coupled with an increase in available nutrients which favored the change of carbonate factory (e.g., Hallock and Schlager, 1986; Mutti and Hallock, 2003; Pomar et al., 2004; Schlager, 2005).

At Dibona Hut, mounds were found only under the mass flow deposits and the clinostratified body representing the falling stage systems tract. Above the falling stage system tract, microbial mounds disappear completely. The demise of the lower Carnian Cassian platforms of the Dolomites was thus a two-step process, in which a first climate and/or oceanographic event (the CPE) killed the km-scale microbial platforms, and then a sea level drop led to the definitive efface of the microbial carbonates. Apart from exposing the shelf, sea level fall may have affected microbial carbonate systems by further increasing the siliciclastic input and associated nutrient availability.



## ***5. General conclusions***

---

Detailed facies analysis carried out on the sedimentary bodies outcropping in the Cortina area (Central Dolomites, Italy), coupled with three dimensional geological modeling techniques, shed light on debated or unknown aspects of the Carnian (Late Triassic) demise of high-relief carbonate platforms of Tethys.

The demise of the last generation of Carnian microbial-dominated high-relief carbonate platforms is linked to a shift of the climate towards more humid conditions (the Carnian Pluvial Event). This climatic event increased in turn the hinterland weathering, the rivers run-off and the siliciclastic input into marginal basins, and so available nutrients, and likely determined a turnover in the carbonate factory. After the death of the km-scale high-relief carbonate platform, the nucleation of relatively small microbial carbonate mounds tightly interfingered with facies typical of a C-factory (i.e. the arenaceous grainstones), documents a initial crisis of the M-factory in the Dolomites. Microbial carbonates were completely wiped out by a fall of the sea level which further increased the siliciclastic input to the basin.

A multidisciplinary approach involving 3D geological modeling and detailed facies analysis permitted to disentangle the timing of climatic change vs. sea level drop, and to understand their effects on the shallow water carbonates realm. Only thanks to this approach the sequence stratigraphy of the studied interval could be depicted.

It was moreover observed as crises of shallow water carbonate systems can generate a geological surface similar to a drowning unconformity without transgression.

The demise of high-relief carbonate platforms triggered the development of a paleogeography characterized by an E-W elongated marine strait connecting two small sub-basins. This system was dominated by tides, as demonstrated by the presence of abundant diagnostic sedimentary structures. In contrast to cases known in the literature, where the topographic confinement is structurally controlled (grabens and canyons), in the Carnian strait of the Cortina area the confinement is produced by the inherited paleogeography with two demised carbonate platforms facing each other.

Photogrammetry and laser scanning allow the rapid and accurate acquisition of field data from the metre-to the km-scale. These data can be used to generate accurate three-dimensional models of sedimentary bodies. Three dimensional acquisition and modeling techniques give also the possibility to retrieve important geological data from inaccessible or exceedingly wide outcrops. In the specific case of this thesis, the identification of a descending trajectory of the shoreline, and hence the position of the sea level fall phase, in turn essential to constrain the sequence stratigraphy of this complex stratigraphic interval, was only possible using the three dimensional reconstruction of the outcrops.

## ***6. Possible implications***

---

Fossil carbonate platforms in the subsurface may constitute sedimentary traps for hydrocarbons. More than half of the present-day oil reserves are stored in carbonate reservoirs. A better understanding of their facies architecture and depositional geometries is of paramount importance in hydrocarbon exploration. The Carnian case study preserves a stacking of carbonate and mixed carbonate-siliciclastic sedimentary bodies and may represent a field analogue for many subsurface hydrocarbon reservoirs.

Although hydrocarbons were not observed, the sedimentary system presented in Chapter 3 of this thesis holds the possibility to be a reservoir outcrop analogue. All the fundamental components of a potential petroleum play are here present and arranged in the right order. The potential source rock coincides with the organic-matter rich San Cassiano Fm. and basal portion of the Heiligkreuz Fm. (Fig. 2, Keim et al., 2006; Neri et al., 2007; Dal Corso et al., 2012), not described in this paper but known from literature. The remaining of the Heiligkreuz Fm., and in particular its sandstone bodies, can be viewed as a potential reservoir capped by an impermeable seal represented by the overlying muddy-evaporitic Travenanzes Fm. (Fig. 2, Breda and Preto 2011). The oil trap setting is completed by the lateral confinement provided by the Cassian Dolomite platforms which display a tight dolomitization and low permeability (Fig. 2, Neri et al 2007). The depicted outcrop analogue shows some similarities with many hydrocarbon reservoirs which have been recently discovered in the North Sea Viking Graben (Galloway 2002; Messina et al., 2009) and between them in particular with the Middle Jurassic Hugin Fm. (Hugin 2 of Folkestad and Satur, 2008). The Hugin 2 unit deposited in a elongated graben in which tidal current amplification and wave-action damping were active. This unit consists of several fining-upward sequences, essentially constituted by the superposition of tidal channels, tidal dunes and tidal flat deposits interpreted as the filling of estuaries during transgressions (i.e. transgressive system tracts). Each fining upward sequence is overlain by a regressive coarsening upward sequence characterized by mixed fluvial and wave dominated deposits,

featuring mouth bars and shoreface facies (i.e. highstand system tracts). The Hugin Fm. was then capped by the marine mudstones of the Heater Fm. and then of the Draupne Fm. (Cockings et al., 1992). Both Hugin 2 and outcrops observed in the Cortina-Tofane area developed in marine laterally-confined conditions, both display the presence of sand-size grained sedimentary bodies deposited in a tidal dominated environment and, although the origin of the seal is widely different, they are both capped by a muddy impermeable succession. Thanks to good exposure and widespread presence of sedimentary structures, the Dolomites case study could probably be used as an outcrop analogue for reservoirs like the Hugin Fm., in order to provide information for example on the drainage pattern of hydrocarbons, which is a key point in heterogeneous and often cross stratified deposits (i.e. deposits with high permeability anisotropy) such as tidal sedimentary bodies.

The high-relief microbial-dominated Cassian carbonate platforms, and more in general several of the high-relief Middle Triassic platforms of the Dolomites, can constitute an outcrop analogue for the Carboniferous carbonate platforms of the Precaspian basin as Kashagan, Tengiz and Karachaganak (Kazakhstan; Weber et al., 2003; Collins et al., 2006; Kenter et al., 2006; 2010a, b; Jones and Xiao, 2006) which are three of the World most important carbonate-hosted oil reservoirs. Similarities between these oil reservoirs and North-eastern Italy platforms can be found in terms of:

- carbonate factory (microbial dominated)
- geometry (isolated and characterized by high-relief and steep slope)
- facies distribution (grainstone-packstone in the inner platform, boundstone on the outermost inner platform, in the margin and upper slope, down to few thousands of meters, megabreccia in the lower slope)
- scale (few to tens of km for the Dolomite platforms, tens of km for the Kazakhstan ones) development of the platform margin (often controlled by faults)

The climatic-triggered turnover of the carbonate factory from M-dominated to C-dominated generates an important change also in terms of petrophysical properties of the sedimentary bodies. The early cemented carbonates (mainly boundstone) of the high-relief Cassian



carbonate platform are substituted by loose mixed carbonate-siliciclastic sediments (mainly arenaceous grainstone) of the Heiligkreutz Fm. In terms of petrophysical properties this is reflected in a switch from tight carbonates, in which primary porosity and permeability are low, to relatively porous and permeable rocks. Moreover, during the Carnian crisis, important shale sequences deposited in the surrounding basins. Thus, a climate change like the Carnian Pluvial Event can create the right conditions for the development of a petroleum play providing both the source rock (basinal shales) and the reservoirs (arenaceous grainstones in this case), at the same time driving diagenetic processes by minimizing the early occlusion of porosity typical of many Mesozoic shallow water carbonate systems.

These developments require detailed petrographic studies and additional modeling of the potential petroleum play analogue which are outside the scopes of this work. However, this thesis set the stage for such developments by providing a sequence stratigraphic framework and a interpretation of processes that governed sedimentation and the turnover of carbonate systems, based on the robust base of a quantitative geological representation of field data.



## References

---

- Anastas, A.S., Dalrymple, R.W., James, N.P., Nelson, C.S., 1997. Cross-stratified calcarenites from New Zealand: subaqueous dunes in a cool-water, Oligo-Miocene seaway. *Sedimentology* 44, 869–891.
- Anthony, E.J., 2002. Long-term marine bedload segregation, and sandy versus gravelly Holocene shorelines in the eastern English Channel. *Marine Geology* 187, 221–234.
- Assereto, R., Brusca, C., Gaetani, M., Jadoul, F., 1977. Le mineralizzazioni Pb–Zn nel Triassico delle Dolomiti. Quadro geologico ed interpretazione genetica. *L'Industria Mineraria* 28, 367–402.
- Barrier, P., 1987. Stratigraphie des dépôts pliocènes et quaternaires du Déroit de Messine. Le Déroit de Messine (Italie). Evolution tectono-sédimentaire récente (Pliocène et Quaternaire) et environnement actuel, 11. Documentés Travaux IGAL, Paris 59–81.
- Beets, D.J., van der Spek, A.J., 2000. The Holocene evolution of the barrier and back-barrier basins of Belgium and the Netherlands as a function of late Weichselian morphology, relative sea-level rise and sediment supply. *Geologie en Mijnbouw* 79, 3–16.
- Berkeley, A., Rankey, E.C., 2012. Progradational Holocene carbonate tidal flats of Crooked Island, south-east Bahamas: an alternative to the humid channelled belt model. *Sedimentology* 59, 1902–1925.
- Betzler, C., Braga, J.C., Martín, J.M., Sánchez-Almazo, I.M., Lindhorst, S., 2006. Closure of a seaway: stratigraphic record and facies (Guadix basin, Southern Spain). *International Journal of Earth Sciences* 95, 903–910.
- Betzler, C., Fürstenau, J., Lüdmann, T., Hübscher, C., Lindhorst, S., Paul, A., Reijmer, J.J.G., Droxler, A.W., 2013a. Sea-level and ocean-current control on carbonate-platform growth, Maldives, Indian Ocean. *Basin Research* 25, 172–196.
- Betzler, C., Hübscher, C., Lindhorst, S., Reijmer, J.J.G., Römer, M., Droxler, A.W., Fürstenau, J., Lüdmann, T., 2013b. Monsoon-induced partial carbonate platform drowning (Maldives, Indian Ocean). *Geology* 37, 867–870.
- Blendinger, W., 1986. Isolated stationary carbonate platforms: the Middle Triassic (Ladinian) of the Marmolada area, Dolomites, Italy. *Sedimentology* 33, 159–183.
- Blendinger, W., 1994. The carbonate factory of Middle Triassic buildups in the Dolomites, Italy — a quantitative-analysis. *Sedimentology* 41, 1147–1159.

- Blendinger, W., Brack, P., Norborg, A.K., Wulff-Pedersen, E., 2004. Three-dimensional modelling of an isolated carbonate buildup (Triassic, Dolomites, Italy). *Sedimentology* 51, 297–314.
- Blondeaux, P., De Bernardinis, B., Seminara, G., 1982. Correnti di marea in prossimità di imboccature e loro influenza sul ricambio lagunare. Paper presented at the Atti XVIII Convegno di Idraulica e Costruzioni Idrauliche, Bologna, Italy, Sept., pp. 21–23.
- Bosellini, A., 1984. Progradation geometries of carbonate platforms: examples from the Triassic of the Dolomites, northern Italy. *Sedimentology* 31, 1–24.
- Bosellini, A., dal Cin, R., Gradenigo, A., 1978. Depositi litorali raibliani nella zona di Passo Falzarego (Dolomiti Centrali). *Annali dell'Università di Ferrara* 5, 223–238.
- Bosellini, A., Gianolla, P., Stefani, M., 2003. Geology of the Dolomites. *Episodes* 26, 181–185.
- Bosellini, A., Masetti, D., Neri, C., 1982. La geologia del Passo del Falzarego. In: Castellarin, A., Vai, G.B. (Eds.), guida alla geologia del Sudalpino centro-orientale. Guide geologiche regionali della Società Geologica Italiana, Bologna, pp. 273–278.
- Brack, P., Rieber, H., Mundil, R., Blendinger, W., Maurer, F., 2007. Geometry and chronology of growth and drowning of Middle triassic carbonate platforms (Cerner and Bivera/Clapsavon) in the southern Alps (northern Italy). *Swiss Journal of Geosciences* 100, 327–347.
- Brandner, R., 1984. Meeresspiegelschwankungen und Tektonik in der Trias der NW-Tethys. *Jahrbuch der Geologischen Bundesanstalt* 126, 435–475.
- Breda, A., Mellere, D., Massari, F., 2007. Facies and processes in a Gilbert-delta-filled incised valley (Pliocene of Ventimiglia, NW Italy). *Sedimentary Geology* 200, 31–55.
- Breda, A., Preto, N., 2011. Anatomy of an Upper Triassic continental to marginal-marine system: the mixed siliciclastic–carbonate Travenanzes Formation (Dolomites, Northern Italy). *Sedimentology* 58, 1613–1647.
- Breda, A., Preto, N., Roghi, G., Furin, S., Meneguolo, R., Ragazzi, E., Gianolla, P., 2009. The Carnian Pluvial Event in the Tofane area (Cortina d'Ampezzo, Dolomites, Italy). *Geo.Alp* 6, 80–115.
- Broglio Loriga, C., Cirilli, S., De Zanche, V., Di Bari, D., Gianolla, P., Laghi, G.F., Lowrie, W., Manfrin, S., Mastandrea, A., Mietto, P., Muttoni, G., Neri, C., Posenato, R., Reichichi, M., Rettori, R., Roghi, G., 1999. The Prati di Stuares/Stuore Wiesen Section (Dolomites, Italy): a candidate global stratotype section and point for the base of the Carnian stage. *Rivista Italiana di Paleontologia e Stratigrafia* 105, 37–78.
- Burne, R.V., Moore, L.S., 1987. Microbialites; organosedimentary deposits of benthic microbial communities. *Palaios* 2, 241–254.

- Cantalamesa, G., Di Celma, C., Ragaini, L. 2005. Sequence stratigraphy of the Punta Ballena Member of the Jama Formation (Early Pleistocene, Ecuador): insights from integrated sedimentologic, taphonomic and paleoecologic analysis of molluscan shell concentrations. *Palaeogeography, Palaeoclimatology, Palaeoecology* 216, 1-25.
- Castellarin, A., Doglioni, C., 1985. A geologic schematic cross-section of the Southern Alps. *Rendiconti della Società Geologica Italiana* 8, 35–36.
- Castellarin, A., Vai, G.B., 1982. Introduzione alla geologia strutturale del Sudalpino. In: Castellarin, A., Vai, G.B. (Eds.), *Guida alla geologia del Sudalpino centro-orientale. Guide geologiche regionali della Società Geologica Italiana*, pp. 1–22.
- Cattaneo, A., Steel, R.J., 2003. Transgressive deposits: a review of their variability. *Earth-Science Reviews* 62, 187-228.
- Catuneanu, O., 2006. *Principles of Sequence Stratigraphy*. Elsevier, Amsterdam (375 pp).
- Catuneanu, O., Abreu, V., Bhattacharya, J.P., Blum, M.D., Dalrymple, R.W., Eriksson, P.G., Fielding, C.R., Fisher, W.L., Galloway, W.E., Gibling, M.R., Giles, K.A., Holbrook, J.M., Jordan, R., Kendall, C.G.St.C, Macurda, B., Martinsen, O.J., Miall, A.D., Neal, J.E., Nummedal, D., Pomar, L., Posamentier, H.W., Pratt, B.R., Sarg, J.F., Shanley, K.W., Steel, R.J., Strasser, A., Tucker, M.E, Winker, C., 2009. Towards the standardization of sequence stratigraphy. *Earth-Science Reviews* 92, 1-33.
- Catuneanu, O., Galloway, W.E., Kendall, C. G., Miall, A.D., Posamentier, H.W., Strasser, A., Tucker, M.E., 2011. Sequence stratigraphy: methodology and nomenclature. *Newsletters on Stratigraphy* 44, 173-245.
- Catuneanu, O., Hancox, P.J., Cairncross, B., Rubidge, B.S., 2002. Foredeep submarine fans and forebulge deltas: orogenic off-loading in the underfilled Karoo Basin. *Journal of African Earth Sciences* 35, 489-502.
- Cockings, J.H., Kessler, L.G.II, Mazza, T.A., Riley, L.A., 1992. Bathonian to mid-Oxfordian sequence stratigraphy of the South Viking Graben, North Sea. In: Hardman, R.F.P. (Ed.), *Exploration Britain, Geological insights for the next decade*. Geological Society of London Special Publication 67, pp. 65–105.
- Collins, J.F., Kenter, J.A.M., Harris, P.M., Kuanysheva, G., Fischer, D.J., Steffen, K.L., 2006. Facies and reservoir-quality variations in the late Visean to Bashkirian outer platform, rim, and flank of the Tengiz buildup, Precaspian Basin, Kazakhstan. In: Harris, P.M., Weber, L.J. (Eds.), *Giant hydrocarbon reservoirs of the world: From rocks to reservoir characterization and modeling*. AAPG Memoir 88/SEPM Special Publication, pp. 55–95.
- Dal Corso, J., Mietto, P., Newton, R.J., Pancost, R.D., Preto, N., Roghi, G., Wignall, P.B., 2012. Discovery of a major negative  $\delta^{13}\text{C}$  spike in the Carnian (Late Triassic) linked to the eruption of Wrangellia flood basalts. *Geology* 40, 79–82.

- D'Alpaos, L., Martini, P., 2005. The influence of the inlet configuration on sediment loss in the Venice Lagoon. In: Fletcher, C.A., Spencer, T. (Eds.), *Flooding and Environmental Challenges for Venice and its Lagoon: State of Knowledge*. Cambridge University Press, pp. 419–430.
- Dalrymple, R.W., Choi, K., 2007. Morphologic and facies trends through the fluvial-marine transition in tide-dominated depositional systems: a schematic framework for environmental and sequence-stratigraphic interpretation. *Earth-Science Reviews* 81, 135–174.
- Davis, R.A., 2006. Precambrian tidalites from the Baraboo Quartzite Wisconsin, USA. *Marine Geology* 235, 247–253.
- Della Porta, G., Kenter, J.A.M., Bahamonde, J.R., 2004. Depositional facies and stratal geometry of an Upper Carboniferous prograding and aggrading high-relief carbonate platform (Cantabrian Mountains, N Spain). *Sedimentology* 51, 267–295.
- Della Porta, G., Kenter, J.A.M., Bahamonde, J.R., Immenhauser, A., Villa, E., 2003. Microbial boundstone dominated carbonate slope (Upper Carboniferous, N Spain): microfacies, lithofacies distribution and stratal geometry. *Facies* 49, 175–207.
- Dercourt, J., Ricou, L.E., Vrielynck, B., 1993. *Atlas Tethys Palaeoenvironmental Maps*. Explanatory Notes. Gauthier-Villars, Paris (307 pp).
- De Zanche, V., Franzin, A., Gianolla, P., Mietto, P., Siorpaes, C., 1992. The Piz da Peres Section (Valdaora-Olang, Pusteria Valley, Italy): a reappraisal of the Anisian stratigraphy in the Dolomites. *Eclogae Geologicae Helvetiae* 85, 127–143.
- De Zanche, V., Gianolla, P., Manfrin, S., Mietto, P., Roghi, G., 1995. A Middle Triassic backstepping carbonate platform in the Dolomites (Italy): sequence stratigraphy and biostratigraphy. *Memorie di Scienze Geologiche* 47, 135–155.
- De Zanche, V., Gianolla, P., Mietto, P., Siorpaes, C., Vail, P.R., 1993. Triassic sequence stratigraphy in the Dolomites (Italy). *Memorie di Scienze Geologiche* 45, 1–27.
- De Zanche, V., Gianolla, P., Roghi, G., 2000. Carnian stratigraphy in the Raibl/Cave del Predil area (Julian Alps, Italy). *Eclogae Geologicae Helvetiae* 93, 331–348.
- Doglioni, C., Carminati, E., 2008. Structural style & Dolomites field trip. *Memorie descrittive della carta geologica d'Italia volume LXXXII*. APAT, Roma (295 pp.).
- Dupraz, C., Reid, R.P., Braissant, O., Decho, A.W., Norman, R.S., Visscher, P.T., 2009. Processes of carbonate precipitation in modern microbial mats. *Earth-Science Reviews* 96, 141–162.

- Emmerich, A., Glasmacher, U.A., Bauer, F., Bechstadt, T., Zühlke, R., 2005. Meso-/Cenozoic basin and carbonate platform development in the SW-Dolomites unraveled by basin modeling and apatite FT analysis: Rosengarten and Latemar (Northern Italy). *Sedimentary Geology* 175, 415–438.
- Feist-Burkhardt, S., Götz, A.E., Szulc, J., (coordinators), Borkhataria, R., Geluk, M., Haas, J., Hornung, J., Jordan, P., Kempf, O., Michalík, J., Nawrocki, J., Reinhardt, L., Ricken, W., Röhling, G.H., Ruffer, T., Török, Á., Zühlke, R., 2008. Triassic. In: McCann, T., (Ed.), *The Geology of Central Europe, Vol. 2*. Geological Society, London, pp. 749-821.
- Fitzgerald, D.M., 1984. Interactions between the ebb-tidal delta and landward shoreline: Price Inlet, South Carolina. *Journal of Sedimentary Research* 54, 1303–1318.
- Flügel, E., 2002. Triassic reef patterns. In: Kiessling, W., Flügel, E., Golonka, J. (Eds.), *Phanerozoic Reef Patterns*. SEPM Special Publication 72, pp. 391–463.
- Flügel, E., 2004. *Microfacies of carbonate rocks*. Springer-Verlag, Berlin-Heidelberg, Germany (976 pp.).
- Folkestad, A., Satur, N., 2008. Regressive and transgressive cycles in a rift-basin: depositional model and sedimentary partitioning of the Middle Jurassic Hugin Formation, southern Viking Graben, North Sea. *Sedimentary Geology* 207, 1–21.
- Föllmi, K.B., Godet, A., 2013. Paleooceanography of Lower Cretaceous Alpine platform carbonates. *Sedimentology* 60, 131–151.
- Frazier, D. E., 1974. Depositional episodes: their relationship to the Quaternary stratigraphic framework in the northwestern portion of the Gulf Basin. University of Texas at Austin, Bureau of Economic Geology Geological Circular 71-1 (28 pp.).
- Furin, S., Preto, N., Rigo, M., Roghi, G., Gianolla, P., Crowley, J.L., Bowring, S.A., 2006. High-precision U–Pb zircon age from the Triassic of Italy: implications for the Triassic time scale and the Carnian origin of calcareous nanoplankton and dinosaurs. *Geology* 34, 1009–1012.
- Gaetani, M., Fois, E., Jadoul, F., Nicora, A., 1981. Nature and evolution of Middle Triassic carbonate buildups in the Dolomites (Italy). *Marine Geology* 44, 25–57.
- Galloway, W.E., 2002. Paleogeographic setting and depositional architecture of a sand dominated shelf depositional system, Miocene Utsira Formation, North Sea Basin. *Journal of Sedimentary Research* 72, 476–490.
- Galloway, W.E., 2008. Depositional evolution of the Gulf of Mexico Sedimentary Basin. In: Miall, A.D. (Ed.), *The Sedimentary Basins of the United States and Canada: Sedimentary Basins of the World, v. 5*, K. J. Hsu, Series Editor, Elsevier Science Amsterdam, pp. 505–550.

Galloway, W.E., Williams, T.A., 1991. Sediment accumulation rates in time and space: Paleogene genetic stratigraphic sequences of the northwestern Gulf of Mexico basin. *Geology* 19, 986-989.

Gattolin, G., Breda, A., Preto, N., 2013. Demise of Late Triassic carbonate platforms triggered the onset of a tide-dominated depositional system in the Dolomites, Northern Italy. *Sedimentary Geology* 297, 38-49.

Gianolla, P., De Zanche, V., Mietto, P., 1998. Triassic sequence stratigraphy in the Southern Alps (northern Italy): definition of sequences and basin evolution. In: De Graciansky, P.C., Hardenbol, J., Jacquin, T., Vail, P.R. (Eds.), *Mesozoic and Cenozoic Sequence Stratigraphy of European Basins*. SEPM Special Publication 60, pp. 719–748.

Gianolla, P., De Zanche, V., Roghi, G., 2003. An upper Tuvallian (Triassic) platform–basin system in the Julian Alps: the start-up of the Dolomia Principale (Southern Alps, Italy). *Facies* 49, 135–150.

Gianolla, P., Jacquin, T., 1998. Triassic sequence stratigraphic framework of Western European basins. In: De Graciansky, P.C., Hardenbol, J., Jacquin, T., Vail, P.R. (Eds.), *Mesozoic and Cenozoic Sequence Stratigraphy of European Basins*. SEPM Special Publication 60, pp. 643–650.

Gianolla, P., Stefani, M., Caggiati, M., Preto, N., 2011. Triassic platform and basinal bodies of the Dolomites as outcrop analogues for hydrocarbon carbonate systems. Preconference Field Trip Guidebook of the AAPG International Conference & Exhibition, Milan, Italy, 19–22 Oct. (78 pp.).

Godet, A., Föllmi, K.B., Spangenberg, J.E., Bodin, S., Vermeulen, J., Adatte, T., Bonvallet, L., Arnaud, H., 2013. Deciphering the message of Early Cretaceous drowning surfaces from the Helvetic Alps: What can be learnt from platform to basin correlations? *Sedimentology* 60, 152–173.

Greene, A.R., Scoates, J.S., Weis, D., Katvala, E.C., Israel, S., Nixon, G.T., 2010. The architecture of oceanic plateaus revealed by the volcanic stratigraphy of the accreted Wrangellia oceanic plateau. *Geosphere* 6, 47–73.

Hallock, P., Schlager, W., 1986. Nutrient excess and the demise of coral reefs and carbonate platforms. *Palaios* 1, 389–398.

Hardie, L.A., Bosellini, A., Goldhammer, R.K., 1986. Repeated subaerial exposure of subtidal carbonate platforms, Triassic, northern Italy: Evidence for high frequency sea level oscillations on a  $10^4$  year scale. *Paleoceanography* 1, 447–457.

Harris, M.T., 1993. Reef fabrics, biotic crusts and syndepositional cements of the Latemar reef margin (Middle Triassic), Northern Italy. *Sedimentology* 40, 383–401.

Hayes, M.O., 1975. Morphology of sand accumulation in estuaries: and introduction to the symposium. In: Cronin, L.E. (Ed.), *Estuarine Research. Geology and Engineering*, 2. Academic Press, London, pp. 3–22.



- Helland-Hansen, W., 1992. Geometry and facies of Tertiary clinothems, Spitsbergen. *Sedimentology* 39, 1013-1029.
- Hernández-Molina, F.J., Fernández-Salas, L.M., Lobo, F., Somoza, L., Díaz-del-Río, V., Dias, J.A., 2000. The infralittoral prograding wedge: a new large-scale progradational sedimentary body in shallow marine environments. *Geo-Marine Letters* 20, 109-117.
- Hofmann, W., 1972. Zur lithofazies und Paläogeographie der Raibler Schichten in der Südtiroler Dolomiten and den östlichen angrenzenden Karnischen Alpen (Italien). *Mitteilungen der Gesellschaft der Geologie und Bergbaustudenten* 21, 225–234.
- Jenkyns, H.C., 1991. Impact of Cretaceous sea level rise and anoxic events on the Mesozoic carbonate platform of Yugoslavia. *AAPG Bulletin* 75, 1007–1017.
- Jones, G.D., Xiao, Y., 2006. Geothermal convection in the Tengiz carbonate platform, Kazakhstan: Reactive transport models of diagenesis and reservoir quality. *AAPG Bulletin* 90, 1251-1272.
- Keim, L., Brandner, R., Krystyn, L., Mette, W., 2001. Termination of carbonate slope progradation: an example from the Carnian of the Dolomites, Northern Italy. *Sedimentary Geology* 143, 303–323.
- Keim, L., Schlager, W., 1999. Automicrite facies on steep slopes (Triassic, Dolomites, Italy). *Facies* 41, 15–25.
- Keim, L., Schlager, W., 2001. Quantitative compositional analysis of a Triassic carbonate platform (Southern Alps, Italy). *Sedimentary Geology* 139, 261–283.
- Keim, L., Spötl, C., Brandner, R., 2006. The aftermath of the Carnian carbonate platform demise: a basinal perspective (Dolomites, Southern Alps). *Sedimentology* 53, 361–386.
- Kenter, J.A.M., 1990. Carbonate platform flanks: slope angle and sediment fabric. *Sedimentology* 37, 777–794.
- Kenter, J.A.M., Harris, P.M., Collins, J.F., Weber, L.J., Kuanysheva, G., Fischer, D.J., 2006. Late Viséan to Bashkirian platform cyclicity in the central Tengiz buildup, Precaspian Basin, Kazakhstan: Depositional evolution and reservoir development. In: Harris, P.M., Weber, L.J. (Eds.), *Giant hydrocarbon reservoirs of the world: From rocks to reservoir characterization and modeling*. AAPG Memoir 88/SEPM Special Publication, pp. 7– 54.
- Kenter, J.A.M., Harris, P.M., Della Porta, G., 2005. Steep microbial boundstonedominated platform margins - examples and implications. *Sedimentary Geology* 178, 5-30.
- Kenter, J.A.M., Playton, T., Harris, P.M., Katz, D., Bellian, J., 2010b. Application of outcrop analogs to characterize carbonate reservoirs in the Pricaspian basin. SPE Caspian Carbonates Technology Conference, Atyrau, Kazakhstan, 8-10 Nov. (13 pp.).

- Kenter, J.A.M., Tankersley, T., Skalinski, M., Harris, P.M., Levy, M., Dickson, T., Jacob, G., 2010a. Tengiz field (Republic of Kazakhstan) Unit 1 platform static model: using a hybrid depositional - diagenetic approach. SPE Caspian Carbonates Technology Conference, Atyrau, Kazakhstan, 8-10 Nov. (9 pp.).
- Kraus, N.C., 2000. Reservoir model of ebb-tidal shoal evolution and sand bypassing. *Journal of Waterway, Port, Coastal, and Ocean Engineering* 126, 305–313.
- Kvale, E.P., 2006. The origin of neap-spring tidal cycles. *Marine Geology* 235, 5–18.
- Lehrmann, D.J., Wei, J.Y., Enos, P., 1998. Controls on facies architecture of a large Triassic carbonate platform: The Great Bank of Guizhou, Nanpanjiang Basin, South China. *Journal of Sedimentary Research* 68, 311–326.
- Longhitano, S.G., 2011. The record of tidal cycles in mixed silici-bioclastic deposits: examples from small Plio-Pleistocene peripheral basins of the microtidal Central Mediterranean Sea. *Sedimentology* 58, 691–719.
- Longhitano, S.G., Nemec, W., 2005. Statistical analysis of bed-thickness variation in a Tortonian succession of biocalcarenitic tidal dunes, Amantea Basin, Calabria, southern Italy. *Sedimentary Geology* 179, 195–224.
- Longhitano, S.G., Sabato, L., Tropeano, M., Gallicchio, S., 2010. A mixed bioclastic-siliciclastic flood-tidal delta in a micro tidal setting: depositional architectures and hierarchical internal organization (Pliocene, Southern Apennine, Italy). *Journal of Sedimentary Research* 80, 36–53.
- Longhitano, S.G., Mellere, D., Steel, R.J., Ainsworth, R.B., 2012a. Tidal depositional systems in the rock record: a review and new insights. In: Longhitano, S.G., Mellere, D., Ainsworth, R.B. (Eds.), *Modern and Ancient Depositional Systems: Perspectives, Models and Signatures*. *Sedimentary Geology* 279, pp. 2–22.
- Longhitano, S.G., Chiarella, D., Di Stefano, A., Messina, C., Sabato, L., Tropeano, M., 2012b. Tidal signatures in Neogene to Quaternary mixed deposits of southern Italy straits and bays. In: Longhitano, S.G., Mellere, D., Ainsworth, R.B. (Eds.), *Modern and Ancient Depositional Systems: Perspectives, Models and Signatures*. *Sedimentary Geology* 279, pp. 74–96.
- Lowenstam, H.A., 1981. Minerals formed by organisms. *Science* 211, 1126–1131.
- Lowenstam, H.A., Weiner, S., 1989. *On Biomineralization*. Oxford University Press, pp. 1–324.
- Lüdmann, T., Kalvelage, C., Betzler, C., Fürstenau, J., Hübscher, C., 2013. The Maldives, a giant isolated carbonate platform dominated by bottom currents. *Marine and Petroleum Geology* 43, 326–340.

- Marangon, A., Gattolin, G., Della Porta, G., Preto, N., 2011. The Latemar: A flat-topped, steep fronted platform dominated by microbialites and synsedimentary cements. *Sedimentary Geology* 240, 97–114.
- Martel, A.T., Allen, P.A., Slingerland, R., 1994. Use of tidal-circulation modeling in paleogeographical studies: an example from the Tertiary of the Alpine perimeter. *Geology* 22, 925–928.
- Martín, J.M., Braga, J.C., Aguirre, J., Puga-Bernabéu, Á., 2009. History and evolution of the North-Betic Strait (Prebetic Zone, Betic Cordillera): a narrow, early Tortonian, tidal-dominated, Atlantic–Mediterranean marine passage. *Sedimentary Geology* 216, 80–90.
- Masetti, D., Neri, C., 1980. L'Anisico della Val di Fassa (Dolomiti occidentali): sedimentologia e paleogeografia. *Annali dell'Università Ferrara* 9, 1–19.
- Massari, F., D'Alessandro, A., 2010. Icehouse, cool-water carbonate ramps: the case of the Upper Pliocene Capodarso Fm (Sicily): role of trace fossils in the reconstruction of growth stages of prograding wedges. *Facies* 56, 47–58.
- Massari, F., Sgavetti, M., Rio, D., D'alessandro, A., Prosser, G., 1999. Composite sedimentary record of falling stages of Pleistocene glacio-eustatic cycles in a shelf setting (Crotone basin, south Italy). *Sedimentary Geology* 127, 85–110.
- Mateu-Vicens, G., Pomar, L., Tropeano, M., 2008. Architectural complexity of a carbonate transgressive systems tract induced by basement physiography. *Sedimentology* 55, 1815–1848.
- Maurer, F., 2000. Growth mode of Middle Triassic carbonate platforms in the Western Dolomites (Southern Alps, Italy). *Sedimentary Geology* 134, 275–286.
- Mazumder, R., Arima, M., 2005. Tidal rhythmites and their implications. *Earth-Science Reviews* 69, 79–95.
- McKinney, M.L., 1985. Mass extinction patterns of marine invertebrate groups and some implications for a causal phenomenon. *Paleobiology* 11, 227–233.
- Mellere, D., Steel, R., 1995. Variability of lowstand wedges and their distinction from forced-regressive wedges in the Mesaverde Group, southeast Wyoming. *Geology* 23, 803–806.
- Mercier, D., Barrier, P., Beaudoin, B., Didier, S., Montenat, J.L., Salinas Zuniga, E., 1987. Les facteurs hydrodynamiques dans la sédimentation plio-quaternaire du Déroit de Messine. Le Déroit de Messine (Italie). Evolution tectono-sédimentaire récente (Pliocène et Quaternaire) et environnement actuel, 11. Documentés Travaux IGAL, Paris 171–183.

- Messina, C., Nemec, W., Longhitano, S. G., 2009. Statistical properties of tidal dunes and their use in reservoir modelling. 27th International Association of Sedimentologists, Alghero, Italy 20-23 Sept., 604.
- Miall, A. D., Arush, M., 2001. The Castlegate Sandstone of the Book Cliffs, Utah: sequence stratigraphy, paleogeography, and tectonic controls. *Journal of Sedimentary Research* 71, 537-548.
- Miall, A. D., Catuneanu, O., Vakarelov, B., Post, R., 2008. The Western Interior Basin. In: Miall, A. D. (Eds.), *The Sedimentary Basins of the United States and Canada: Sedimentary basins of the World*, v. 5, K. J. Hsü, Series Editor, Elsevier Science, Amsterdam, pp. 329–362.
- Mietto, P., Manfrin, S., 1995. A high resolution Middle Triassic ammonoid standard scale in the Tethys Realm; a preliminary report. *Bulletin de la Société géologique de France* 166, 539–563.
- Mutti, M., Bernouilli, D., Stille, P., 1997. Temperate carbonate platform drowning linked to Miocene oceanographic events: Maiella platform margin, Italy. *Terra Nova* 9, 122–125.
- Mutti, M., Droxler, A.W., Cunningham, A.D., 2005. Evolution of the Northern Nicaragua Rise during the Oligocene-Miocene: drowning by environmental factors. *Sedimentary Geology* 175, 237–258.
- Mutti, M., Hallock, P., 2003. Carbonate systems along nutrients and temperature gradients: some sedimentological and geochemical constraints. *International Journal of Earth Sciences (Geologische Rundschau)* 92, 465–475.
- Muttoni, G., Kent, D.V., Channell, J.E., 1996. Evolution of Pangea: paleomagnetic constraints from the Southern Alps, Italy. *Earth and Planetary Science Letters* 140, 97–112.
- Neri, C., Gianolla, P., Furlanis, S., Caputo, R., Bosellini, A., 2007. Note illustrative della Carta Geologica d'Italia alla scala 1:50000, foglio 029 Cortina d'Ampezzo. APAT, Roma (200 pp.).
- Neri, C., Stefani, M., 1998. Sintesi cronostratigrafica e sequenziale dell'evoluzione permiana superiore e triassica delle Dolomiti. *Memorie della Società Geologica Italiana* 53, 417–463.
- Pasquier, J.B., Strasser, A., 1997. Platform-to-basin correlation by high-resolution sequence stratigraphy and cyclostratigraphy (Berriasian, Switzerland and France). *Sedimentology* 44, 1071-1092.
- Pomar, L., 2001. Ecological control of sedimentary accommodation: evolution from a carbonate ramp to rimmed shelf, Upper Miocene, Balearic Islands. *Palaeogeography, Palaeoclimatology, Palaeoecology* 175, 249-272.

- Pomar, L., Brandano, M., Westphal, H., 2004. Environmental factors influencing skeletal-grain sediment associations: a critical review of Miocene examples from the Western-Mediterranean. *Sedimentology* 51, 627–651
- Pomar, L., Tropeano, M., 2001. The Calcarenite di Gravina Formation in Matera (southern Italy): new insights for coarse-grained, large-scale, cross-bedded bodies encased in offshore deposits. *AAPG Bulletin* 85, 661-689.
- Posamentier, H.W., Jervey, M.T., Vail, P.R., 1988. Eustatic controls on clastic deposition I —conceptual framework. In: Wilgus, C.K., Hastings, B.S., Kendall, C.G.St.C., Posamentier, H.W., Ross, C.A., Van Wagoner, J.C. (Eds.), *Sea Level Changes—An Integrated Approach*. Special Publication, vol. 42. Society of Economic Paleontologists and Mineralogists (SEPM), pp. 110–124.
- Preto, N., 2012. Petrology of carbonate beds from the stratotype of the Carnian (Stuores Wisen section, Dolomites, Italy): the contribution of platform-derived microbialites. *Geo.Alp* 9, 12-29.
- Preto, N., Franceschi, M., Gattolin, G., Massironi, M., Riva, A., Gramigna, P., Bertoldi, L., Nardon, S., 2011. The Latemar: a Middle Triassic polygonal fault-block platform controlled by synsedimentary tectonics. *Sedimentary Geology* 234, 1–18.
- Preto, N., Hinnov, L.A., 2003. Unraveling the origin of carbonate platform cyclothems in the Upper Triassic Durrenstein Formation (Dolomites, Italy). *Journal of Sedimentary Research* 73, 774–789.
- Preto, N., Spötl, C., Mietto, P., Gianolla, P., Riva, A., Manfrin, S., 2005. Aragonite dissolution, sedimentation rates and carbon isotopes in deep-water hemipelagites (Livinallongo Formation, Middle Triassic, northern Italy). *Sedimentology* 181, 173–194.
- Preto, N., Kustatscher, E., Wignall, P.B., 2010. Triassic climates—state of the art and perspectives. *Palaeogeography, Palaeoclimatology, Palaeoecology* 290, 1–10.
- Pugh, D.T., 1987. *Tides, Surges and Mean Sea-Level*. John Wiley and Sons, Chichester (472 pp).
- Rankey, E.C., Reeder, S.L., 2011. Holocene oolitic marine sand complexes of the Bahamas. *Journal of Sedimentary Research* 81, 97–117.
- Raup, D.M., 1979. Size of the Permo-Triassic bottleneck and its evolutionary implications. *Science* 206, 217–218.
- Reeder, S.L., Rankey, E.C., 2009. Controls on morphology and sedimentology of carbonate tidal deltas, Abacos, Bahamas. *Marine Geology* 267, 141–155.
- Reijmer, J.J.G., 1998. Compositional variations during phases of progradation and retrogradation of a Triassic carbonate platform (Picco di Vallandro/Durrenstein, dolomites, Italy). *Geologische Rundschau* 87, 436–448.

- Rigo, M., Preto, N., Roghi, G., Tateo, F., Mietto, P., 2007. A rise in the carbonate compensation depth of western Tethys in the Carnian (Late Triassic): deep-water evidence for the Carnian Pluvial Event. *Palaeogeography, Palaeoclimatology, Palaeoecology* 246, 188–205.
- Rüffer, T., Zühlke, R., 1995. Sequence stratigraphy and sea-level changes in the Early to Middle Triassic of the Alps: a global comparison. In: Haq, B.U. (Ed.), *Sequence Stratigraphy and Depositional Response to Eustatic, Tectonic and Climatic Forcing*. Kluwer, Amsterdam, pp. 161–207.
- Russo, F., Neri, C., Mastandrea, A., Baracca, A., 1997. The mudmound nature of the Cassian platform margins of the Dolomites. A case history: the Cipit boulders from Punta Grohmann (Sasso Piatto Massif, Northern Italy). *Facies* 36, 25–36.
- Russo, F., Neri, C., Mastandrea, A., Laghi, G., 1991. Depositional and diagenetic history of the Alpe di Specie (Seelandalpe) fauna (Carnian, northeastern Dolomites). *Facies* 25, 187–210.
- Schlager, W., 1981. The paradox of drowned reefs and carbonate platforms. *Geological Society of America Bulletin* 92, 197-211.
- Schlager, W., 1991. Depositional bias and environmental change - important factors in sequence stratigraphy. *Sedimentary Geology* 70, 109-130.
- Schlager, W., 1993. Accommodation and supply - a dual control on stratigraphic sequences. *Sedimentary Geology* 86, 111-136.
- Schlager, W., 1999a. Scaling of sedimentation rates and drowning of reefs and carbonate platforms. *Geology* 27, 183–6.
- Schlager, W., 1999b. Type 3 sequence boundaries. In: *Advances in Carbonate Sequence Stratigraphy: Application to Reservoirs, Outcrops and Models* (Eds. P.M. Harris, A.H. Sallet and T. Simo), SEPM Special Publication 63, pp. 35–45.
- Schlager, W., 2003. Benthic carbonate factories of the Phanerozoic. *International Journal of Earth Sciences* 92, 445–464.
- Schlager, W., 2005. Carbonate sedimentology and sequence stratigraphy. *SEPM concept in sedimentology and paleontology* 8 (200 pp.).
- Schlager, W., Reijmer, J.J.G., Droxler, A., 1994. Highstand shedding of carbonate platforms. *Journal of Sedimentary Research* 64, 270-281.
- Schlager, W., Schöllnberger, W., 1974. Das Prinzip stratigraphischer Wenden in der Schichtfolge der Nördlichen Kalkalpen. *Mitteilungen. Österreichische Geologische Gesellschaft* 66–67, 165–193.
- Seilacher, A., 2007. *Trace Fossil Analysis*. Springer (238 pp.).

- Senowbari-Daryan, B., Zühlke, R., Bechstädt, T., Flügel, E., 1993. Anisian (Middle Triassic) buildups of the Northern Dolomites (Italy): the recovery of reef communities after the Permian/Triassic crisis. *Facies* 28, 181–256.
- Shanmugam, G., Shrivastava, S.K., Das, B., 2009. Sandy debrites and tidalites of Pliocene reservoir sands in upper-slope canyon environments, offshore Krishna–Godavari Basin (India): implications. *Journal of Sedimentary Research* 79, 736–756.
- Simms, M.J., Ruffell, A.H., 1989. Synchronicity of climatic change and extinctions in the Late Triassic. *Geology* 17, 265–268.
- Simms, M.J., Ruffell, A.H., 1990. Climatic and biotic change in the late Triassic. *Journal of the Geological Society of London* 147, 321–327.
- Siorpaes, C., Gianolla, P., 1991. Stratigrafia triassica del versante settentrionale delle cime di San Sebastiano (Dolomiti orientali). *Rendiconti della Società Geologica Italiana* 14, 155–156.
- Sloss, L.L., Krumbein, W.C., Dapples, E.C., 1949. Integrated facies analysis. In: Longwell, C.R. (Ed.), *Sedimentary Facies in Geologic History*. Memoir, vol. 39. Geological Society of America, pp. 91–124.
- Stanley, S.M., Hardie, L.A., 1998. Secular oscillations in the carbonate mineralogy of reef-building and sediment-producing organisms driven by tectonically forced shifts in seawater chemistry. *Palaeogeography, Palaeoclimatology, Palaeoecology*, 144, 3-19.
- Stefani, M., Furin, S., Gianolla, P., 2010. The changing climate framework and depositional dynamics of Triassic carbonate platforms from the Dolomites. *Palaeogeography, Palaeoclimatology, Palaeoecology* 290, 43-57.
- Sztanò, O., De Boer, P.L., 1995. Basin dimensions and morphology as controls on amplification of tidal motions (the Early Miocene North Hungarian Bay). *Sedimentology* 42, 665–682.
- Tape, C.H., Cowan, C.A., Runkel, A.C., 2003. Tidal-bundle sequences in the Jordan sandstone (Upper Cambrian), southeastern Minnesota, USA: evidence for tides along inboard shorelines of the Sauk Epicontinental Sea. *Journal of Sedimentary Research* 73, 354–366.
- Tropeano, M., Sabato, L., 2000. Response of Plio-Pleistocene mixed bioclastic-lithoclastic temperate-water carbonate systems to forced regressions: the Calcarenite di Gravina Formation, Puglia, SE Italy. In *sedimentary responses to forced regressions* (Eds. D. Hunt, R.L. Gawthorpe), Geological Society, London, Special Publications 172, 217-243.
- Tucker, M.E., Wright, V.P., 1990. *Carbonate sedimentology*. Blackwell, Oxford (492 pp).

Vail P.R., Audemard, F., Bowman, S.A, Eisner, P.N., Perez Cruz, C., 1991. The stratigraphic signatures of tectonics, eustasy and sedimentology-an overview. In: Einsele, G., Ricken, W., Seilacher, A. (Eds.), *Cycles and events in stratigraphy*. Springer-Verlag, Berlin-Heidelberg, pp. 617-659.

Von Mojsisovics, E., 1879. *Die Dolomit-Riffe von Südtirol und Venetien*. Beiträge zur bildungsgeschichte der Alpen 13, Wien (552 pp.).

Weber, L.J., Francis, B.P., Harris, P.M., Clark, M., 2003. Stratigraphy, lithofacies and reservoir distribution, Tengiz field, Kazakhstan. In: Ahr, W.M., Harris, P.M., Morgan, W.A., Somerville, I.D. (Eds.), *Permo-Carboniferous carbonate platform and reefs*. SEPM Special Publication 78/AAPG Memoir 83, pp. 351-394.

Weissert, H., Lini, A., Föllmi, K.B., Kuhn, O., 1998. Correlation of Early Cretaceous carbon isotope stratigraphy and platform drowning events: a possible link? *Palaeogeography, Palaeoclimatology, Palaeoecology* 137, 189–203.

Williams, G.E., 1989. Tidal rhythmites: geochronometers for the ancient Earth–Moon system. *Episodes* 12, 162–171.

Wilson, P.A., Jenkyns, H.C., Elderfield, H., Larson, R.L., 1998. The paradox of drowned carbonate platforms and the origin of Cretaceous Pacific guyots. *Nature* 392, 889-894

Ziegler, P.A., 1988. Evolution of the Arctic–North Atlantic and Western Tethys. *AAPG Memoir* 43, 164–196 (Tulsa).